DISSERTATION

submitted to the
Combined Faculties for the Natural Sciences and for Mathematics
of the Ruperto-Carola University of Heidelberg, Germany
for the degree of
Doctor of Natural Sciences

presented by
Dipl. Mol. Biomed. **Christoph Schneider**
born in Bremerhaven, Germany

Oral-examination:

_____

Clock controlled gene-9 is a trehalose phosphorylase which does not contribute to growth or development in *Neurospora crassa*

Referees:

Prof. Dr. Michael Brunner

PD Dr. Johannes Lechner

Acknowledgements

First of all I want to thank my girlfriend **Michaela Schäfer**

You were strong when I was weak.

You were confident when I was hopeless.

You were at my side, when my spirit left me alone.

I thought about how all this could have ended without your help, your care, your endless patience and without everything that I obtained from you:

I could not imagine…

I also owe special thanks to **my family** for continuously supporting me and my (sometimes weird) ideas and future plans. I am glad that you have been and will be there whenever I need someone to talk, to lough or to discuss.

I especially thank **Christoph Pille** and **Daniela Marzoll** who I learned to know as colleagues and who I will keep in memory as friends. We had a beautiful time together which I enjoyed very much. I wish you all the best for your future plans and I really hope that we will stay in contact.

Furthermore, I want to thank my supervisor **Prof. Dr. Michael Brunner**. We did not always share the same opinion but I see him as a great mentor and I really learned a lot from him about scientific and non-scientific topics during my time as a PhD student. I also gratefully recognize his attempts to improve my personal and professional development.

Finally, I want to thank **the whole team of AG Brunner** for a nice and productive working atmosphere. It is the small and funny moments which we had together and which made my time as a PhD student much more fun than it would have been without you guys. Special thanks to **Martina Franke** who helped me so much even in tricky situations as well as to **Nai Ha** who invested his time and helped me to analyze the RNAseq data.

Table of contents

Summary

This study was originally designed to investigate the role of global cellular processes like the cell cycle in mediating signal from the circadian clock to rhythmic growth and development in *Neurospora crassa*. In a first attempt clock control over growth and cell cycle related genes was tested by real-time monitoring of gene expression with a luciferase based assay. It was observed that under conditions, which restrict growth and conidiation, the target genes showed no or poor rhythmicity. In contrast, under native growth conditions or in cultures which overcome growth repression by aging rhythmic gene expression could be observed in any of the target genes. Surprisingly, this included also typical “housekeeping” genes like *tubulin*, *histoneH1* or *actin* for example. A further hallmark of these rhythms was that they were equal in phase even in genes which had previously been reported to be expressed antiphasic (Sancar et al., 2011). These observations suggest that the luciferase assay may interfere with clock controlled processes which are related to native growth.

With a further project the role of clock control over metabolism for rhythmic growth should be analyzed. For this purpose a mutant was characterized which had been shown to be defective in the trehalose synthase *clock controlled gene 9* (*ccg-9*^{RIP}) (Shinohara et al., 2002). The mutant displays the loss of clock control over conidiation and a severe defect in vegetative growth and asexual development. These observations strongly suggested a link between clock control over carbohydrate metabolism and circadian growth. Changes in the transcriptome during conidiation were analyzed in *ccg-9*^{RIP}. The majority of misregulated genes are related to metabolic functions. However, genotype and phenotype of *ccg-9*^{RIP} did not cosegregate during backcrossing. A knockout of *ccg-9* by gene replacement grew rhythmic and did not show any defect during vegetative growth and asexual development under several conditions. These results demonstrate that *ccg-9* does not have any role in circadian growth. Furthermore, the phenotype of *ccg-9*^{RIP} must be caused by disruption of other genes than *ccg-9*.

Zusammenfassung

In der vorliegenden Arbeit sollte zunächst die Bedeutung des Zellzyklus für zirkadianes Wachstumsverhalten in *Neurospora crassa* analysiert werden. Dafür wurde die Expression von mit Wachstum und Zellzyklus assoziierten Genen mit Hilfe eines Luziferase-basierenden Verfahrens in Echtzeit gemessen. Unter wachstumshemmenden Bedingungen konnte bei diesen Genen nur ein schwacher Expressionsrhythmus beobachtet werden. Native Wachstumsbedingungen und späte Kulturstadien, die ein zunehmend natürliches Wachstum erlauben, resultierten in rhythmischer Expression sämtlicher getesteter Gene. Dies wurde überraschender Weise auch für typische Haushaltsgene wie *Tubulin*, *Aktin* oder *HistonH1* beobachtet. Eine weitere Eigenschaft dieser Rhythmen war die Phasengleichheit, selbst bei Genen, die zu verschiedenen Tageszeiten exprimiert werden (Sancar et al., 2011). Diese Beobachtungen zeigen, dass die Methode durch zelluläre Prozesse beeinflusst wird, die von der zirkadianen Uhr kontrolliert werden und mit Wachstum in Verbindung stehen.

In einem weiteren Projekt sollte die Rolle des Metabolismus bei der Entstehung von Wachstumsrhythmen untersucht werden. Dafür wurde eine Mutante charakterisiert, die einen Gendefekt im „*clock controlled gene-9*“, welches eine Trehalose-Synthase codiert, trägt (*ccg-9*^{RIP}) (Shinohara et al., 2002). *ccg-9*^{RIP} wächst langsam, arrhythmisch und weist einen erheblichen Defekt in der asexuallen Entwicklung auf. Dies impliziert einen Zusammenhang zwischen rhythmischem Wachstum und Kohlenhydrat-Stoffwechsel. Die Genexpression im Verlauf der Konidienbildung wurde analysiert. In *ccg-9*^{RIP} konnten die fehlregulierten Gene dabei überwiegend dem Metabolismus zugeordnet werden. Nach einer Rückkreuzung mit dem Wildtyp wurde jedoch festgestellt, dass Genotyp und Phänotyp nicht gekoppelt sind. Weiterhin zeigt eine in dieser Studie generierte Nullmutante keinen vom Wildtyp abweichenden Phänotyp. Diese Ergebnisse zeigen, dass *ccg-9* keine Funktion in der Regulation von zirkadianem Wachstum in *Neurospora* hat und dass der Phänotyp von *ccg-9*^{RIP} durch andere Gendefekte als die im *ccg*-9-Lokus verursacht worden sein muss.

1 Introduction

1.1 *Neurospora crassa* - an overview

1.1.1 Discovery as a model organism

First studies using *Neurospora* date back to the early years of the 18th century. *Neurospora*, formerly known as a family of fungi that was named the "*Monilia sitophila"* group, was found to grow in bakeries, which also gave it the name "red bread-mold fungi" (Davis, 2000). In the 1920s, when scientists became increasingly interested in the nature of genes, their inheritance and their role in life, Bernhard O. Dodge and Cornelius L. Shear published their first studies on meiotic segregation of mating types with *Neurospora* (Shear and Dodge, 1927). The following years *Neurospora* became a model organism to study eukaryotic genetics. Due to its haploid genome and its easy accessibility to mutagenesis people soon found out that *Neurospora* may serve as a good model organism to investigate the physiological function of single genes in the context of growth, nutrition and metabolism. George Beadle and his colleague Edward L. Tatum could isolate a series of metabolic mutants using UV light or X-ray induced mutagenesis and auxanography (Beadle and Tatum, 1945). Their studies finally resulted in the one gene – one enzyme hypothesis, for which they were awarded the Nobel Prize in 1958. However, the advantages of using *Neurospora* as a model organism were not just limited to genetics. Formulation of synthetic media allowed an easy and defined cultivation. Simple extraction of nucleic acids and proteins even from little biomass made this fungus becoming a very convenient tool for protein biochemistry and molecular biology. Today *Neurospora* is established as an eukaryotic model organism in a variety of research topics ranging from biochemistry and cell biology to fungal growth and development as well as circadian biology. Sequencing of the *N. crassa* genome at the beginning of the 21st century (Galagan et al., 2001) raised opportunities towards high-throughput gene knockout projects and analysis of gene

functions (Borkovich et al., 2004; Colot et al., 2006). With respect to the advantages of this model organism and the increasing technical possibilities in the field of molecular biology, *N*. *crassa* will serve as an important tool for life science research also in the future.

1.1.2 Growth and reproduction

Neurospora crassa is a filamentous fungus. In contrast to budding species it grows by elongation of so called vegetative hyphae and thereby covers the substrate with a network of biomass. As a syncytial organism the hyphae of *N. crassa* do not grow by cell division. All hyphae together rather form one cellular compartment and growth is accompanied by continuous division and duplication of the organelles. However, these processes are mainly restricted to the growth front, while old hyphae become vacuolized. Despite the syncytial vegetative growth of *N. crassa* it can also undergo differentiation into different tissues and even cellular compartments. This feature becomes especially visible during growth in native light/dark rhythms (L/D) as well as in constant darkness (DD). Under these conditions a phase of vegetative growth alternates with a phase of asexual development. These alterations in growth behavior, namely the rhythmic switch between vegetative growth and asexual development, are controlled by the circadian clock. They are accompanied by rhythmic alteration of biomass production (Castro-Longoria et al., 2002) and therefore made *N. crassa* becoming a powerful tool for circadian research, as described later.

As summarized in figure 1 *N. crassa* shows a sexual and asexual way of reproduction. For asexual reproduction, which is the more common way, *N. crassa* forms so called conidia. There are two types of conidia, the micro- and macroconidia. Microconidia are less prominent as they are smaller and typically occur in much lower abundance compared to macroconidia. They arise out of the vegetative mycelium by the formation of phialidae. A technical advantage of microconidia is that they harbor just one single nucleus (Baylis and DeBusk, 1967). Hence, for genetic work it is possible to obtain homocaryotic strains with a single transformation. Their formation can be stimulated with iodoacetate (Rossier et al., 1973) but still the yield is low. Therefore, scientists

usually come back to using macroconidia for genetic modification by transformation. For the process of macroconidiation vegetative hyphae branch out growing vertically to so-called aerial hyphae. These form a multitude of branches themselves, which are finally compartmentalized first by minor, then by major constrictions. The result of this developmental program is distinct cells harboring 2-4 nuclei, the macroconidia. Scientists addressed the molecular biology behind this process in several studies and a number of genes, which are expressed in specific stages during asexual development, were identified and characterized (Berlin and Yanofsky, 1985; Roberts et al., 1989; Hager and Yanofsky, 1990). Factors that show a specific expression pattern during the course of asexual development include for example *aconidiate-2* (*acon-2*), a cyclic adenosinemonophosphate (cAMP) phosphodiesterase, *all development altered-7* (*ada-7*) and *conidial separation-1* (*csp-1*), which are transcription factors as well as several conidiation specific (*con*) genes. They all orchestrate a complex signaling network and seem to have a specific role during asexual development. Hence, knockout mutants of these factors are blocked in different stages of conidiation (Springer and Yanofsky,

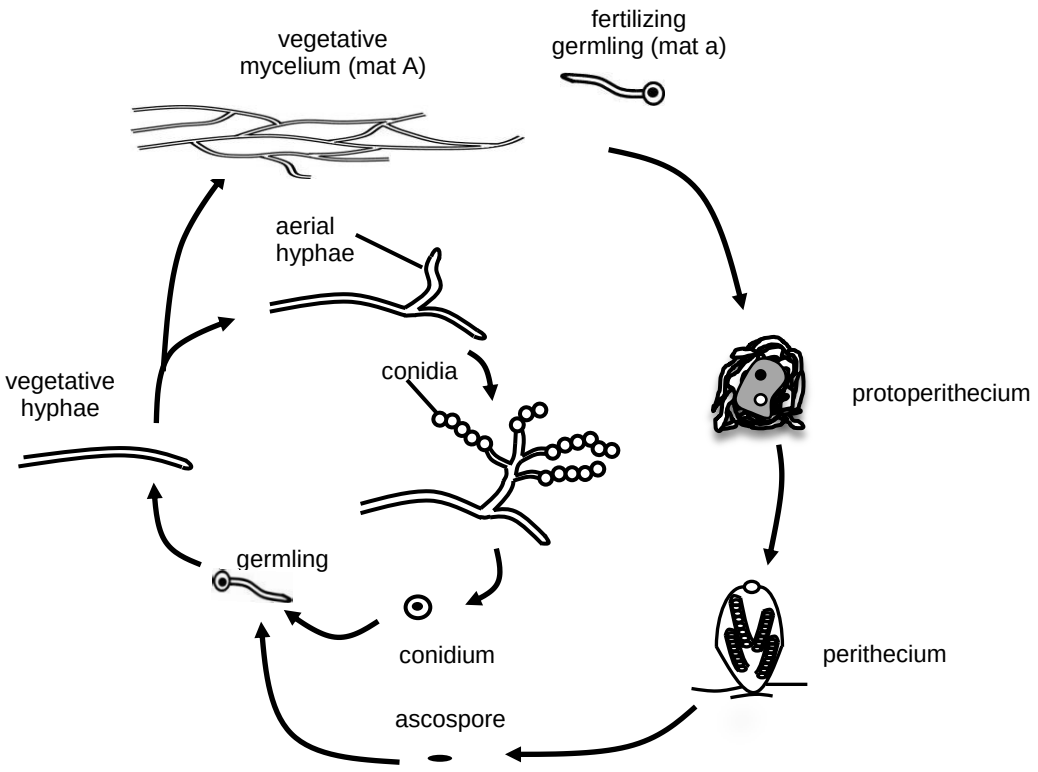

Figure 1: The sexual and asexual reproduction cycle of *N. crassa*
For description see text.

1989). The most prominent regulator in this context, however, is *fluffy*, which has been identified as a zink-finger transcription factor. Its expression is induced 6 h after onset of development and mutants are blocked during formation of major constrictions (Springer and Yanofsky, 1989; Bailey and Ebbole, 1998). Later studies showed that its expression is not only required but also sufficient to induce conidiation (Bailey-Shrode and Ebbole, 2004) and thereby clarified the role of *fluffy* as a major regulator of conidiation. It furthermore became of particular interest because it was shown that *fluffy* is a target of the circadian clock (Correa and Bell-Pedersen, 2002; Olmedo et al., 2010), providing a link to circadian growth. However, it has been shown that *fluffy* mutants still grow rhythmically (Correa and Bell-Pedersen, 2002).

Occurrence of sexual reproduction in contrast is more depending on environmental conditions. It is favored by poor nitrogen supply and fusion of two strains with the opposite mating type (mat A and mat a) is a prerequisite. Fertilization takes place either by fusion of vegetative hyphae or of a hypha with an asexual spore. Upon fertilization protoperithecia are formed, which carry several so-called croziers. Within these croziers nuclear fusion followed by meiotic divisions are taking place. Finally croziers develop to asci, which harbor a number of eight ascospores in a fully developed perithecium. Ascospores are eventually released into the air to find a substrate and germinate.

1.1.3 Carbohydrate metabolism and sensing

General metabolism of carbohydrates in *N. crassa* relies on the metabolic pathways, which are most highly conserved among higher eukaryotes. These are glycolysis, gluconeogenesis, the citric acid cycle and the pentose phosphate pathway. Hence, glucose as well as fructose and sucrose are easily fermentable carbon sources for *N. crassa,* but it can utilize a variety of sugars as carbon source with varying efficiency. Disaccharides and more complex carbohydrates are generally hydrolyzed by extracellular enzymes before the resulting monomeric sugars can enter the cell. Sucrose for example is cleaved into glucose and fructose by invertase. This enzyme seems to have a substantial role in growth on medium containing sucrose as a single carbon source, as a lack of invertase activity results in a severely reduced growth under

these conditions (Sargent and Woodward, 1969). The most abundant carbohydrate on earth, however, is cellulose. Under native conditions *N. crassa* is found growing in regions of burned vegetation and therefore is well adapted to utilization of cellulose. For this purpose it secretes a variety of enzymes, presumably cellulases and glycosyl-hydrolases, which degrade the cellulose to glucose. In numerous studies the identity of these secreted enzymes during growth on complex sugars like cellulose and even native substrates like *Miscanthus* was discovered by purification with subsequent sequence analysis and by mass spectrometry (Yazdi et al., 1990; Tian et al., 2009; Phillips et al., 2011).

The breakdown of mono- or disaccharides normally generates direct precursors for glycolysis or the pentose phosphate pathway. However, metabolism of more complex carbon sources like cellulose generally requires very specific sets of enzymes. This is necessary to make fermentation of complex substrates accessible to the aforementioned catabolic pathways. Expression of these enzymes is usually repressed during the presence of readily fermentable carbon sources. This mechanism is called “carbon catabolite repression” (CCR). It helps to restrict expression to genes which will guarantee a sufficient energy supply. Under carbon-rich conditions these are usually enzymes for fermentation of easily fermentable carbohydrates like glucose, fructose or sucrose. Under starvation conditions, however, a variety of genes become derepressed. In *S. cerevisiae* for example a shift to starvation conditions results in a severe transcriptional response inducing genes for utilization of alternative carbon sources (Wu et al., 2004). Abundance of multiple proteins is controlled by CCR including secreted enzymes like cellulases and other glycosyl-hydrolases, enzymes for utilization of alternative carbon sources and finally enzymes, which start degrading the intracellular reserve carbohydrates (Zink, 1967; Hanks and Sussman, 1969; Flavell and Woodward, 1971). In *N. crassa* one regulator of CCR is CELLULOLYTIC REGULON-1 (CRE-1), a C_2H_2-type zinc-finger transcription factor, which has been shown to be involved in repression of genes coding for cellulolytic enzymes (Sun and Glass, 2011; Znameroski et al., 2012). Unfortunately, a detailed mechanism about the sensing of carbohydrate abundance is still missing for *N. crassa*. In yeast as well as in other filamentous fungi it

has been reported that G-protein coupled receptors, RAT SARCOMA (RAS), cAMP and PROTEIN KINASE A (PKA) signaling seem to be involved in glucose sensing (Dong et al., 1995; Wang et al., 2004). Several studies show interdependency between substrate abundance, enzyme (cellulase) production and the activity of the aforementioned signaling factors (Dong et al., 1995; Wang et al., 2004; Schmoll et al., 2009; Schuster et al., 2012). Additionally phosphorylation of glucose may be important for sensing the intracellular carbohydrate status as double-knockouts of hexokinase and glucokinase resulted in a decreased activation of RAS signaling in *S. cerevisiae* (Colombo et al., 2004). However, a dedicated sensor protein for intra- or extracellular carbohydrate levels has not been identified so far. REGULATOR OF CONIDIATION-3 (RCO-3), a protein with high similarity to a glucose transporter in *S. cerevisiae*, has been suggested to have a role as a glucose sensor for *N. crassa* (Madi et al., 1997). However, so far this hypothesis lacks further evidence. In fact another important mechanism to respond to extracellular carbon supply may be the regulation of carbohydrate transporters. These may also transport disaccharides like cellobiose, a direct product of cellulose degradation (Tian et al., 2009). These observations implicate, that (I) a complex substrate does not necessarily have to be digested to monomers in the extracellular space to serve as a nutrient and (II) other carbohydrates than glucose may as well act as signaling molecules for the nutrient status.

1.1.4 Circadian clocks and the clock of *Neurospora crassa*

Circadian clocks are molecular systems that drive the expression of clock controlled genes (*ccgs)* depending on the time of the day. They can be found in organisms across all kingdoms ranging from archaebacteria to mammals. Circadian clocks entrain to and anticipate environmental changes like day and night rhythms or nutrient supply. These rhythmic cues provide an important input for the circadian clock as they are needed for its synchronization. Therefore they are called “zeitgeber”. The basic principle of circadian clocks is highly conserved: different zeitgebers entrain and synchronize an oscillator consisting of an interdependent negative feedback loop with a positive and one or more negative element(s). The positive element is a transcription factor, controlling expression of its own repressors, the negative elements. This

interdependency results in an oscillating activity of the transcription factor and, hence, expression of target genes. This will have a major influence on several output pathways like e.g. metabolism, development or stress resistance. Thereby circadian clocks enable the cell to adapt its molecular physiology to environmental changes and challenges before they actually occur. This behavior may finally increase the fitness of the organism. Several microarray studies in different eukaryotic model organisms found up to 10% of the analyzed transcripts to be rhythmically expressed (Harmer et al., 2000; McDonald and Rosbash, 2001; Storch et al., 2002; Koike et al., 2013; Hurley et al., 2014). Furthermore by controlling expression of transcription factors and repressors circadian clocks have an influence on gene expression over several levels of transcriptional hierarchy (Sancar et al., 2011). These findings point out that circadian clocks may have a substantial impact on an organisms transcriptome. One further general hallmark of circadian clocks is their so-called self-sustainability: even under constant conditions without application of a zeitgeber they are still able to possess and maintain a constant circadian rhythm with a characteristic endogenous period-length. The word “circadian” refers to the fact that this period-length is always found close to the 24 h diurnal rhythm (circa = about, dies = day). The endogenous period length for *N. crassa* is approximately 22.5 h.

The circadian clock of *N. crassa* consists of positive and negative elements, which generate an oscillating feedback loop to drive rhythmic expression of *ccgs* (figure 2). The positive element is a GATA-type zinc finger transcription factor complex, the White Collar Complex (WCC), which directly regulates the expression of *ccg´s*. WCC itself is a heterodimer consisting of the transcription factors WHITE COLLAR 1 (WC-1) and WHITE COLLAR 2 (WC-2). In the nucleus they interact with each other over so-called Per-Arnt-Sim (PAS) domains (Ballario et al., 1998). Interaction with the DNA is in both, WC-1 and WC-2, mediated by a zinc-finger motif (Linden and Macino, 1997; Ballario et al., 1996). Beside its function as a transcription factor the WCC is also a blue light receptor, which couples light input to the circadian clock. For light activation the LOV domain in WC-1 is essential (He et al., 2002). Upon light irradiation a bound Flavin adenine dinucleotide (FAD) cofactor forms a photoadduct with a cysteine residue of the

LOV domain, which enables light-driven dimerization of WCC (Mahlzahn and Ciprianidis et al., 2010). Together they form a light complex, which specifically enhances the expression of light-activated genes. Constant light leads to a permanent activation of WCC which will prevent rhythmicity of the circadian clock. Circadian rhythms can also be entrained by rhythmic temperature changes (Liu et al., 1997). As temperature critically affects reaction kinetics of molecular interactions one would expect a faster clock and, hence, a shorter period-length at higher temperature. The opposite should be true for lower temperatures. However, the period-length remains stable within a defined range of temperatures. This phenomenon is called temperature compensation. It is a general hallmark of circadian clocks and its discovery goes back to the early years of circadian research (Pittendrigh et al., 1959; Enright, 1967; Zimmerman et al., 1968).

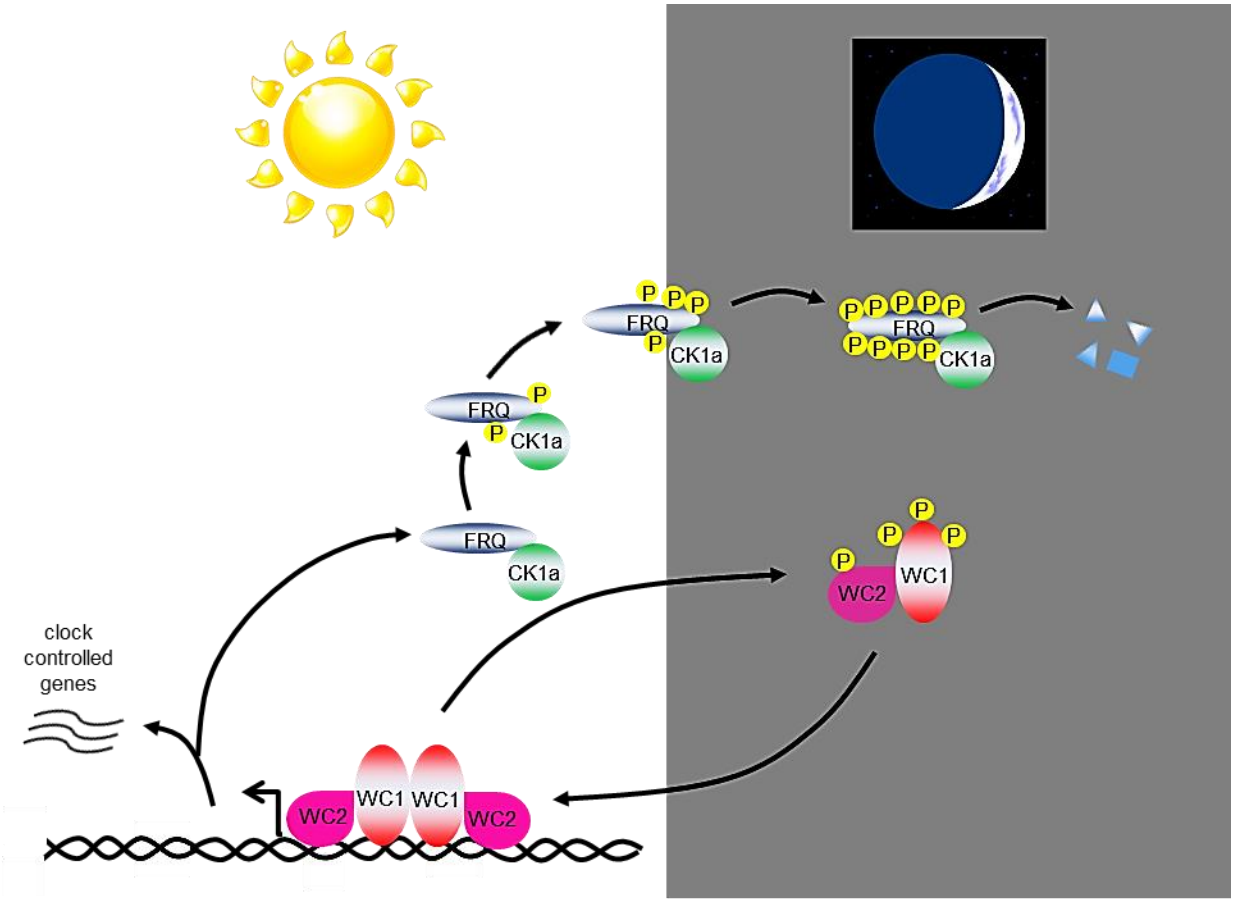

Figure 2: A molecular model of the circadian clock in *Neurospora crassa*

For description see text.

The FREQUENCY (FRQ) protein represents the negative element in the circadian clock of *N. crassa*. Its expression is controlled by rhythmic and light-dependent binding of the WCC to a clock box (C box) and a light-responsive element (LRE) in the *frequency* promoter, respectively (Froehlich et al., 2002, Froehlich et al., 2003). It is interacting with CASEIN KINASE 1a (CK1a) (Görl et al., 2001). The interaction as well as a nuclear localization signal (NSL) of FRQ targets the kinase to the nucleus. CK1a promotes the phosphorylation of WCC (Querfurth et al., 2007). This results in a FRQ-dependent inactivation of WCC and its translocation to the cytoplasm (Schafmeier et al., 2005; Schafmeier et al., 2008). FRQ itself becomes heavily phosphorylated over the course of a circadian day (Garceau et al., 1997; Liu et al., 2000). This process essentially depends on CK1a activity. Hyperphosphorylated FRQ shows reduced ability to enter the nucleus and will finally be degraded in the cytosol (Querfurth et al., 2011). A reduced FRQ abundance eventually results in reactivation of the WCC by dephosphorylation. This is mediated by PROTEIN PHOSPHATASE 2A (PP2A) (Schafmeier et al., 2005) in contrast to PROTEIN PHOSPHATASE 1 (PP1), which rather dephosphorylates FRQ (Yang et al., 2004). The timing of phosphorylations is critical for the period length of the circadian clock (Liu et al., 2000). Hence, a model has been suggested in which these posttranslational modifications and their consequences are the result of equilibrium between kinase and phosphatase activities (Schafmeier et al., 2008).

As already mentioned the circadian clock serves to control several output pathways. However, in *Neurospora* the most prominent physiological properties, which are under clock control, are growth and asexual development. This can be well observed during unidirectional growth. In constant darkness or under L/D entrainment a phase of vegetative growth alternates with asexual spore development in a circadian manner. For *Neurospora* this phenomenon has first been described by Wiliam H. Brand (Brand, 1953). Later in 1959 Pittendrigh and colleagues were the first who observed that this alternation follows a circadian rhythm and thereby related it to the circadian clock (Pittendrigh et al., 1959). Furthermore, the results of this study already implicate two general hallmarks of the *N. crassa* circadian clock, namely its light sensitivity and temperature compensation, as mentioned before. As scientists now had an easily

assessable output to study the circadian clock, the so-called “racetube-assay” was developed and became a standard in circadian research with *Neurospora* (figure 3). It allows unidirectional growth by filling glass tubes with a solid substrate and inoculating them with conidia on one end. *Neurospora* will now grow in the tube until it will reach the other end. The change of vegetative growth to asexual development can easily be analyzed by densitometry as conidia appear as a dense orange area in the tube, the so-called “*band*” (*bd*). The rhythmic appearance of these bands can be related to the circadian day by simply putting marks at the growth front every 24 h. This procedure allows an easy evaluation of changes in period-length or phase shifts in mutants or on different media for example.

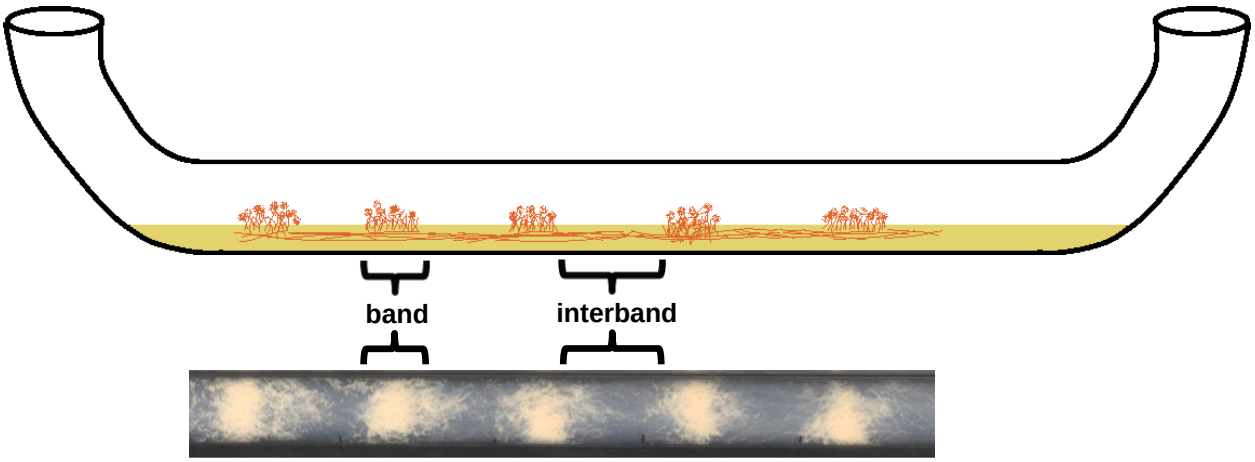

Figure 3: *Neurospora crassa* grows rhythmic during unidirectional growth in race tubes
For description see text.

1.2 Trehalose – a versatile sugar molecule

1.2.1 Biosynthesis and metabolism of trehalose

Trehalose is a disaccharide which consists of two glucose moieties (figure 4). Due to its α,α-1.1-glycosidic bond it has a non-reducing nature. In the past it has been connected to a variety of biological processes. Furthermore, it can be found in a variety of organisms from bacteria to fungi, plants and invertebrate animals (for review see Elbein, 1974). With this broad spectrum of organisms different ways for trehalose biosynthesis evolved. A very common mechanism uses the intermediate trehalose-6-phosphate (T6P). This is generated by TREHALOSE-6-PHOSPHATE SYNTHASE (TPS) from UDP-glucose and glucose-6-phosphate as substrates. T6P is subsequently dephosphorylated by TREHALOSE-6-PHOSPHATE PHOSPHATASE (TPP) to yield trehalose (Cabib and Leloir, 1958). This mechanism is found in bacteria (e.g. *E. coli*), plants *(*e.g. *A. thaliana)*, fungi (e.g. *S. cerevisiae*) and insects (Cabib and Leloir, 1958; Candy and Kilby, 1959; Giæver et al., 1988; Kaasen et al., 1992; Vogel et al., 1998; Blazquez et al, 1998). Trehalose can further be synthesized by TREHALOSE PHOSPHORYLASE (TreP). For this reaction TreP uses glucose-1-phosphate and glucose as substrates. As the name of the enzyme implicates it can also catalyze the

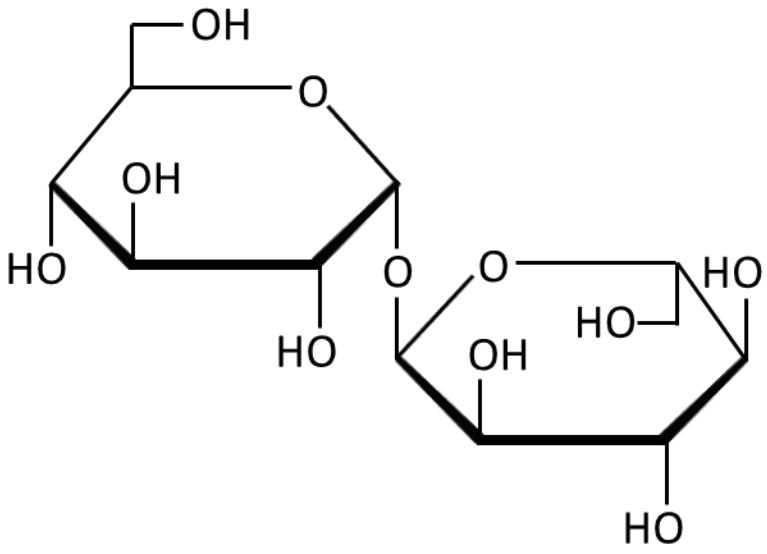

Figure 4: α, α-Trehalose

reverse reaction. TreP can also cleave trehalose in the presence of inorganic phosphate (Belocopitow and Marechal, 1971; Wannet et al., 1998). This pathway has been found in fungi, bacteria and protists. In addition to the aforementioned ways of trehalose biosynthesis some bacteria can generate trehalose by using ADP-glucose and glucose or by converting maltose or maltooligosaccharides (Nishimoto et al., 1996; Maruta et al., 1996; Qu et al., 2004). The *N. crassa* genome contains three genes coding for two putative trehalose-phosphate synthases (NCU09715 and NCU00793) as well as one trehalose-phosphatase (NCU05041). The protein sequences show high homology to the respective trehalose synthase complex in yeast. However, despite the fact that this complex has been well-characterized in yeast during the recent decades, in *Neurospora* little is known about it. In *N. crassa clock controlled gene-9* (*ccg-9*) has been suggested to be a trehalose synthase. Inactivation of *ccg-9* has been reported to result in severe growth and sporulation defects (Shinohara et al., 2002).

The degradation of trehalose is mainly catalyzed by trehalases. The reaction is a simple hydrolysis of the glycosidic bond, which releases two glucose molecules. Hence, trehalases belong to the class of α-glucosidases. In fungi it is commonly differentiated between two types of trehalases depending on their pH-optimum, namely acid and neutral trehalases. While neutral trehalases are regulated by cAMP signaling and rather participate in intracellular breakdown of trehalose, acid trehalases localize to vesicles and cell membranes, are not regulated by cAMP and involved in degradation of extracellular breakdown of trehalose (Thevelein, 1984). Surprisingly trehalases have also been detected in mammals in contrast to their biosynthetic counterparts (Yoneyama and Lever, 1988). In *N. crassa* Sussaman and colleagues isolated mutants that were unable to grow on medium containing trehalose as the sole carbon source in the early 1970´s (Sussmann et al., 1971). Later one gene coding for trehalase was mapped to linkage group one in the *N. crassa* genome (White et al., 1985). Today it is known that the *N. crassa* genome codes for two trehalases: one neutral trehalase (NCU04221), that is Ca^{2+} dependent and can be activated by cAMP and an aforementioned acid trehalase (NCU00943) (dÉnfert et al., 1999).

1.2.2 Biological functions of trehalose

Trehalose is a reserve carbohydrate in fungi

The most prominent function that has been attributed to trehalose is its role as a reserve carbohydrate. In the 1950´s and in the following years trehalose was found as a major reserve carbohydrate in spores of different fungi (Sussman and Lingappa, 1959; Mandels et al., 1965). The same studies already indicated that it is rapidly consumed during germination or after exposure to stress as confirmed in a variety of studies using different model organisms. Moreover, in *Saccharomyces cerevisiae* it was demonstrated that the consumption of trehalose is critical for fueling the cell cycle upon exit of cellular quiescence (Shi et al., 2010). Furthermore, the authors of the same study found, that trehalose is preferentially metabolized over other reserve carbohydrates like glycogen upon entry into an active cell cycle. These findings connected trehalose to cell cycle control and suggested it as a potential growth regulator.

Trehalose and/or derivatives may be growth regulators and signaling molecules

In fungi first implications of trehalose or rather its close relative trehalose-6-phosphate (T6P) playing a role in growth came from studies with *S. cervisiae*. It was found that mutants lacking T6P synthase were unable to grow on glucose as a single carbon source (Van Aelst et al., 1993). This finding raised the hypothesis that trehalose may be involved either in the uptake, the sensing of glucose or it may participate in the regulation of the glycolytic flux (Thevelein and Hohmann, 1995). In fact it had been demonstrated that in yeast T6P regulates glycolysis by competitive inhibition of hexokinase, the enzyme that catalyzes a very initial step of glucose breakdown by converting glucose to glucose-6-phosphate (Blazquez et al., 1993). However, the physiological relevance of this mechanism remains controversial. It was argued that T6P may be converted to trehalose immediately due the close proximity of the enzymes (TPS and TPP) in the complex. Hence, the effective cytosolic concentration of T6P may be far too low for outcompeting the glucose in the hexokinase (Thevelein and Hohmann, 1995). Furthermore, in plants it has been demonstrated that T6P has a key role in embryonic development, vegetative growth and transition to flowering (Eastmond et al., 2002; van Dijken et al., 2004). In a recent study the presence of TPS1 and T6P were

connected to transcription factor signaling during the flowering process (Wahl et al., 2013). These findings point out the role of T6P as a signaling molecule in *A. thaliana*.

Role of Trehalose as a potent stress protectant

In several studies and model organisms trehalose has been shown to be important to cope with various forms of environmental stress. Already in the 1960´s trehalose has been detected in insects as a part of the haemolyphatic system (Tanno, 1964; Sømme, 1967; Ring, 1977). There it is thought to protect from frost during cold periods together with other compounds like glycerol or mannitol (for review see Sømme, 1982). A similar function has been suggested in *E. coli* as mutants defective in trehalose biosynthesis were found to have a decreased resistance to low temperatures (Kandror et al., 2002). In various microorganisms like *E. coli* and *S. cerevisiae* an increased intracellular trehalose concentration has been associated with protection against heat shock, desiccation, and osmotic stress (Hottiger et al., 1987; Giæver et al., 1988; De Virgilio et al., 1994). Furthermore, the stress changes transcription of trehalose biosynthetic enzymes. Subunits of the trehalose synthase complex in yeast are induced during heat shock (Bell et al., 1992). These results suggest that eukaryotes actively use trehalose biosynthesis to increase their stress resistance. How trehalose acts as a stress protectant on a molecular level is not fully understood so far. In case of a dehydrated environment the cell suffers from fusion and phase transitions of lipids as well as protein denaturation. Similar processes may play a role during heat shock or osmotic stress. However, by X-ray diffraction and infrared spectroscopy trehalose has been shown to stabilize the lipid bilayer as well as protein conformations. The stereochemistry of trehalose and its ability to substitute for water by providing hydrogen bonds seem to play a central role in these processes (Carpenter and Crowe, 1989; Rudolph et al., 1990; Allison et al., 1999).

1.3 The aim of this study

The aim of this study was to test, whether rhythmic growth may be the result of a global clock control on physiological processes like cell cycle or metabolism. It is a very fascinating phenomenon that the circadian clock in *Neurospora crassa* provides a rhythmic switch between vegetative growth and asexual development. Analysis of the kinetics of biomass production during rhythmic growth and have revealed that it follows a circadian rhythm as well (Castro-Longoria et al., 2007). These findings implicate that *Neurospora* does not simply shift between two developmental programs but also its cellular physiology should be in accordance with these rhythms of biomass production. In a first approach it was postulated that circadian rhythmicity of growth may base on a clock controlled cell cycle. To test this hypothesis, expression profiles of genes that were assumed to participate in or reflect cell cycle activity were measured by a luciferase activity assay. However, due to contradictory results, the experimental conditions apparently did not suffice to draw clear conclusions. Therefore, an alternative concept was developed. Rhythmic biomass production could as well be the result of clock control over metabolism. In yeast for example ultradian metabolic cycles have been associated with periodic growth phases (Tu et al., 2005). For this hypothesis the abundance of reserve carbohydrates was assumed to define a good measure as they should be representative for the homeostasis between anabolic and catabolic processes in the cell. Furthermore, *clock controlled gene-9* (*ccg-9*) had been suggested to be a trehalose synthase and a mutant with a non-functional allele not only displayed severe defects in growth and development but also grew arrhythmic (Shinohara et al., 2002). Taken together, these observations suggested that metabolism and especially reserve carbohydrates may play a role in mediating a clock signal towards rhythmic growth and *ccg-9* seemed to be a good candidate gene for this study.

2 Results

2.1 Studies with a luciferase based reporter assay in *N. crassa*

2.1.1 Entrainment increases rhythmicity of growth related genes

As mentioned before circadian growth is accompanied with a rhythmicity of biomass formation (Castro-Longoria et al., 2007). This implies that the circadian clock may have an influence on fundamental processes like the cell cycle which regulate cellular growth. Circadian expression of cell cycle related genes would strongly support this hypothesis. Hence, a selection of candidate genes was tested for rhythmic expression with a luciferase based reporter assay. Among them were cell cycle related genes that have been found in close proximity to a WCC binding site in the promoter e.g. *cyclinB3* (NCU01242) (Smith et al., 2010). Unbiased control genes without a WCC binding site but with a relation to growth or cell cycle progression such as *tubulin* and *histoneH1* were selected. If the circadian clock controls growth or cell cycle, these genes should show rhythmic expression even without being direct target genes of the WCC.

To test rhythmicity of target genes, their promoters were cloned in front of the firefly luciferase gene as has been reported before (Gooch et al., 2008). Luciferase activity was recorded after synchronizing the clock with a 2 h light pulse. A stable and clear rhythm was detected in the p*frq*::*luc* strain which served as a positive control. However, with the same synchronization scheme it was nearly impossible to observe rhythms in growth or cell cycle related reporter strains. And if there were any, they showed a very low amplitude and high noise due to fluctuations in signal intensity (figure 5). Interestingly the luciferase activity of these strains became clearly rhythmic when the cultures were entrained with a light / dark (12 h / 12 h) regime (LD) for 3.5 days before release to constant darkness (DD). As can be seen in figure 5, after LD entrainment

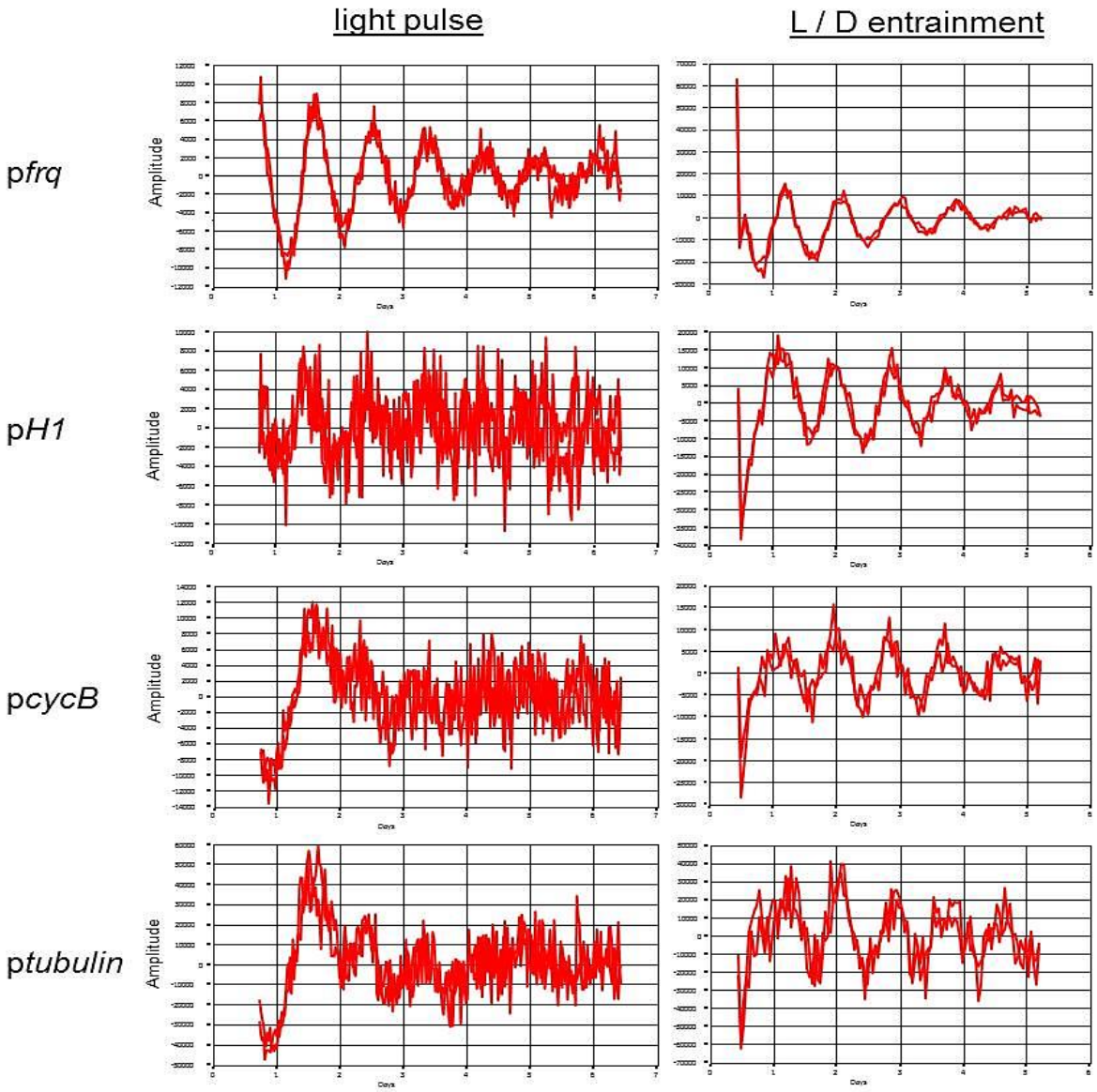

Figure 5: Entrainment for 3.5 days significantly increases rhythm quality

While growth and cell cycle related genes showed a noisy and low amplitude rhythm after light synchronization, the quality and amplitude clearly increased after 3.5 days of light / dark entrainment. The diagrams show two representative traces after detrending.

quality and amplitude of the rhythms increased remarkably. This also held true for reporters that are not shown in figure 5 like p*actin*::*luc* or p*apc11*::*luc*. However, in a *frq*^{10} background (*frq* knockout) no rhythmicity was observed at all. The improvement of circadian rhythms after entrainment was apparently independent of the presence of a WCC binding site in the promoter since p*H1*::*luc* and typical “housekeeping genes” like

p*tubulin*::*luc* showed the same phenomenon as p*cycB3*::*luc.* However, this observation was not always reproducible. Sometimes growth and cell cycle reporters showed poor or no rhythmicity at all even after 3.5 days entrainment. It was also observed that a reduction in entrainment time to 2.5 days for example was not sufficient to generate high quality and stable rhythms. Moreover, the phase response with respect to dark transfer was extremely unstable.

2.1.2 Stable and equiphase rhythms in race tube assays

To study the expression of selected target genes in the context of rhythmic growth a race tube assay with the aforementioned reporter strains was performed. Bioluminescence was recorded with a highly sensitive CCD camera during growth in DD. Again all reporter strains showed strong but equiphase rhythms (figure 6). The rhythms were stable over the complete duration of growth in the race tubes. In order to test whether the assay would display phase differences properly a p*desat*::*luc* strain was included. Expression of *desaturase* has been reported to be controlled by the transcriptional repressor *csp-1*, which itself is a direct target of WCC. This mechanism causes antiphasic gene expression of *csp-1* target genes compared to directly WCC controlled genes (Sancar et al., 2012). However, signal rhythmicity from the p*desat*::*luc* reporter strain was in phase with rhythms generated with other reporters. Interestingly, luciferase activity in the p*frq*::*luc* strain strongly localized to asexual structures (in the “band”) and remained there for several days. A slight rhythmicity could be observed but it was in phase with others as well. Taken together, these results suggested that the reporter assay may not reflect promoter activity under the applied experimental conditions.

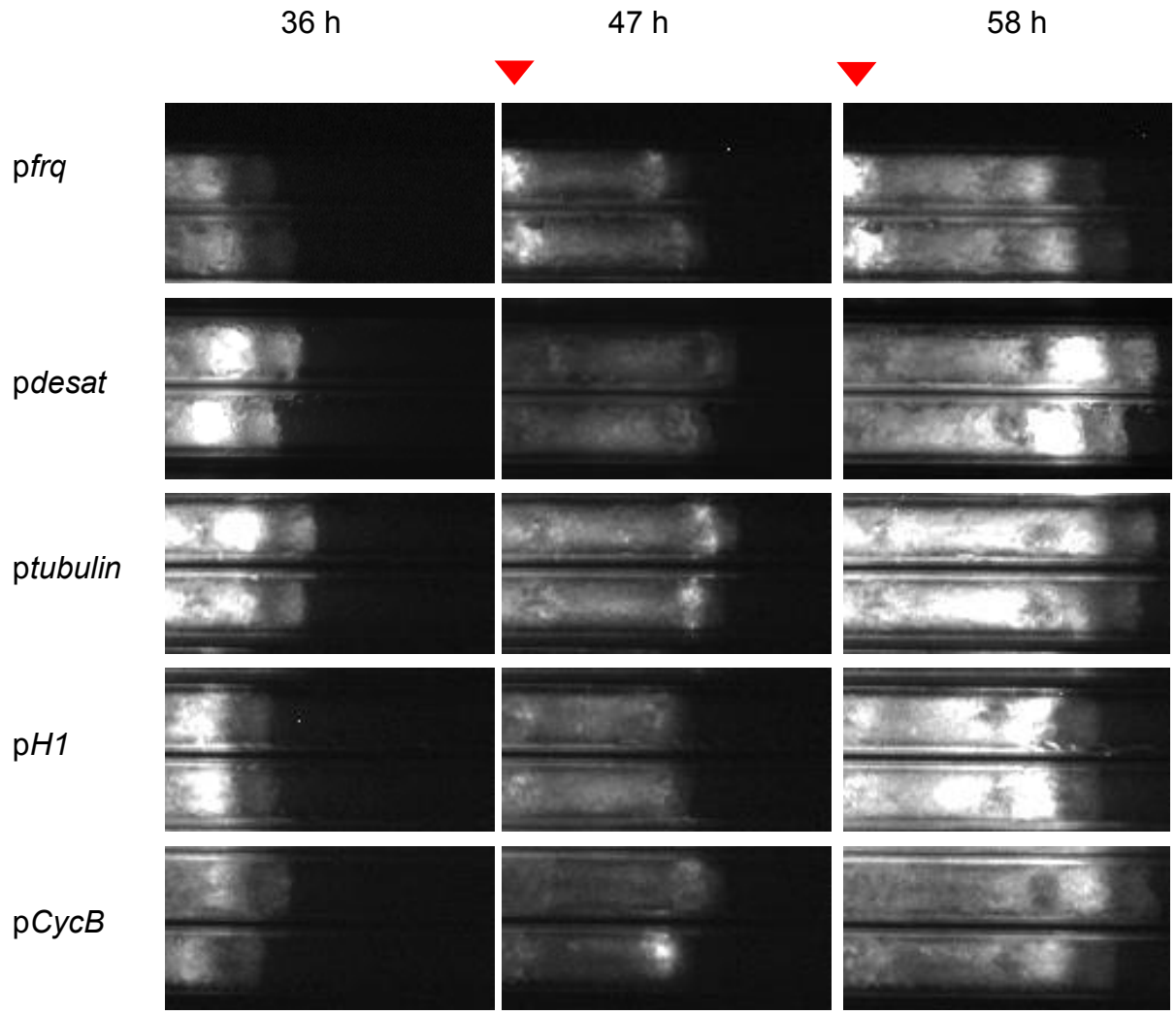

Figure 6: Luminescence signals from different reporters are equiphase during growth in race tubes

Images show the luminescence signal of the respective reporter strain growing in two race tubes with a delay of 11 hours. Please note the stable luminescence signal in the conidial band in the p*frq*::*luc* reporter (red arrows).

2.1.3 Phase synchronization of aged cultures in 96-well plate assays

In the 96-well plate assay asexual development is inhibited by adding 2% sorbose to the medium. This is important in order to prevent early formation of conidia in the well. As conidia are metabolically inactive they do not give any luciferase signal and would severely disturb the assay. In race tube experiments asexual development is possible. The conidia can be seen as a shadow in the images (figure 6). The previous

experiments suggested that the luciferase assay may be biased by asexual development. To test this hypothesis aged cultures previously entrained for 3.5 days and grown in dark for further 5 days were subjected to resynchronization by a 1 h light pulse. This was the time when asexual development became visible as the formation of aerial hyphae in the wells. Interestingly, the light pulse was now sufficient to drive high amplitude rhythms in reporter strains for growth and cell cycle related genes like p*cycB*::*luc* (figure 7). Furthermore, a shift in the relative phase response between p*frq*::*luc* and p*desat*::*luc* was detectable. Compared with young cultures the phase difference between both seemed to be smaller. In experiments with higher glucose concentration in the medium even a global synchronization could be observed after some days of free running in DD (figure 8). However, these rhythms rather had a shape of a pulse instead of a sine wave. The observations in the 96-well format phenomenologically related to what has been observed before in race tubes. Under the

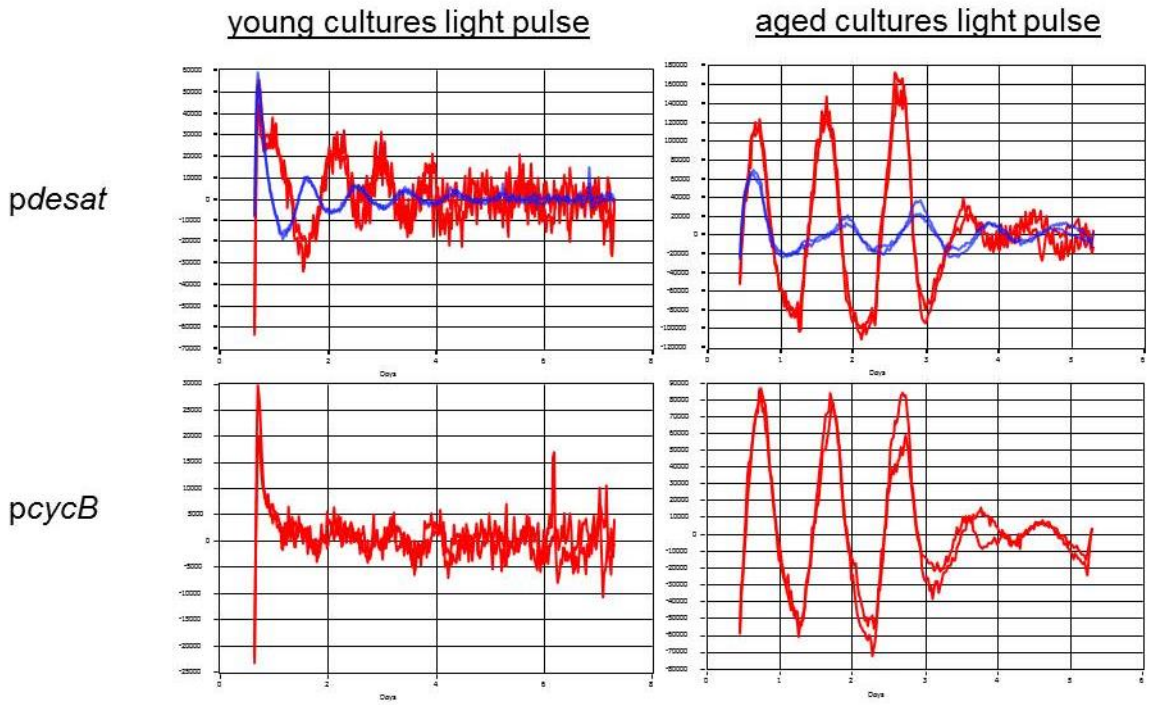

Figure 7: In aged cultures a light pulse is sufficient to drive high amplitude rhythms

Growth and cell cycle reporters showed dampened and low amplitude rhythms in young cultures after light pulse synchronization (left panel). However, the same synchronization scheme caused clear and high amplitude rhythms but also phase shifts between p*frq*:*luc* and p*desat*:*luc* in approx. eight-day-old cultures. Each graph shows two representative traces of the respective reporter. Traces of p*frq*:*luc* are shown in blue for phase comparison.

described conditions both assays shared the asexual development as a common feature. Therefore, it was concluded, that this may be the key to the aforementioned observations.

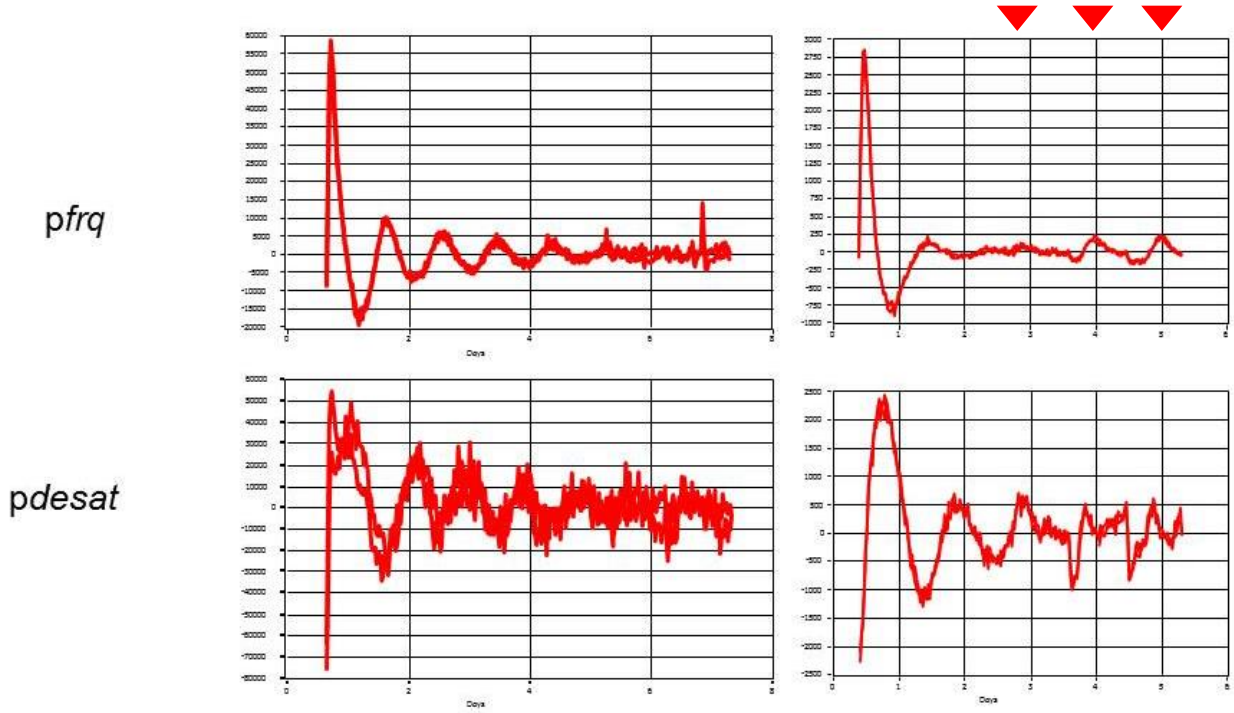

Figure 8: Higher glucose concentrations synchronize *frequency* and *desaturase* rhythms

While p*frq::luc* and *desat*::*luc* reported antiphasic rhythms under standard conditions (0.025% glucose), synchronization was observed using high glucose media (0.5% glucose). The graphs show two representative traces from the respective reporter. Red arrows indicate beginning of coherency.

Taken together, circadian rhythms in growth or cell cycle reporters appeared under conditions which were permissive for asexual development. Furthermore, these conditions apparently synchronized the phase behavior of well-established and otherwise antiphasic reporters. These results suggest that asexual development may interfere with the assay by driving artificial rhythms. It could be possible that under conditions which allow unrestricted growth and asexual development the luciferase assay no longer reflects pure promoter activity of the reporter. Considering the origin of this project, which was investigating circadian control of growth and development, this otherwise very powerful technique was no longer useful under these conditions. Hence, the project was not pursued any longer.

2.2 Characterization of a *ccg-9*^{RIP} mutant strain

As mentioned before in a former study *ccg-9* had been identified as a trehalose synthase in *N. crassa*. Moreover, inactivation of *ccg-9* by repeat-induced point mutation (RIP) resulted in severe defects in vegetative growth and asexual development. For this thesis it was particularly interesting that the *ccg-9*^{RIP} mutant has been described to grow arrhythmic (Shinohara et al., 2002). The phenotypes related to *ccg-9* suggest that trehalose has an important role in regulation of vegetative and asexual development in *N. crassa*. Furthermore, it implicates that clock control over metabolism of reserve carbohydrates is critical to maintain the growth rhythm. In order to test this hypothesis, the *ccg-9* gene and its function as well as the aforementioned *ccg-9*^{RIP} strain should be analyzed in more detail.

2.2.1 Genomic characterization of *ccg-9*^{RIP}

To generate a RIP mutant a second copy of the gene of interest is introduced into the genome. Then the strain is crossed and during meiotic recombination a variety of nucleotide exchanges, mainly purines to pyrimidines, will eventually silence both copies by generating premature stop-codons. This process is most probably a defense mechanism against viral transposons. However, in *Neurospora* genetics it became useful to study genes by generating non-functional alleles. In order to characterize the *ccg-9* locus of the *ccg-9*^{RIP} mutant, PCR fragments were sent to sequencing. Indeed, an accumulation of nucleotide polymorphisms at the *ccg-9* locus was observed. Several of those were found to generate a stop-codon in the open reading frame. The one that has been localized closest to the 5´ end of the open reading frame is shown in figure 9. The premature termination of translation led to a truncated protein that lacks its entire

```
wt          CCCAACCCTCTGTTCGCGGCTCTGGCTCGAGGTGGATATTGTGCCCATCGTTATGCGCCC 480
ccg-9RIP    CCCAACCCTCTATTTACGGCTTTAGTTCGAGGTAGATATTGTACCTATCGTTATGCGTCT 397
            ***********.** .***** *.* *******.********.** *********** *
```

Figure 9: A stop codon generated by nucleotide exchanges in the *ccg-9* locus

catalytic domain and thereby was considered being non-functional with respect to trehalose biosynthesis.

2.2.2 Inducible expression of *ccg-9* does not affect growth rhythmicity

The most interesting phenotype of *ccg-9*^{RIP} for circadian research is its arrhythmic growth in constant darkness. Figure 10 shows the growth of *ccg-9*^{RIP} in comparison with the wild type (*frq*$^{+}$ *bd*) and a clock mutant that does not express any FRQ protein (*frq*^{10} *bd*). Not only vegetative growth was severely impaired in *ccg-9*^{RIP} but, very similar to the *frq*^{10} *bd* strain, it also did not show the circadian conidiation pattern as it occurred in the wild type. This result indicates that *ccg-9* either feeds back to the core oscillator or is critical for mediating a clock signal to rhythmic growth and development. As it had been demonstrated earlier the mutant showed rhythmic abundance and phosphorylation of FRQ protein (Shinohara et al., 2002). Furthermore, during the course of this study conditions were found under which the mutant exhibited a clearly visible and circadian growth pattern. These results make it very unlikely that a non-functional clock is the reason for the arrhythmic growth behavior of the *ccg-9*^{RIP} mutant.

Figure 10: Growth behavior of *ccg-9*^{RIP} in constant darkness

While the wild type (*frq*$^{+}$ *bd*) conidiated in a circadian fashion, *ccg-9*^{RIP} showed an arrhythmic conidiation pattern as well as the clock-null mutant *frq*^{10}. Vegetative growth was severely affected in *ccg-9*^{RIP}. This image shows growth for five days on standard race tube medium containing 0.1% glucose.

Furthermore it should be tested, whether circadian conidiation is linked to *ccg-9* expression. By gene replacement homocaryotic knockin strains were generated which expressed *ccg-9* under control of the *qa-2* promoter. The *qa-2* gene belongs to a gene cluster which is inducible by quinic acid and is responsible for its catabolism. In the knockin strains this promoter allowed conditional expression of N-terminally Flag-tagged CCG-9 protein upon addition of quinic acid to the medium. Sequence information that was available in the databases[1,2] predicted another translational start site for *ccg-9* compared to the literature (Shinohara et al., 2002). In order to not express a truncated and possibly less functional protein the knockin cassette was designed to drive expression of a long isoform. In fact Western Blots showed two inducible and Flag-specific signals which were detectable even without the inducer (figure 11 a). This is suboptimal because *ccg-9* expression itself was observed to be very low under standard growth conditions (see chapter 2.3). Hence, the residual activity of the *qa*-2 promoter might be sufficient to drive wild type levels of *ccg*-9 expression. Furthermore, as demonstrated with a native expressing p*ccg-9*::*ccg-9-Flag* knockin strain, the large isoform was just weakly expressed compared to the smaller one (figure 11 b). Analysis of the short isoform by mass spectrometry confirmed the start site predicted in the literature (see appendix figure S1). However, compared to the wild type a change in growth rhythmicity could be observed neither with nor without quinic acid added to the growth medium (figure 11 c). In liquid cultures *ccg*-9 was expressed approximately 6- to 50-fold over the wild type level after induction with quinic acid compared to 0.2- to 0.5-fold without the inducer. These results show that *ccg*-9 expression is inducible in the knockin strain and that induced expression of *ccg-9* does not change the growth behavior. This suggests that circadian growth does not depend on native *ccg-9* promoter activity. However, at this time point the leakage of the *qa-2* promoter as well as the possibility that native promoter activity could reside between the two translation initiation sites made a clear interpretation of the observations very difficult.

[1] http://www.broadinstitute.org/annotation/genome/neurospora/MultiHome.html
[2] http://www.ncbi.nlm.nih.gov/

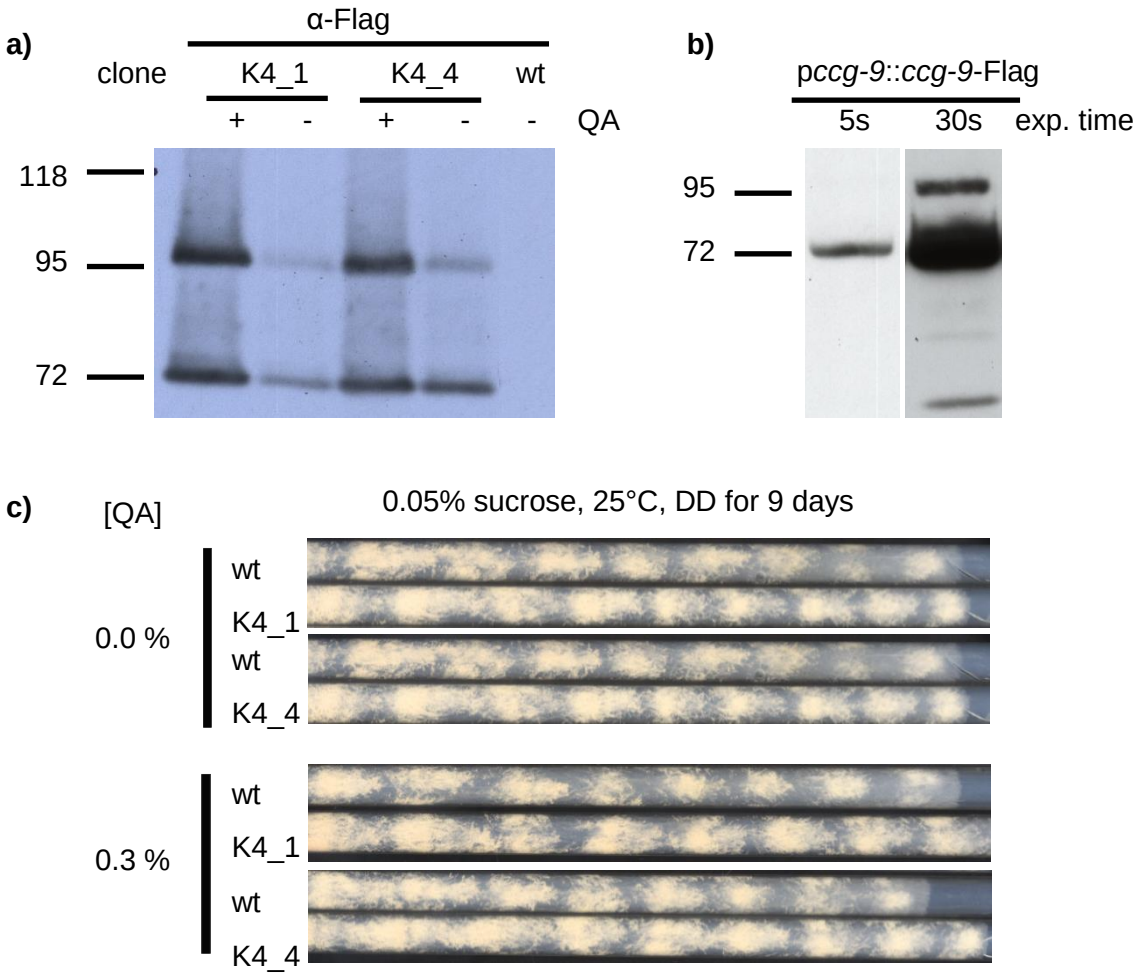

Figure 11: Inducible expression of *ccg-9* and its effect on growth rhythmicity

Homocaryotic strains (K4_1 and K4_4) were generated which allowed induction of *ccg-9* by addition of quinic acid (QA) to the medium **(a)**. From the two isoforms observed in these knockin strains the large one showed low abundance under native expression conditions **(b)**. Growth rhythmicity was comparable to the wild type (wt) under inducing (0.3% QA) and non-inducing (0.0% QA) conditions **(c)**.

2.2.3 Nutrient dependency and growth behavior of *ccg-9^{RIP}*

Nutrient dependency of vegetative growth behavior

In addition to its clock phenotype *ccg-9^{RIP}* displayed a severe defect in vegetative and asexual development. In yeast impaired trehalose metabolism had been associated with growth defects on glucose containing media and the regulation of the glycolytic flux on the level of hexokinase (Van Aelst et al., 1993; Blazquez et al., 1993; compare chapter 1.2.2). These results suggest a role for trehalose in carbon source sensing and

fermentation. Similar mechanisms might lead to the growth defect of *ccg-9*^{RIP}. Hence, it was tested whether the growth defect of the *ccg-9*^{RIP} mutant persists on media containing alternative carbon sources which partially or completely bypass glycolysis as the major route of carbon source catabolism. To exclude starvation effects due to low fermentation efficiency higher carbon source concentrations were used compared to standard conditions. As the results show the *ccg-9*^{RIP} mutant retained its phenotype on different carbon sources (figure 12). Sucrose containing medium is shown as an easily fermentable sugar for comparison. Even though slight variations could be observed the

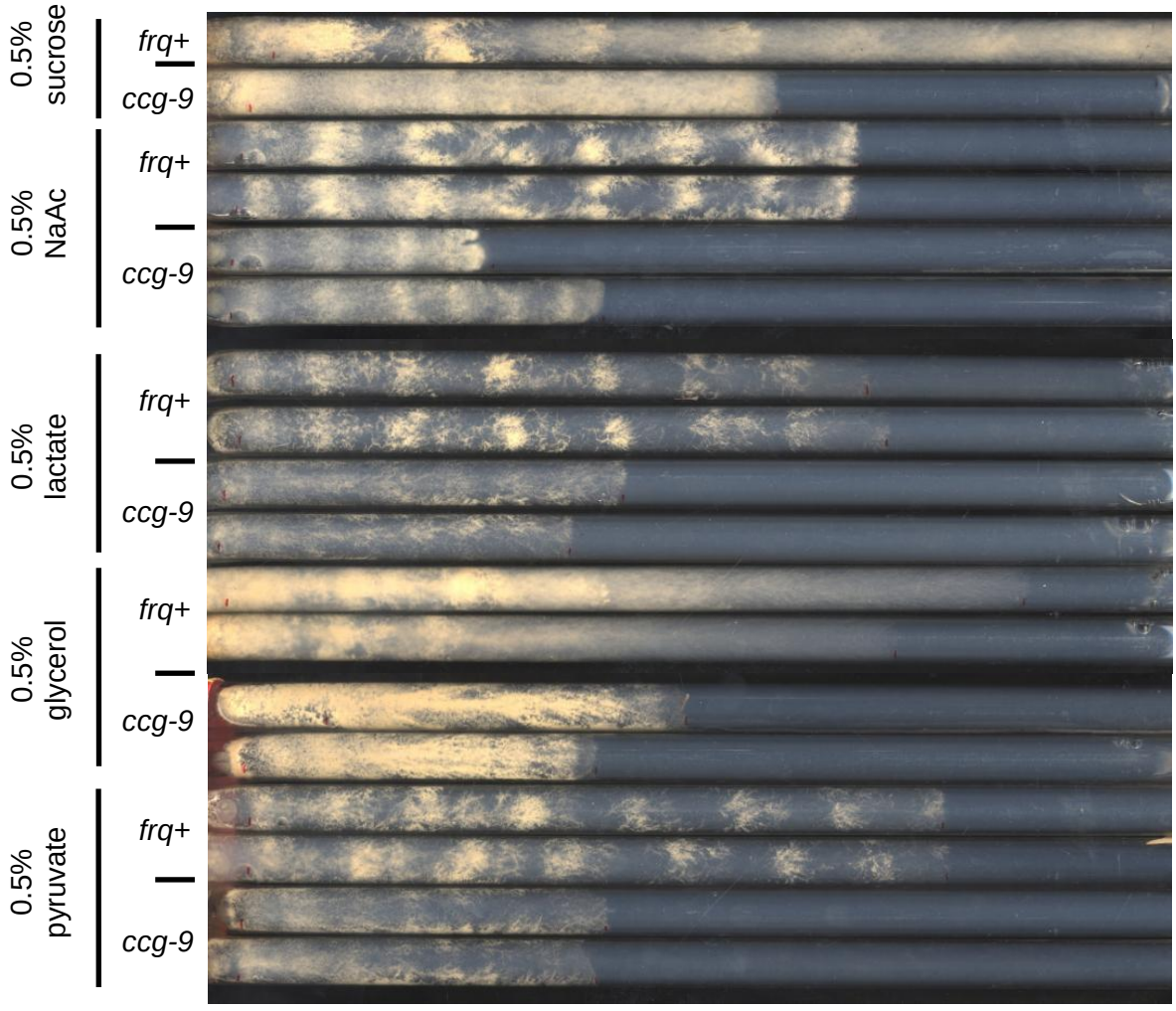

Figure 12: The phenotype of *ccg-9*^{RIP} persists on different carbon sources

To test, whether the phenotype of *ccg-9*^{RIP} was caused by a (partial) block in glycolysis, growth was compared on carbon sources which bypass glycolysis partially (glycerol) or completely (acetate, lactate and pyruvate). Race tubes were grown in constant darkness for seven days. Sucrose, which completely relies on glycolytic fermentation, is shown for comparison.

mutant always showed approximately half the growth rate of the wild type and poor asexual development. The same held true for medium containing trehalose as a carbon source. This was expected because due to secretion of trehalases trehalose was probably degraded to glucose in the extracellular space (Thevelein, 1984). In later experiments a severe misregulation of genes encoding enzymes and transporters for nitrogen and phosphate assimilation was observed. However, even in rich media supplemented with casamino acids as well as arginine and glutamine as donors for amino moieties *ccg-9*^{RIP} displayed the typical defects in vegetative growth and asexual development (figure 13). The same held true for high phosphate media. Together, these results suggest that the phenotype of the mutant is at least not exclusively caused by insufficient primary assimilation of carbon, nitrogen or phosphate sources. Interestingly, under starvation conditions a clear conidiation rhythm was observed. This was visible under low-phosphate conditions or with DNA as a poor phosphate source (figure 14). A similar observation was made before with medium containing acetate which can be

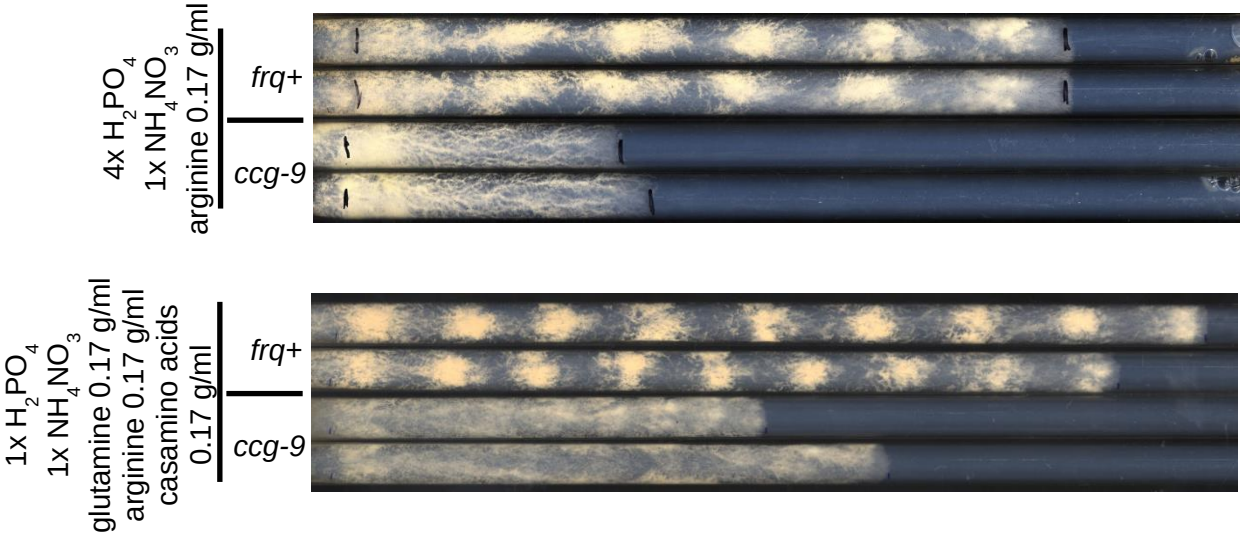

Figure 13: Supplementation of media with phosphate or amino acids does not rescue the phenotype of *ccg-9*^{RIP}

The images show race tube experiments with 4x phosphate concentration (20 mg / ml, top) compared to standard Vogel´s medium or on medium supplemented with amino acids as donors for amino moieties (bottom).

seen as a rather poor carbon source (figure 12). These results show that the circadian clock is functional in the *ccg-9*^{RIP} background and that the growth arrhythmicity of this mutant may be a consequence of nutritive effects. Furthermore, it suggests that *ccg-9* is not necessary to control circadian growth supporting the previous findings.

Figure 14: Poor phosphate conditions reconstitute the growth rhythmicity in *ccg-9*^{RIP}

The image shows representative race tube experiments using media with either low phosphate content or 0.05% DNA as a poor phosphate source. Cultures were grown in constant darkness for at least seven days.

2.2.4 Glucose dependency of asexual development

The previous experiments rather showed nutritive effects on vegetative growth but not essentially on asexual development. However, the latter can be much more sensitive to nutritional changes in the environment. Furthermore, if trehalose is a carbohydrate sensor it should enable the organism to discriminate between different sugar concentrations in the substrate. Hence, for *ccg-9*^{RIP} and the wild type the formation of conidia in response to different glucose concentrations was quantified by photodensitometry. This was done by harvesting conidia from the race tubes after four days of growth in constant light. Regardless of the glucose concentration in *ccg-9*^{RIP} the total amount of conidia was always lower compared to the wild type (figure 15). However, the mutant showed mainly the same response to increased glucose concentrations as the wild type did. The fold change normalized to the lowest concentration behaved the same except a minimal but significant difference at 1%

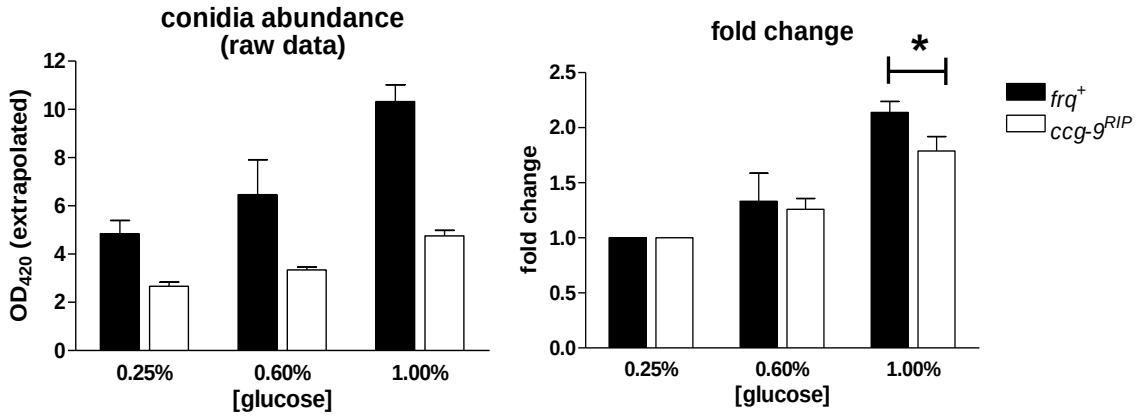

Figure 15: The *ccg-9*^{RIP} mutant shows reduced conidiation but a similar glucose response as the wild type in race tubes

Even though the total amount of conidia is decreased in *ccg-9*^{RIP} the fold change normalized to the lowest glucose concentration is similar to the wild type strain. Error bars show the standard deviation of the mean (n=3). Significance was calculated with a two-way ANOVA test.

glucose. These results show that *ccg-9*^{RIP}, even though it has a general defect in conidiation, is generally able to sense different glucose concentrations in the medium.

To summarize these experiments it was observed that *ccg-9*^{RIP} showed a general defect in vegetative growth and formation of asexual spores as it has been described before (Shinohara et al., 2002). However, these growth defects could neither be rescued on substrates containing different carbon sources, nor with supplementing alternative nitrogen or phosphate sources. Furthermore, *ccg-9*^{RIP} was still able to respond to different glucose concentrations in the medium. Together, these results suggest that impaired carbon, nitrogen or phosphate assimilation are not the major reason for the *ccg-9*^{RIP} phenotype and that the mutant can at least sense different concentrations of simple carbohydrates in the substrate.

2.2.5 Transcriptome analysis of *ccg-9*^{RIP} during asexual development

In the past *ccg-9* has been found to be induced during asexual development (Bell-Pedersen et al., 1996). Furthermore, CCG-9 protein seemed to be enriched in asexual structures compared to vegetative mycelia (figure 16). Together with the phenotype of the *ccg-9*^{RIP} mutant these observations suggest a specific role of *ccg-9* during asexual

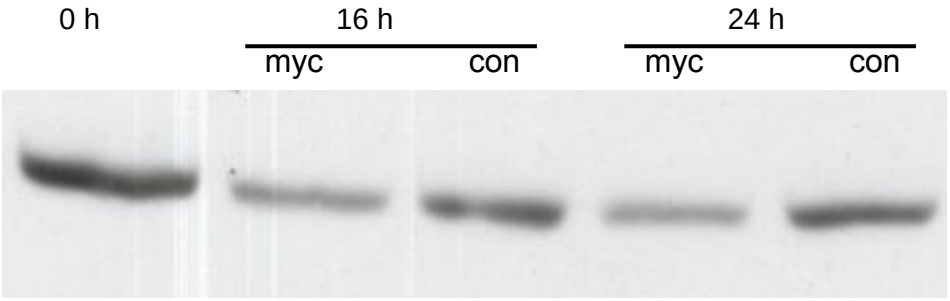

Figure 16: CCG-9 protein is enriched in asexual structures

The Western Blot shows total protein extracts of a p*ccg-9*::*ccg-9-Flag* knockin strain prepared either from vegetative mycelia (myc) or from asexual structures (con). Vegetative mycelia were transferred from liquid to solid culture and covered with filter paper to separate vegetative from asexual structures. Samples were taken from submerged culture (0 h), after 16 h and 24 h.

development. To evaluate this role on a molecular level, changes in the transcriptome during conidiation were analyzed in both wild type and *ccg-9*^{RIP}. For this purpose asexual development was induced by air exposure of mycelia that were previously grown in submerged culture (Berlin and Yanofsky, 1985). Samples were harvested before (0 h), 8 h and 24 h after induction of conidiation. Two independent experiments were sent for RNA sequencing. In agreement with previous data the *ccg*-9 transcript was dramatically induced 8 h and 24 h after air exposure in the wild type while it was nearly not expressed at all in liquid culture. Interestingly in *ccg-9*^{RIP} the *ccg*-9 transcript was already expressed 40- to 70-fold over wild type level in liquid culture. Moreover, induction of other conidiation specific genes was observed in the wild type but not always in *ccg-9*^{RIP} (see appendix figure S2). This shows that the assay induces a response on a molecular level according to the phenotypes of both strains.

The data sets were now filtered for significantly induced genes in the wild type during the course of the experiment (figure 17 a). In the next step identified candidates were compared with *ccg-9*^{RIP} (figure 17 b) and filtered for those which did not show the induction as detected in the wild type (figure 17 c). The remaining candidate genes were subjected to *in silico* functional analysis (figure 18 a and b) (Ruepp et al., 2004). To test whether enrichment of functional gene categories in this set is specifically due to a lack of *ccg-9* or simply reflects the functional distribution of genes induced by conidiation

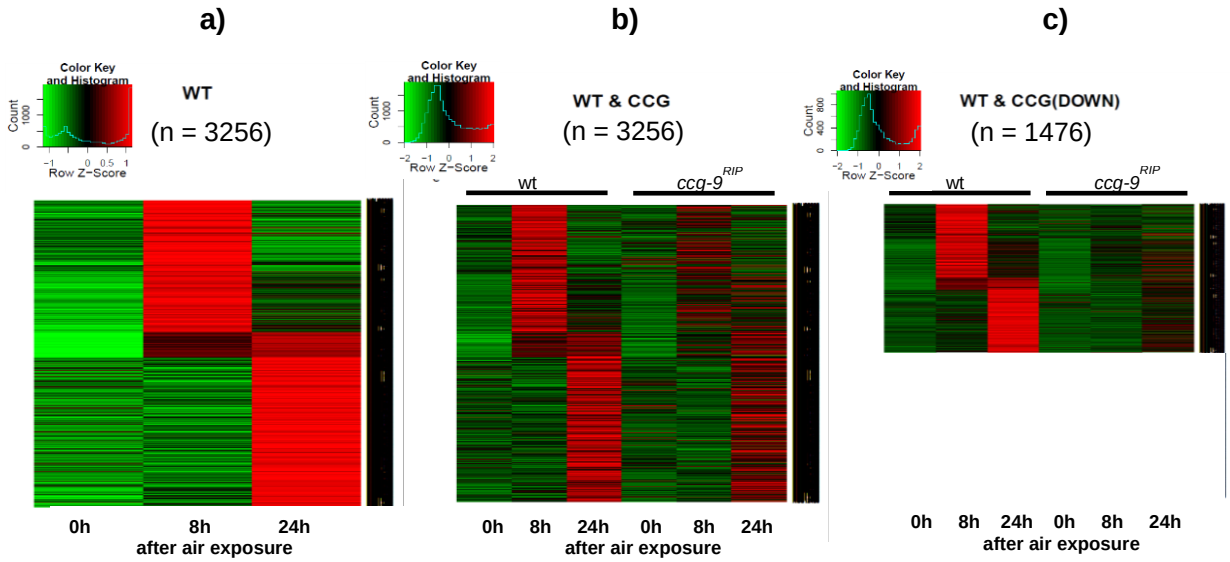

Figure 17: Genes that are induced during conidiation in the wild type but not in *ccg-9*^{RIP} were selected for further analysis

The figure shows the heat maps which were generated during the selection process. First genes were selected which were induced during conidiation in both experiments **(a)**. According to their expression pattern three classes of genes are clearly distinguishable. This set of genes was compared with *ccg-9*^{RIP} **(b)** and filtered for those which did not follow the same expression pattern **(c)**.

(figure 17 a) a functional analysis of the latter is shown for comparison. The data showed that a nonfunctional *ccg-9* allele did not result in a specific enrichment of any functional gene category. The majority (49.3%) of identified genes related to metabolism, which also represented the most significantly enriched category, followed by cellular transport (23.4%) as well as cell rescue, defense and virulence (20.4%). Interestingly, genes related to development just represented a small fraction (1.29%, not shown). Significantly enriched subcategories are shown in figure 18 b. Here the most dominant subcategory relates to C-compound and carbohydrate metabolism. The genes in this category are predicted to participate in a variety of metabolic reactions ranging from polysaccharide to catabolism to degradation of aromatic compounds. However, in agreement with previous experiments, genes participating in glycolysis or the TCA cycle were not misregulated (figure 19). Apart from that, in *ccg-9*^{RIP} a severe misregulation of genes participating in nitrate and phosphate assimilation was oberved. However as described earlier, growth experiments with high phosphate media or on media supplemented with amino acids as additional nitrate sources failed to restore the growth

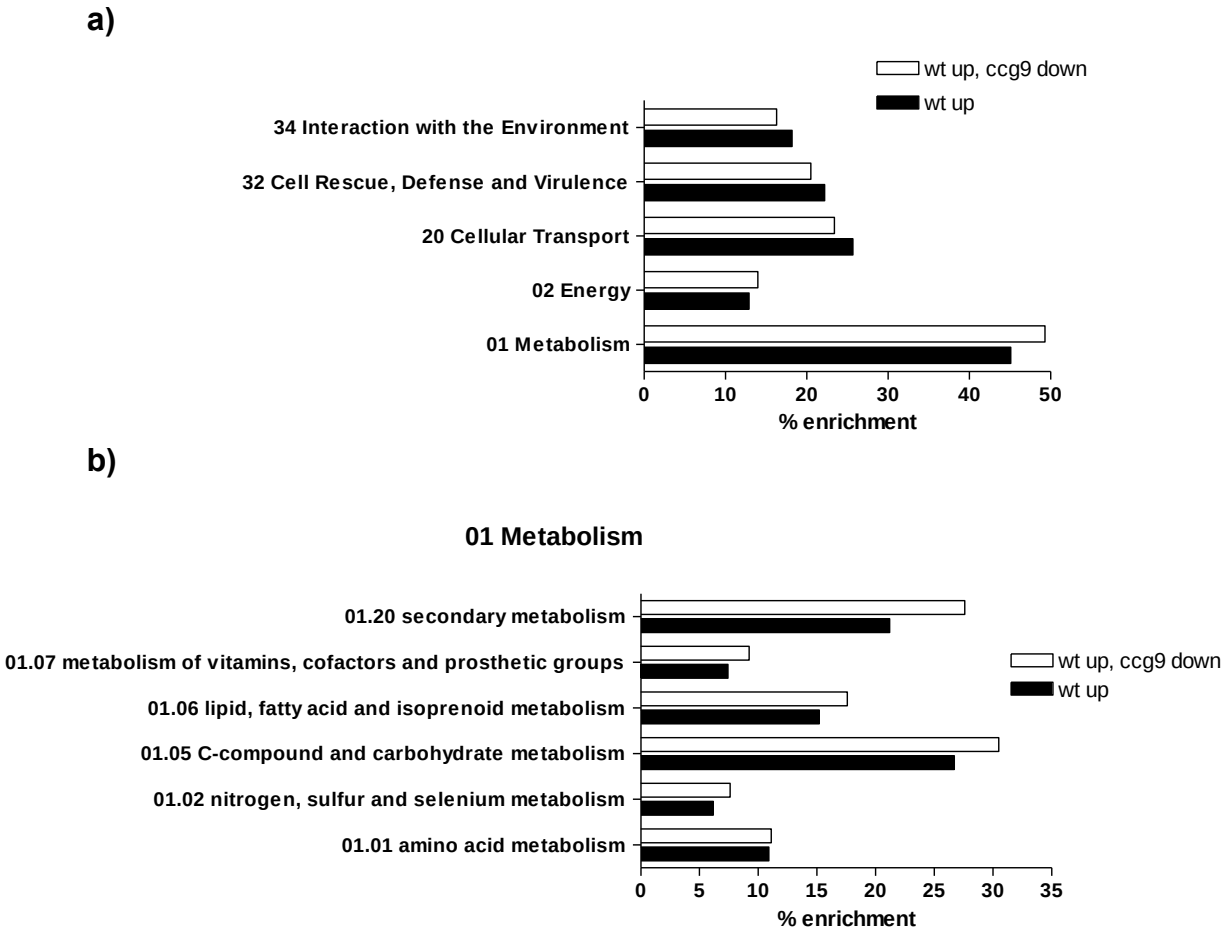

Figure 18: *In silico* functional analysis of candidate genes

The functional distribution within the analyzed sets of genes is shown in the top diagrams. To test for a specific enrichment due to a lack of *ccg-9*, the functional distribution of non-induced candidates (wt up, ccg-9 down) was compared with the total set of induced genes (wt up). The diagrams show significantly enriched major functional classes **(a)** as well as significantly enriched subcategories of metabolism related genes **(b).**

defect of *ccg-9*^{RIP} (see chapter 2.2.3). Finally, the data were also filtered for genes which were repressed in the wild type but not in *ccg-9*^{RIP} but this approach did not yield enough candidates for functional analysis. One major aim of the transcriptome analysis was to find candidates that could be responsible for the phenotype of *ccg-9*^{RIP}. In a recent study putative transcription factor genes had been identified and their knockouts analyzed on a genome wide basis (Colot et al., 2006). Based on this study a broad set of transcription factor genes was screened for individual expression patterns during the course of the experiment. While the majority of these behaved comparable to the wild type, *fluffy* and *ada-1* were severely misregulated (figure 20). In both experiments *ada-1*

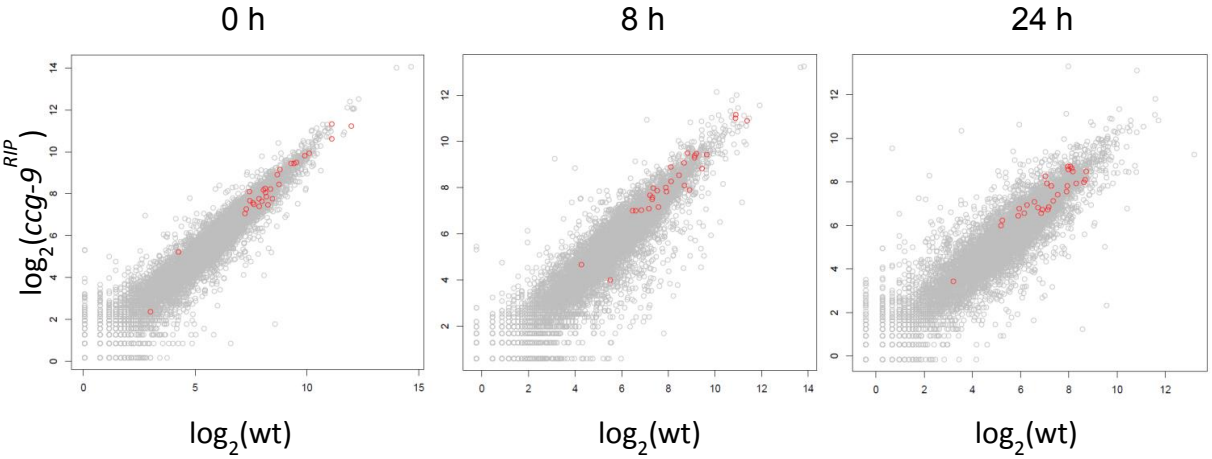

Figure 19: Distribution of genes for glycolysis and the TCA cycle within the dataset

The dot-plots show the reads of *ccg-9*^{RIP} over the wild type during the process of asexual development. Maped genes are shown in gray. Genes with a function in glycolysis or the TCA cycle are highlighted in red. A misregulation that was consistent for two experiments could not be detected.

was severely repressed at all time points in the *ccg-9*^{RIP} strain compared to the wild type. The *fluffy* transcript, however, was not repressed in submerged cultures of *ccg-9*^{RIP} but induction failed during the course of the experiment as it could be observed in the wild type. Both transcription factors play a major role in regulation of vegetative growth and asexual development as knockout mutants grow poor and fail to conidiate (Colot et al., 2006). Therefore, they were listed as strong candidates for rescue experiments.

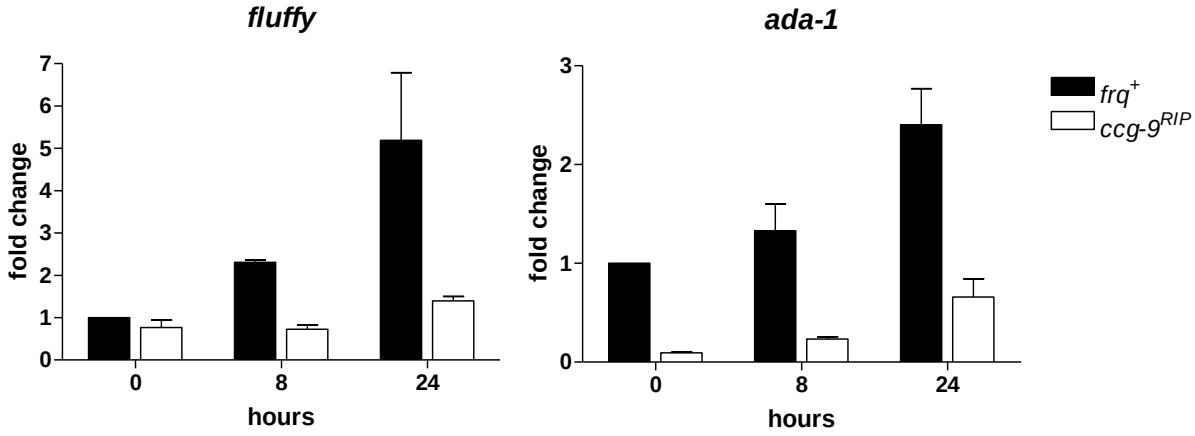

Figure 20: *Fluffy* and *ada-6*, two major regulators of growth and development, are severely misregulated in *ccg-9*^{RIP}

The diagrams show the fold change normalized to the mean expression at 0 h. Error bars show the standard deviation of the mean (n=2). Significance was calculated with a two-way ANOVA test.

2.2.6 Falsification of the *ccg-9^{RIP}* mutant

In order to perform rescue experiments *ccg-9^{RIP}* was crossed with a *frq^{+} His^{-}* strain to yield a histidine auxotroph mutant. This new strain would allow stable genomic integration of an extra copy of a gene of interest. After crossing the offspring was characterized by genotyping as it had been done with *ccg-9^{RIP}* earlier (compare chapter 2.2.1). Four independent strains which grew poorly in slants were sequenced at the *ccg-9* locus. Surprisingly, for three of them a wild type *ccg-9* allele was found (figure 21 a). For one of the clones the amplification of the locus as well as the sequencing of the PCR product was repeated with different primers to cover the whole open reading frame. However, no difference to the genomic sequence of the wild type could be detected. For better comparison of the phenotype the strains were grown in race tubes. All four strains showed the same arrhythmic growth defect as *ccg-9^{RIP}* (figure 21 b). Apparently, the genotype did not correlate with the phenotype. The promoter region was not sequenced and the *ccg-9* transcript was not quantified because the RIP-induced SNPs can be seen as markers for the chromosomal region surrounding the *ccg-9* locus. Three strains containing a meiotic recombination in the proximal promoter region close to the open reading frame were assumed to be very unlikely. Therefore, promoter sequence and activity in these strains should be the same as in the wild type. The results strongly suggest that the phenotype may not be related to a non-functional *ccg-9* allele.

a)

```
ccg-9_a4        CCCACCACGGCTTGCTTGACTGCGTCGACGTTTCATGCTAATATTGGATGTCCCATAGAC 60
ccg-9_a8        CCCACCACGGCTTGCTTGACTGCGTCGACGTTTCATGCTAATATTGGATGTCCCATAGAC 126
wt              CCCACCACGGCTTGCTTGACTGCGTCGACGTTTCATGCTAATATTGGATGTCCCATAGAC 180
ccg-9_a1        CCCACCACGGCTTGCTTGACTGCGTCGACGTTTCATGCTAATATTGGATGTCCCATAGAC 126
                ************************************************************

ccg-9_a4        GCTCTATCTTGGTATCTCTGCCGTCTTTGCTGACGACCATACGGCCGTTGTGGCCCTGGC 120
ccg-9_a8        GCTCTATCTTGGTATCTCTGCCGTCTTTGCTGACGACCATACGGCCGTTGTGGCCCTGGC 186
wt              GCTCTATCTTGGTATCTCTGCCGTCTTTGCTGACGACCATACGGCCGTTGTGGCCCTGGC 240
ccg-9_a1        GCTCTATCTTGGTATCTCTGCCGTCTTTGCTGACGACCATACGGCCGTTGTGGCCCTGGC 186
                ************************************************************

ccg-9RIP        ACTTTGCCTACTACGGTTTGCTTGATTGCGTCGACGTTTCATACTAATATTAGATATCCT 91
ccg-9_a3        ACTTTGCCTACTACGGTTTGCTTGATTGCGTCGACGTTTCATACTAATATTAGATATCCT 120
                ************************************************************

ccg-9RIP        ATAGACGCTCTATTTTGGTATCTCTGCCGTCTTTGCTGACGACTATACGGCTGTTGTGGC 151
ccg-9_a3        ATAGACGCTCTATTTTGGTATCTCTGCCGTCTTTGCTGACGACTATACGGCTGTTGTGGC 180
                ************************************************************
```

b)

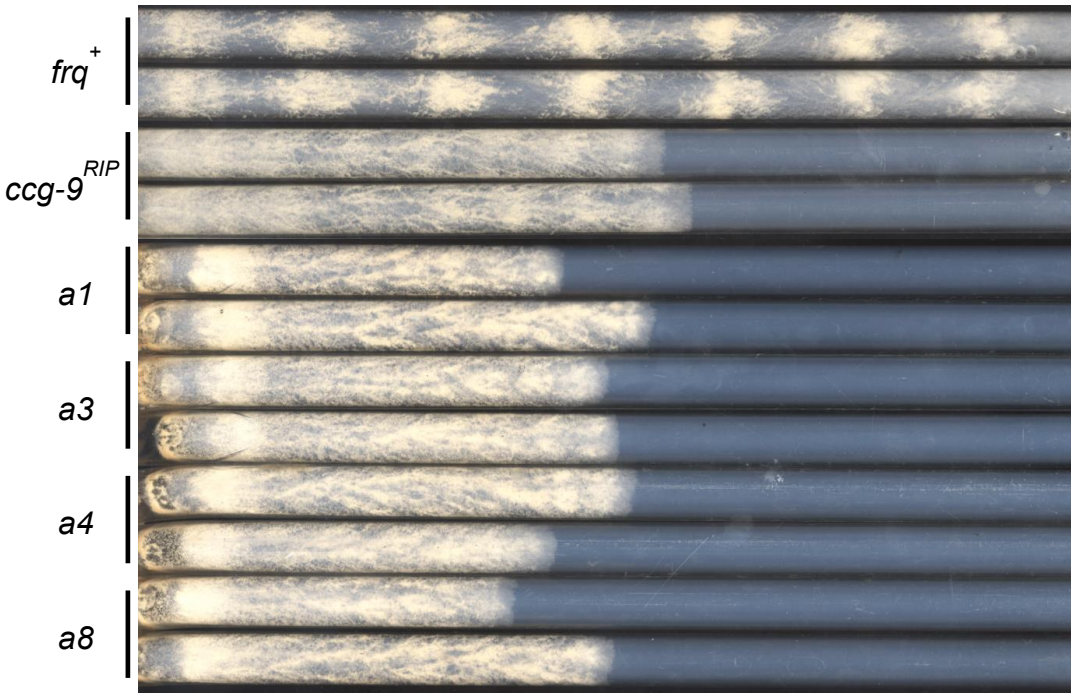

Figure 21: The *ccg-9*^{RIP} phenotype does not cosegregate with the genotype

After crossing in three of four clones (a1, a4 and a8) a wild type *ccg-9* allele was found by sequencing. The figure **(a)** shows 120 bp of the respective sequence alignments with the wild type and *ccg-9*^{RIP}. Stars indicate mismatches. In **(b)** representative race tubes are shown.

2.3 Characterization of a *ccg-9* knockout mutant

2.3.1 Generating a *ccg-9* knockout by gene replacement

In order to confirm the previous findings homocaryotic *ccg*-9 knockout mutants were generated by transformation and backcrossing to the wild type (for details see chapters 4.5.5 and 4.5.9). For this purpose the entire *ccg-9* open reading frame was replaced by the *hph* gene, which codes for a hygromycin B phosphotransferase and renders the organism resistant to hygromycin B. Offspring of the cross was then selected for hygromycin resistance. The homologous recombination of the *hph* cassette with the *ccg-9* locus was detected by PCR for three independently generated strains (figure 22 a). In agreement with this result in all three clones the copy number of *ccg*-9 loci was reduced to the detection limit as quantified by qPCR (figure 22 b). In addition, for one of the crosses (cross s2) the copies of *ccg*-9 loci were quantified in eight different clones. The *ccg-9* locus could not be detected in any of them. In contrast, the copy number of the *hph* gene was detected in a comparable amount to a homocaryotic reference strain obtained from the Fungal Genetics Stock Center (FGSC) (appendix figure S3). These data indicate that in cross s2 the resistance to hygromycin co-segregates with a deletion of the *ccg-9* locus. Hence, the resistance is conferred by the single insertion of the *hph* gene at the *ccg-9* locus and not by any ectopic insertion.

To complete the genetic characterization of the knockout strains the *ccg-9* transcript abundance was detected. Unfortunately, in the wild type *ccg-9* expression was already very low under standard conditions and the C_t values in qPCR experiments were very high. To be sure about the absence of a *ccg*-9 transcript it was also quantified under conditions which usually force the induction of *ccg*-9 expression. Therefore, the assay for induction of conidiation was repeated in a reduced setup with the mutants and the wild type. While the *ccg-9* transcript was induced after 8 h in the wild type it still could not be detected in the knockouts (figure 22 c; for the raw data see appendix table S4). The samples derived from the knockout mutants showed C_t values above 35 which were comparable to the control without any template. These data show, that, as a result of the homologous gene replacement, *ccg-9* is no longer expressed even under

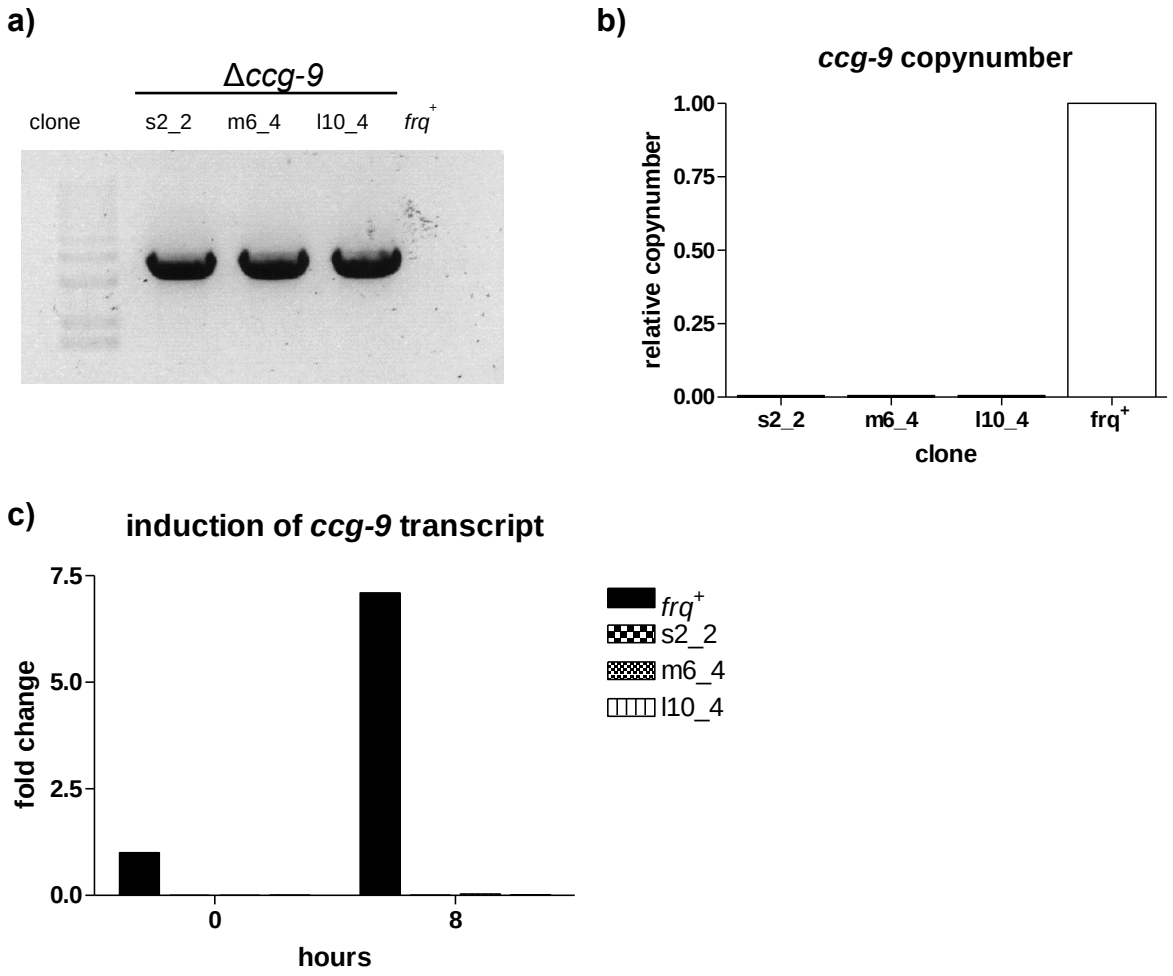

Figure 22: Validation of *ccg-9* knockout clones

Homologous integration of the knockout construct was tested by PCR. The 3 kb fragment was generated with a locus and a construct specific primer and could be detected for three independently generated clones (s2_2, m6_4, l10_4) **(a)**. Wild type copies of the *ccg-9* gene could not be detected by qPCR **(b)**. Transcript levels were low and could not be induced by asexual development as it was the case in the wild type (*frq*$^{+}$) **(c)**.

conditions that favor the induction of *ccg-9* transcript.

2.3.2 Growth characteristics of the *ccg-9* knockout mutant

To test whether the knockout strains show the same phenotype as the *ccg-9*^{RIP} mutant, all strains were grown in race tubes in constant darkness. In contrast to *ccg-9*^{RIP} all knockout strains grew rhythmic and did not show any growth defect on standard race tube medium containing 0.1% glucose (figure 23). Furthermore, any severe differences in the endogenous period length could not be detected indicating that *ccg-9* did not feed

back to the circadian clock. The genotype as well as the general phenotype appeared to be the same in all knockout strains. Hence, strain s2_2 was chosen as a representative for further experiments.

To further characterize the response of the knockout strain to different concentrations of the carbon source in the substrate, conidia were harvested from race tubes and counted as it had been done before with *ccg-9*^{RIP} (compare chapter 2.2.4). Conidial density was not significantly different between the wild type and the *ccg-9* knockout strain neither on low glucose nor on high glucose media (figure 24 a). However, in previous experiments the *ccg-9*^{RIP} mutant showed impaired growth behavior on complex carbohydrates compared to wild type (see appendix figure S5). Extracellular enzymes like cellulases are highly regulated in response to the intracellular carbohydrate supply. If this regulatory system depended on *ccg-9* or trehalose, a glucose medium would completely bypass any (feasibly *ccg*-9 dependent) regulatory mechanism and thereby mask possible growth effects. Therefore, the experiment was repeated on medium containing a complex carbohydrate. As cellulose is the most abundant carbohydrate on earth and *Neurospora* is usually found growing on burned plants, cellulose was chosen as a

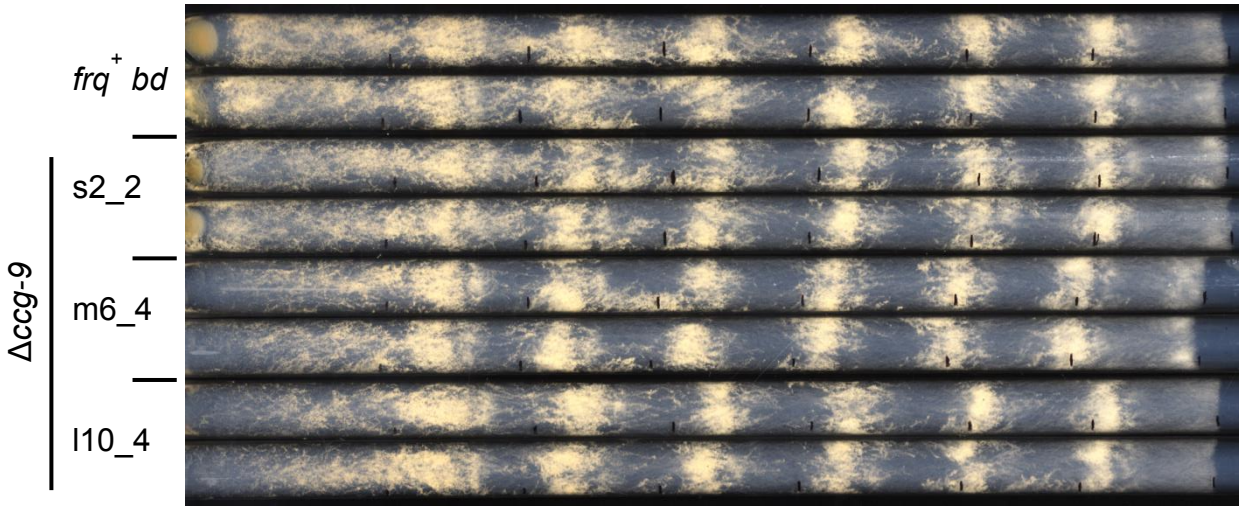

Figure 23: Growth phenotype of the *ccg-9* knockout mutants

Race tube experiments showed that rhythmicity and the vegetative growth of the *Δccg-9* knockout strains (s2_2, m6_4, l10_4) behave absolutely like the wild type (*frq*$^{+}$ *bd*). The image shows a representative race tube experiment under standard conditions in constant darkness.

carbon source. However, even on cellulose medium the amount of conidia harvested from the race tubes was not significantly different from the wild type independently of the concentration (figure 24 b). As trehalose is suggested to act as a stress protectant the experiment was repeated under application of thermal stress at 37°C. At low glucose concentration it was not possible to detect conidia in a significant amount. High glucose concentration yielded equal amounts of conidia from the *ccg-9* knockout and the wild type (figure 24 c). These data show that, with respect to conidiation, *ccg-9* is not needed for carbohydrate sensing neither on glucose nor on cellulose. Furthermore, *ccg-9* apparently does not have a protective effect regarding thermal stress.

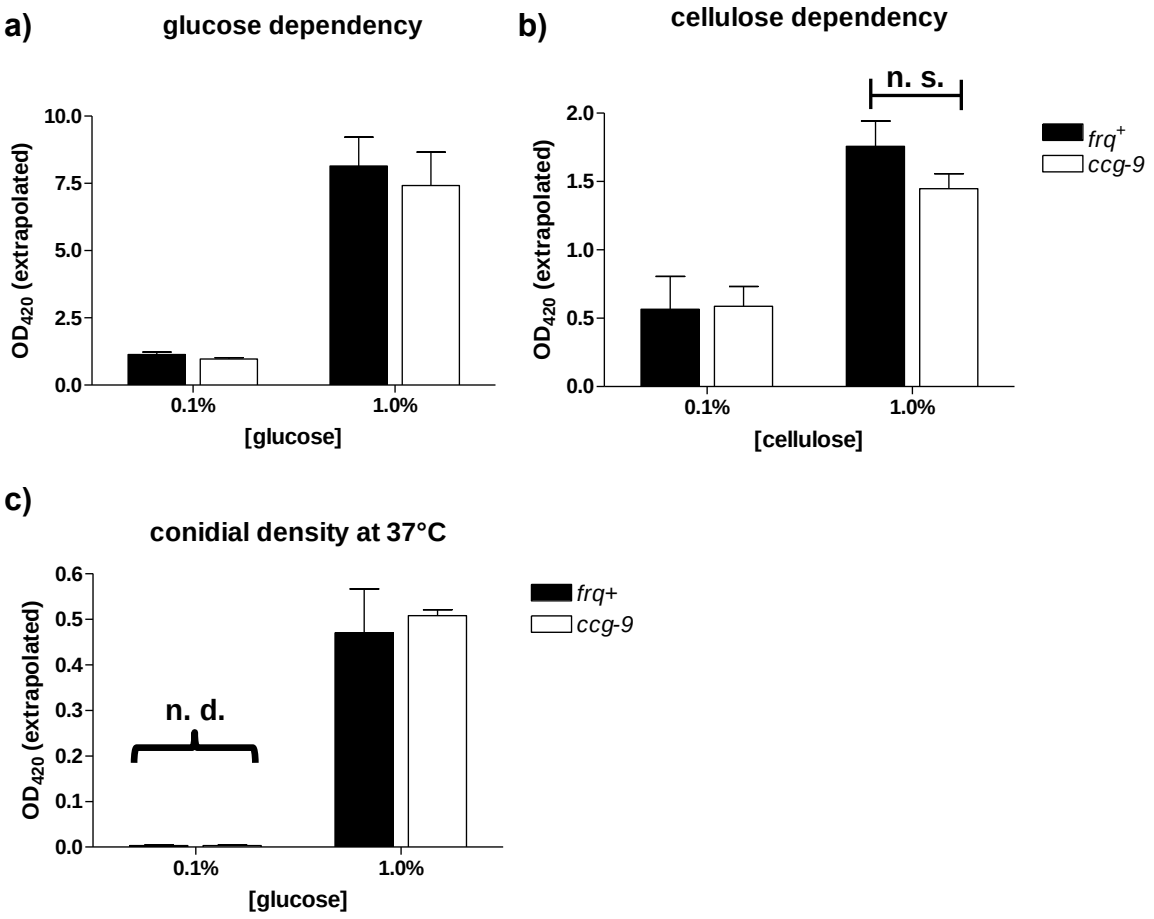

Figure 24: Conidiation and carbon source sensing are not affected in the *ccg-9* knockout

The amount of conidia produced by the *ccg-9* knockout was not significantly different from the wild type (*frq*$^+$) neither on low nor on high glucose **(a)** or cellulose **(b)** medium. Thermal stress at 37°C did not affect conidial density as well **(c)**. The graphs show the optical density of conidial suspensions after harvesting from race tubes. Error bars show the standard deviation of the mean (n=3). Significance was calculated with a two-way ANOVA test. n. s. = not significant; n. d. = not detectable

While asexual development is nearly discontinued under minimal conditions on a solid substrate, vegetative growth is maintained even on extremely poor substrates. Furthermore, *Neurospora* is easily capable of utilizing the agar as a carbon source. Therefore, the race tube assay was not an appropriate tool to measure the function of *ccg-9* in carbohydrate sensing with respect to vegetative growth. However, in liquid culture dry mass of the vegetative mycelium strictly depends on carbon source concentration. Determination of the mycelial dry mass did not reveal any differences between the wild type and the *ccg-9* knockout mutant. Both strains grew equally well on low (0.2%) and high (2%) glucose media (figure 25 a). This held also true for initial tests with other carbon sources like sucrose and starch and under thermal stress at 37°C. Cellulose was quite difficult to test as it was insoluble and *Neurospora* tended to form mycelial aggregates with agglomerated cellulose material. As an initial experiment gave promising results growth was tested under osmotic stress with 4% NaCl. However, three more independent replicates did not show a significant difference between the wild type and *ccg-9* knockout neither on low nor on high glucose media (figure 25 b). All these experiments were performed in constant light in order to test general effects without any clock influence. On the other hand as *ccg-9* is controlled by the circadian clock it may need clock activity to see a difference between the wild type and the

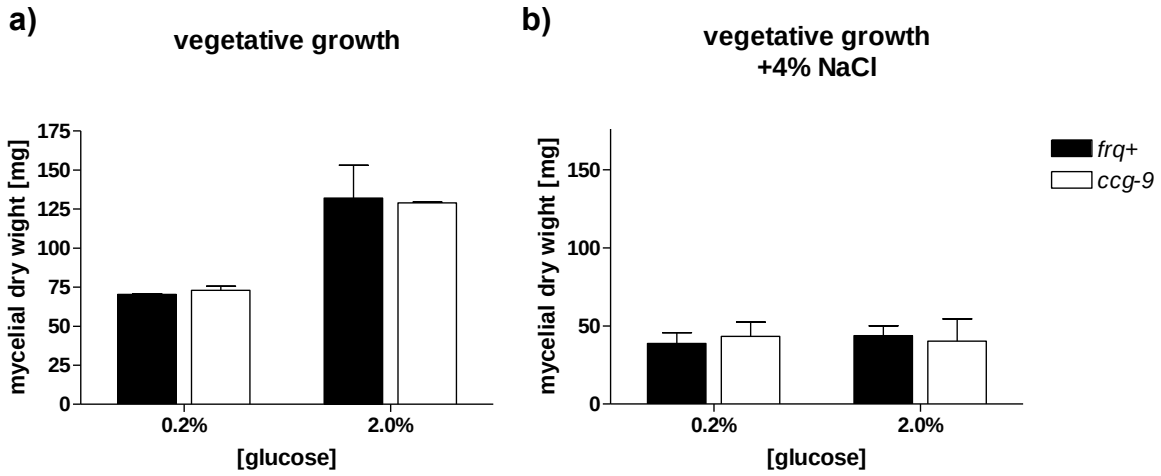

Figure 25: Vegetative growth is glucose responsive and not affected even under osmotic stress

Mycelial pads grown in petri dishes were transferred to liquid cultures without **(a)** or with 4% NaCl **(b)**. The graphs show the mycelial dry weight of the wild type (frq^+) and the knockout strain (*ccg-9*) after 24 h of growth in liquid culture. Error bars show the standard deviation of the mean (n=3).

knockout. However, in tests with light / dark (12 h / 12 h) entrainment the knockout grew as well as the mutant. These results show that, in agreement with previous data, *ccg-9* is not mandatory neither for vegetative growth itself nor for the dependency of growth on carbohydrate availability.

2.3.3 *ccg-9* is a trehalose phosphorylase instead of a trehalose synthase

To get deeper insights into the nature and a putative physiological role of CCG-9 the protein sequence was compared to other enzymes which had been related to trehalose metabolism in fungi and other microorganisms. Shinohara and colleagues had characterized CCG-9 as a trehalose synthase (Shinohara et al., 2002). Surprisingly, CCG-9 did not show a significant sequence homology to (putative) trehalose synthases in other fungi like *S. cerevisiae*, *Magnaporthe oryzae* or *Aspergillus nidulans*. However, especially in the C-terminal catalytic domain a remarkable homology to well characterized trehalose phosphorylases of other fungi like *Shizophyllum commune* or *Agaricus bisporus* was found (Wannet et al., 1998; Eis et al., 1999). These observations strongly suggested that *ccg-9* was a trehalose phosphorylase instead of a trehalose synthase. Trehalose phosphorylases use inorganic phosphate to degrade trehalose to glucose and glucose-1-phosphate. To test this hypothesis, CCG-9-Flag was purified and then tested for trehalose phosphorylase activity. This was done by using a discontinuous assay: In a first reaction trehalose was degraded using the purified enzyme. Subsequently, liberated glucose was determined by a simple glucose oxidase assay using quantification of nicotinamide adenine dinucleotide phosphate (NADPH) by spectrophotometry. A mock-purification from the *ccg-9* knockout strain was used in a control reaction. The results show that trehalose degradation could be significantly enhanced by adding inorganic phosphate to the reaction using CCG-9-Flag extracts. This dependency could not be observed using mock-extracts obtained from the *ccg-9* knockout strain (figure 26). These results show that phosphate-dependent trehalose degradation is a specific result of CCG-9 activity. Therefore, CCG-9 is a trehalose phosphorylase instead of a trehalose-synthase which assigns it to a very different group of enzymes within trehalose metabolism.

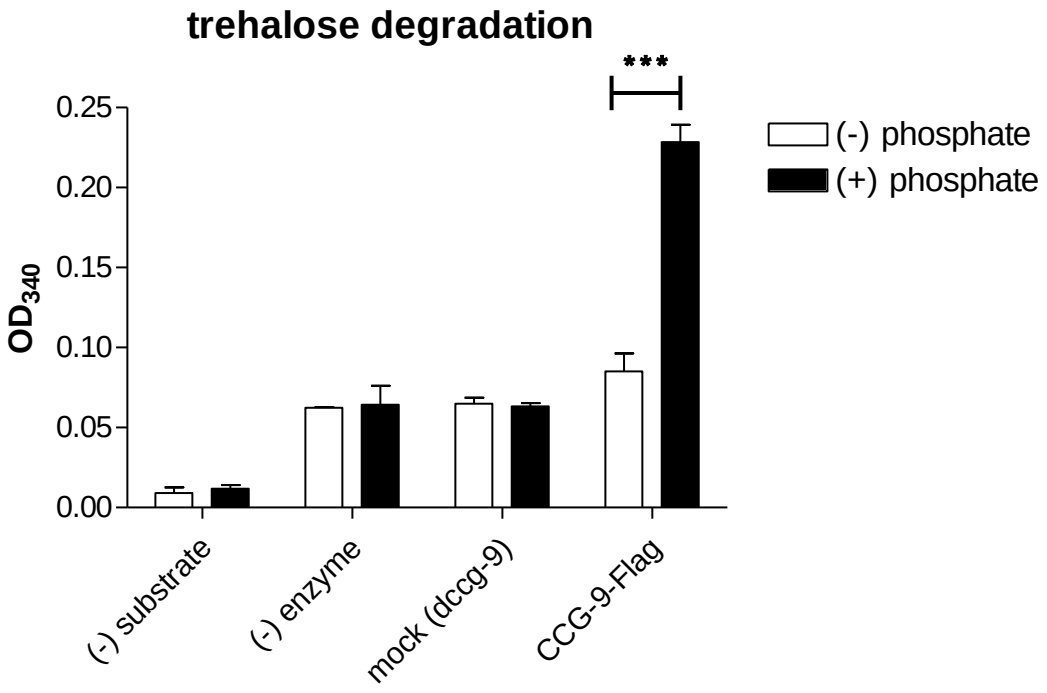

Figure 26: CCG-9 can degrade trehalose in a phosphate dependent manner
For the assay CCG-9-Flag was purified. Extracts from a *ccg-9* knockout strain (mock) were purified as a control to exclude unspecific activity in the elution. Trehalose phosphorylase activity was assayed in the presence ((+) phosphate) and absence ((-) phosphate) of inorganic phosphate. Error bars show the standard deviation of the mean (n=3). Significance was calculated with a two-way ANOVA test.

3 Discussion

3.1 Luciferase assays and their limitations in *Neurospora crassa*

In recent years luciferase assays have become a powerful and intuitive technique for realtime-monitoring of circadian promoter activity. In contrast to other methods like semi-quantitative transcript determination by qPCR luciferase assays allow very precise analysis of circadian rhythms with respect to amplitude, period-length, rhythm quality and phase shifts. So far this method has been established in a 96-well plate format under growth repressive conditions as well as in race tubes allowing free vegetative growth and asexual development (Gooch et al., 2008). However, in this study it was discovered that the assay apparently has its limitations under certain conditions, which may probably relate to rhythmic asexual development. Coherent rhythms in race tubes were observed even from reporters which have recently shown to oscillate antiphasic (Sancar et al., 2012). Furthermore, the same phenomenon could be induced in the 96-well plate assay as soon as cultures overcame growth repression and start asexual development. A reason for these observations might be the luciferase reaction suffering from superimposing substrate rhythms, which may relate to asexual development. The luminescence intensity not only depends on the luciferin but also on the oxygen concentration (Gooch et al., 2008). It has been reported that the intracellular concentration of reactive oxygen species (ROS) is clock controlled (Yoshida et al., 2011) and the homeostasis between oxygen and ROS seems to be critical for the circadian control of asexual development (Belden et al., 2007). Moreover, a knockout of superoxide dismutase induces circadian banding in race tubes similar to *frq*$^{+}$ *bd* while a knockout of the ROS-generating NADP oxidase rather represses circadian conidiation (Yoshida et al., 2008; Yoshida et al, 2011). Therefore, conditions which are permissive for circadian asexual development may at least coincide with rhythmic changes in

intracellular oxygen concentration and may thereby severely interfere with the assay. In fact, interference of ROS with luciferase intensity has been demonstrated elsewhere (Czupryna and Tsourkas, 2011). Furthermore, in our lab the assay was established with a relatively high concentration (150 µM) of the substrate compared to other studies (Gooch et al., 2008; Larrondo et al., 2012; Gooch et al., 2014; Hong et al., 2014). If it holds true that circadian control over substrate availability interferes with the assay, a high luciferin concentration may even enhance these artificial rhythms.

If the observations of this study were related to growth and asexual development this may also explain the low reproducibility which was observed in the 96-well plates but not in race tubes. While race tubes constitute a relatively stable and reproducible environment especially with respect to rhythmic growth, the well plate does not. A well can rather be seen as a microenvironment which may suffer from the variance of different parameters like e.g. conidial density, the volume of the medium and the overlaying gas phase, humidity as well as oxygen supply and more. These variances may result in a different pace of development of the culture and thereby a different time may be needed to overcome growth repression caused by the sorbose medium.

The data can therefore be explained with the assumption that under certain conditions the assay does not exclusively reflect promoter activity but at least in part a rhythmic intracellular redox homeostasis. This hypothesis is difficult to proof because it is hard to find an experimental setup which allows clear differentiation between rhythmic bioluminescence caused by either clock control on the promoter activity or substrate availability. The observed bioluminescence signal will most probably be the result of both. Biochemical comparison of intracellular luciferase abundance with substrate (oxygen) concentration over the course of a circadian day may give an impression. However, from a technical perspective with 96-well plates it should be nearly impossible and from race tubes it is at least difficult to gain sufficient amounts of biomass for biochemical analysis. Aconidial strains like *fluffy* may not necessarily help since most of them are unable to complete the development of conidia but are not totally blocked in asexual development. Furthermore, these strains are difficult to handle and they are not

necessarily a suitable tool to address the core issue. Asexual development itself may not simply be the origin but the phenotypic consequence or side effect of a molecular mechanism which possibly causes artificial bioluminescence rhythms.

3.2 *ccg-9^{RIP}* - still an interesting tool for circadian research?

During this study it was shown that the phenotype of the *ccg-9^{RIP}* mutant is not caused by a non-functional *ccg-9* allele. Nevertheless, the growth arrhythmicity of this strain may be a reason to use it for investigations on the link between the circadian clock and rhythmic conidiation which is still poorly understood. As a consequence any future work with this strain should primarily aim at finding the true cause for the *ccg-9^{RIP}* phenotype. In the following paragraphs it will be discussed whether it is reasonable to spend further efforts on characterizing the *ccg-9^{RIP}* mutant in more detail.

One question to ask is whether the signaling from the circadian clock to rhythmic growth is indeed defective. *Ccg-9* does apparently not promote induction of a specific functional set of genes during conidiation. Nevertheless, it was demonstrated that the majority of genes which were induced during conidiation in the wild type, functionally related to metabolism, especially of C-compounds and carbohydrates (compare figure 10). This may provide an explanation for the arrhythmic phenotype of the mutant which fails to induce a huge set of metabolic genes during asexual development. A functional

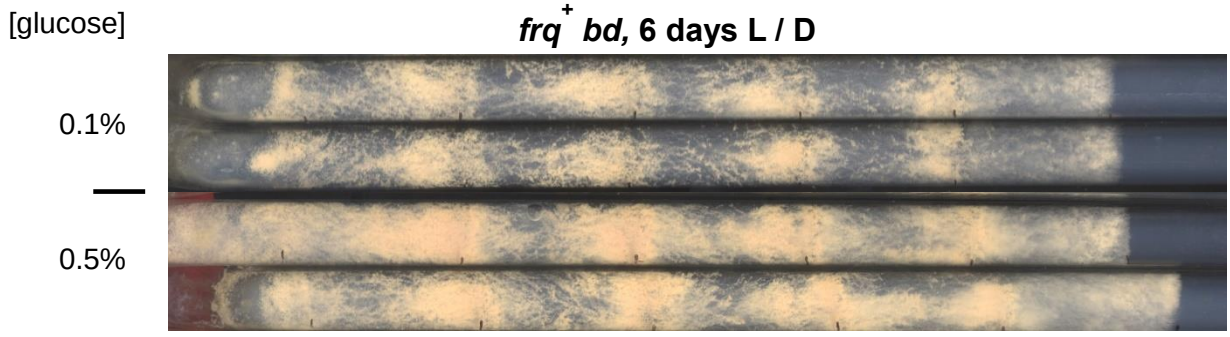

Figure 27: Example for nutritive effects on growth rhythmicity

Even though the growth rhythm is clearly visible under both conditions, high glucose conditions increase conidiation also in the interband. This effect dampens the visual impression of growth rhythmicity.

metabolism can be seen as a central essence for successful growth and reproduction. Metabolic cycles have been reported in yeast (which is not known to have a circadian clock) as well as mammalian cells and were connected to growth and cell cycle progression (Tu et al., 2005; Tu et al., 2007; Xu et al., 2009). The circadian clock of *N. crassa* may coordinate growth and metabolic cycles to assure optimal utilization of nutrients for a most effective reproduction. In *ccg-9*^{RIP} the clock could still be able to control growth rhythmicity by dedicated signaling pathways, but reduced expression of metabolic genes will possibly dampen the output to such an extent that a conidiation rhythm is hardly visible. As expected, nutrient supply seems to have a major impact on the manifestation of rhythmicity: rhythmic growth of *ccg-9*^{RIP} could be restored on various media containing acetate or low phosphate (compare figures 12 and 14). Similar observations were made with the wild type on media with high carbon source content such as 0.5% glucose (figure 27). Compared to low glucose medium (0.1%) enhanced conidiation started to mask the growth rhythm on high glucose medium. The peak-to-trough ratio seemed to be decreased. These observations support the hypothesis that a growth rhythm per se exists in *ccg-9*^{RIP} but may be masked by nutritional effects.

If *ccg-9*^{RIP} should serve as a tool for a better understanding of clock control over growth rhythmicity, its phenotype should be clearly attributable to a narrow range of causalities. Since the transcriptome analysis of the *ccg-9*^{RIP} has its limitation in functional interpretation of the results the mutant was further characterized. Mitogen-activated protein (MAP) kinases have been reported as important regulators of growth and asexual development (Park et al., 2011). Furthermore, it has been demonstrated that

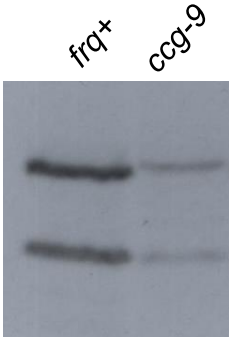

Figure 28: Phosphorylation of MAK-1 and MAK-2 is reduced in *ccg-9*^{RIP}

Total extracts from cultures grown under standard conditions were decorated with phospho-specific MITOGEN ACTIVATED KINASE 1 and 2 (MAK-1 / MAK-2) antibody after Western Blotting. Please note the slight upshift of the MAK-1 signal in extracts from *ccg-9*^{RIP}.

phosphorylation of MAP kinases and signaling activity of MAPK pathways are controlled by the circadian clock (Vitalini et al., 2007; Bennett et al., 2013). A signaling from trehalose biosynthesis to MAP kinase cascades seemed reasonable, since both have been related to stress resistance in fungi (Maerz et al., 2008; Teichert et al., 2014). Therefore, MAP kinases were interesting targets to explain the growth phenotype of *ccg-9*^{RIP}. The activity of two MAP kinase signaling pathways was tested using phospho-specific antibodies against MITOGEN ACTIVATED PROTEIN KINASE-1 and -2 (MAK-1, MAK-2). In fact, a consistent reduction of MAK-1 phosphorylation compared to wild type was found in *ccg-9*^{RIP} (figure 28). This may suggest that MAP kinase signaling is involved in the phenotype of the mutant. However, a slight upshift of the p-MAK-1 signal was observed as well in *ccg-9*^{RIP} indicating an unknown posttranslational modification which could disturb the affinity of the antibody. Furthermore, MAP kinase pathways are well investigated and known as central regulators of cellular physiology. They regulate a huge variety of genes and, moreover, they receive input from a variety of cellular signaling pathways themselves (Li et al., 2005; Gras et al., 2013; Gosh et al., 2014). Therefore, this observation may be a first hint but will not necessarily ease the quest for the link between clock activity and rhythmic conidiation.

The results of this study demonstrate that the *ccg-9*^{RIP} phenotype is caused by a mutation in another gene beside *ccg-9* itself. Moreover, the method, which has been used to generate the mutant, relies on insertion of genomic single nucleotide polymorphisms (SNPs). In contrast to targeted approaches this may affect neighboring genes or genes with high sequence similarity. Therefore, it is possible that the cause of the phenotype is even multigenic. Sequence data from the transcriptome analysis were analyzed for distribution and density of SNPs in the wild type and in *ccg-9*^{RIP}. In fact, enrichment of SNPs was found at multiple sites distributed over the whole genome. However, the data were not reproducible in different samples and therefore not reliable. The accurate and convenient method to find and evaluate genomic alterations in the mutant would be whole genome sequencing.

Taken together, *ccg-9*^{RIP} does probably not provide a reliable tool for circadian research. Its growth arrhythmicity may be the result of nutritional and metabolic effects on the conidiation behavior instead of a defect in a single gene or a dedicated signaling pathway. Hence, further investigations on this mutant at least with respect to circadian research may be complicated, because it could involve a variety of genes along several metabolic pathways. Furthermore, the mutant may have accumulated a high number of genomic SNPs during the RIP process. As a consequence, the phenotype could be the cumulative result of various mutations. The *ccg-9*^{RIP} mutant harbors too many instability factors. Therefore, it will be very difficult to draw any clear and straightforward conclusions.

3.3 ccg-9 and trehalose metabolism in *N. crassa*

In this study the *ccg-9* knockout strain did not show any phenotype, which raised the question for the physiological relevance of the *ccg-9* gene. In *N. crassa ccg-9* was described as a trehalose synthase (Shinohara et al., 2002). These findings were based on sequence homology to an enzyme found in the basidomycete *Grifola frondosa* (Saito et al., 1998). In fact, the enzyme which was characterized in this study belongs to the class of trehalose phosphorylases (EC 2.4.1.64), which has initially been found in the protist *Euglena gracilis* (Maréchal and Belocopitow, 1970). This makes a remarkable difference, because in contrast to trehalose synthases, trehalose phosphorylases can catalyze the forward and the reverse reaction. Furthermore, they use glucose and glucose-1-phosphate as substrates for trehalose synthesis and inorganic phosphate for trehalose degradation. However, the physiological role of this class of enzymes is still poorly understood. The reason may be that in various fungi trehalose biosynthesis and degradation seem to be regulated redundantly by several enzymes. The enzymes for the trehalose synthase complex, which was found and intensively studied in *S. cerevisiae*, are also encoded in the genome of *N. crassa* and other fungi. Furthermore, two trehalases have been identified in *Neurospora* so far (Sussman et al., 1971; d´Enfert et al., 1999). It could be possible that *ccg-9* plays a minor role in trehalose metabolism compared to these highly specialized enzymes. In fact, latest experiments

of this study showed that a knockout of the *N. crassa* TREHALOSE-6-PHOSPHATE PHOSPHATASE (NCU05041), which catalyzes the dephosphorylation of trehalose-6-phosphate to trehalose, renders the organism sensitive for temperature stress (figure 29 a). Trehalose is generally known as a thermal stress protectant which has also been found for *Neurospora* (Plesofsky and Brambl, 1999). However, a similar observation could not be made for the *ccg-9* knockout mutant (figure 29 b). Nevertheless, it has to be considered, that the genetic background of both knockout strains is different and therefore both experiments are not exactly comparable.

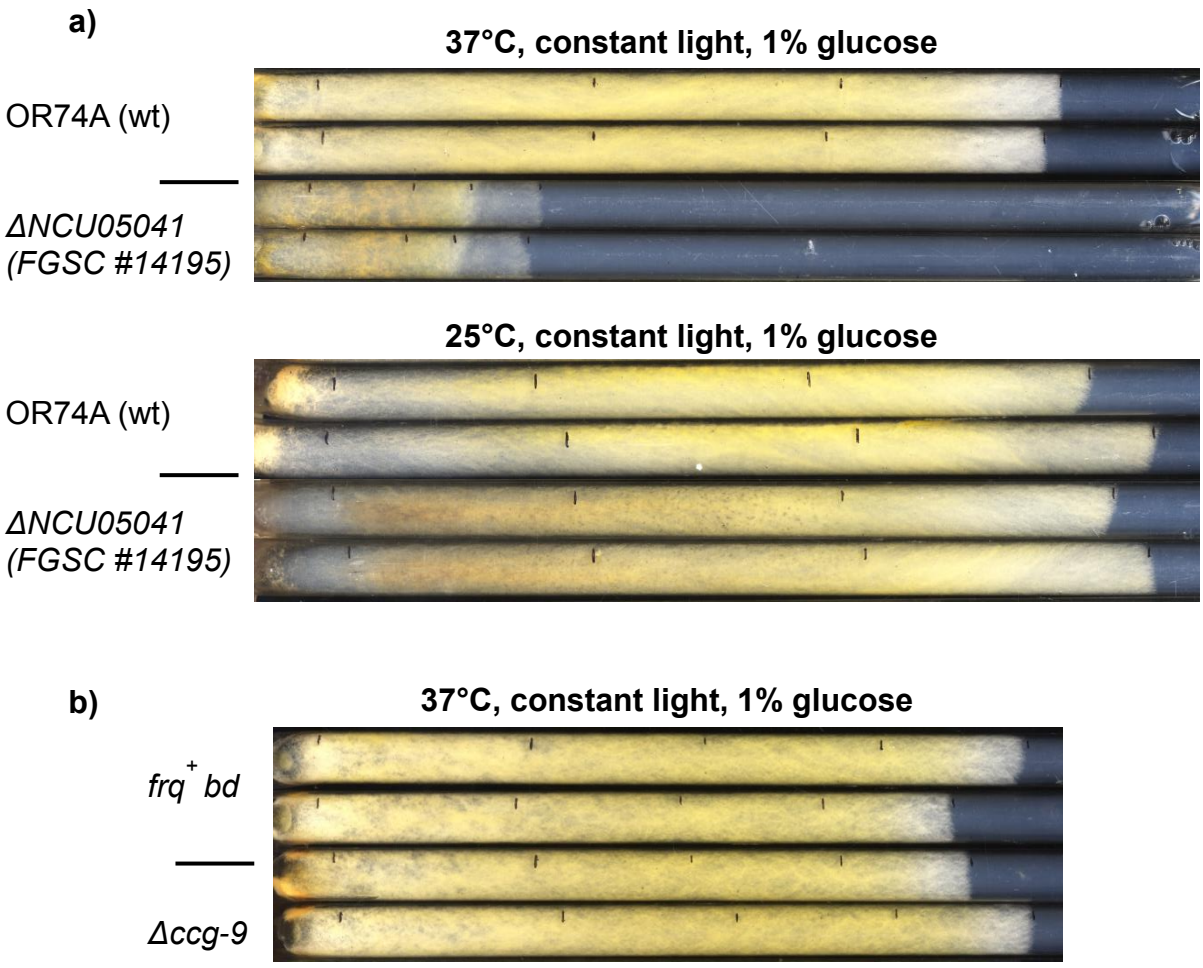

Figure 29: Trehalose-6-phosphate phosphatase seems to be essential for thermal stress resistance

The images show representative race tube experiments grown under the indicated conditions. Please note that the FGSC mutant **(a)** is based on the genomic background of the OR74A wild type. This strain grows faster in race tubes compared to *frq*$^{+}$ *bd* and Δ*ccg-9* **(b)**.

In *Shizophyllum commune* a homologue of *ccg*-9 has been intensively studied and characterized as a trehalose phosphorylase by Nidetzky and colleagues. It has been hypothesized, that the equilibrium for the reaction catalyzed by trehalose phosphorylase lies far on the side of trehalose phosphorolysis *in vivo* (Eis and Nidetzky, 1999). This theory would also partially explain the aforementioned observation. The fact, that *ccg-9* is rather repressed under high glucose conditions but inducible by glucose starvation may support this hypothesis as well (Shinohara et al., 2002). As a consequence, mobilization of trehalose by phosphorolysis would conserve the energy of the glycosidic bond in a phosphoester (Maréchal and Belocopitow, 1970; Eis and Nidetzky, 1999). This suggests a role of *ccg-9* in more effective use of reserve carbohydrates during stress situations. Interestingly it was observed that, in contrast to *ccg-9*, NEUTRAL TREHALASE (NCU04221), which catalyzes intracellular breakdown of trehalose (d'Enfert et al., 1999), is downregulated during conidiation (appendix figure S6). If the global energetic balance benefited from trehalose breakdown by phosphorolysis over simple hydrolysis this should improve energy dependent processes like growth and asexual development. However, the results of this study indicate that *ccg-9* does not play a role for either under a variety of conditions including stress and low carbon supply. Nevertheless, it could be possible that *ccg-9* still occupies a functional niche in trehalose metabolism. Its enzymatic properties may result in a very specific physiological advantage which was not identified in this study.

3.4 Conclusion and outlook

The first project aimed to explain rhythmic growth by clock control over the cell cycle. Studies have reported connections between the circadian clock and the cell cycle in mammalian cells but also in *Neurospora* (Matsuo et al., 2003; Prequeiro et al., 2006; Hong et al., 2014). However, first attempts to address this issue resulted in inconsistent observations with different luciferase assays. These may be caused either by technical (e.g. luciferase concentration) or by biological (e.g. by cellular redox state) circumstances or both. Furthermore, for evaluation of racetubes the spatial distribution

of the signal has to be considered as well, since the hyphal growth front forms a distinct cellular compartment compared to the vacuolized vegetative hyphae. The challenge for future experiments is to find natural growth conditions which still display native promoter activity.

Otherwise circadian growth could be the phenotypic manifestation of clock control over metabolism. The circadian clock of *Neurospora crassa* has been reported to control a variety of metabolic genes either directly or indirectly (Smith et al., 2010; Sancar et al., 2011). C*lock controlled gene-9* represented a promising candidate to test this hypothesis. However, in this study it was demonstrated that *ccg-9* did not have any obvious function in rhythmic growth and asexual development as it has been shown elsewhere (Shinohara et al., 2002). Nevertheless, *ccg-9* may have distinct functions in *Neurospora* which just do not show any phenotypic expression under the conditions tested. Moreover, the role of *ccg-9* in trehalose metabolism may be negligible due to functional redundancy of other enzymes. However, with its substrates it theoretically connects a variety of metabolic pathways. Glucose-1-phosphate for example can be converted to UDP-glucose, which is important as a metabolite in galactose and glucuronate metabolism as well as for the synthesis of glycogen and trehalose itself. The final question about the physiological role of *ccg-9*, however, remains speculative.

A functional cell cycle and metabolism are accepted as prerequisites for viable growth in any organism. However, the genetic interdependency between growth and cell cycle or metabolism becomes a complex issue because this project especially addresses the role of the circadian clock in this context. Therefore, the question is not whether metabolism or cell cycle are critical for growth behavior. It is rather interesting to know whether rhythmic growth is the result of circadian regulation of metabolism or cell cycle related genes. Several thousands of genes may be involved either in a direct or in an indirect manner. Hence, engineering suitable mutants for *in* vivo studies may be difficult. For future attempts it may be helpful to characterize the metabolism of *N. crassa* during circadian growth. High performance liquid chromatography (HPLC) as well as nuclear magnetic resonance (NMR) are powerful techniques for quantitative metabolomics and

have also been successfully applied to *Neurospora* (Schmit and Brody, 1975; Kim et al., 2011). Furthermore, modern high-throughput methods from metabolomics, fluxomics and proteomics allow a detailed analysis of metabolism and signaling pathways. Together with these data one may address this issue by rather using modern *in silico* methods of systems biology than with genetic models.

4 Materials and Methods

4.1 Media, stock solutions and buffers

4.1.1 Growth media

Standard liquid medium

3x Vogel´s salts		33.3 ml
3x L-arginine/HCl		33.3 ml
3x D-glucose monohydrate		33.3 ml

Standard solid medium for flasks and slants

D-glucose monohydrate		2.2 g
L-arginine/HCl		0.6 g
50x Vogel´s		2 ml
Biotin	ad	50 ng/ml
Agar		2 g
H_2O bidest.	ad	100 ml

Supplement with histidine to a final concentration of 0.5 mg/ml and then autoclave.

Race tube medium

50x Vogel´s		2 ml
L-arginine/HCl		0.17 g
D-glucose monohydrate		0.1 g
Biotin	ad	50 ng/ml
Agar		2.2 g
H_2O bidest.	ad	100 ml

Autoclave and pour 10 ml into a short race tube.

Bottom agar

50x Vogel´s		10 ml
L-arginine/HCl		1.8 g
Agar		7.5 g
H_2O bidest.	ad	450 ml

Autoclave and then add 50 ml 10x FIGS. When cooled down to 50°C add Hygromycin to a final concentration of 300 µg/ml if needed. Pour 25 ml into a petri dish.

Top agar

50x Vogel´s		5 ml
Sorbitol		45.5 g
Agar		7 g
H_2O bidest.	ad	225 ml

Autoclave and then add 25 ml 10x FIGS.

Crossing medium

5x Westergard´s		100 ml
Sucrose		2.5 g
Agar		10 g
Biotin	ad	50 ng/ml
H_2O bidest.	ad	500 ml

Autoclave and pour 25 ml into a petri dish.

Ascospore plating medium

50x Vogel´s		2 ml
Agar		1 g
H_2O bidest.	ad	90 ml

Autoclave, then add 10 ml 10x FIGS and, if needed, Hygromycin to a final concentration of 100 µg/ml.

Luciferase assay medium A

D-glucose-monohydrate		0.05 g
D-fructose		0.05 g
Sorbose		2 g
H_2O bidest.	ad	50 ml

Autoclave and store at 4°C.

Luciferase assay medium B

3x Vogel´s		33.3 ml
Biotin	ad	50 ng/ml
Agar		1.8 g
H_2O bidest.	ad	50 ml

Autoclave and mix 1:1 with medium A, add Luciferin to a final concentration of 150 µM.

LB medium

Tryptone		10 g
Yeast extract		5 g
NaCl		5 g
H_2O bidest.	ad	1000 ml

Autoclave and store at 4°C when opened. Add selection marker as needed.

YPD medium

Yeast extract		10 g
Peptone		20 g
D-glucose-monohydrate		20 g
H_2O bidest.	ad	1000 ml
pH to 5.8 with HCl		

Autoclave and store at room temperature.

SDC medium

D-glucose-monohydrate		20 g
Yeast nitrogen base w/o selection marker		6.7 g
H_2O bidest.	ad	1000 ml
pH to 5.8 with HCl		

Autoclave and store at room temperature.

SOB and SOC medium

Yeast extract		0.5 g
Tryptone		2 g
NaCl		58.4 mg
KCl		20 mg
autoclave, then add		
$MgCl_2$ 1 M		1 ml
$MgSO_4$ 1 M		1 ml
H_2O bidest.	ad	100 ml

To get SOC medium add 20 mM D-glucose.

4.1.2 Stock solutions

50x Vogel´s salts (Vogel, 1956)

Na_3citrate x $2H_2O$		123.5 g
KH_2PO_4		250 g
NH_4NO_3		100 g
$MgSO_4$ x 7 H_2O		10 g
$CaCl_2$ x 2 H_2O		5 g
Micronutrients		5 ml
Biotin	ad	0.25 µg/ml
H_2O bidest.	ad	1000 ml

Add some ml of chloroform for preservation and store at room temperature.

Media stocks

3x L-arginine/HCl	18 g on 1000 ml
3x D-glucose monohydrate	66 g on 1000 ml
3x Vogel´s	60 ml 50x Vogel´s complete to 1000 ml

Autoclave and store at room temperature.

10x FIGS

Sorbose		100 g
D-fructose		2.5 g
D-glucose (monohydrate)		2 g (3 g)
H_2O bidest.	ad	500 ml

Autoclave and store at 4°C.

5x Westergard´s (Westergard and Mitchell, 1947)

KNO_3		2.5 g
KH_2PO_4		2.5 g
$MgSO_4$ x 7 H_2O		1.25 g
NaCl		0.25 g
$CaCl_2$		0.25 g
Micronutrients		0.25 ml
H_2O bidest.	ad	500 ml

Do not autoclave and store at 4°C. The white precipitate is not harmful. It should be resuspended by shaking before preparing the medium to distribute it evenly.

Micronutrients stock

Citric acid x H_2O		5 g
$ZnSO_4$ x 7 H_2O		5 g
$(NH_4)_2Fe(SO_4)_2$ x 6 H_2O		1 g
$CuSO_4$ x 5 H_2O		0.25 g
$MnSO_4$ x H_2O		0.05 g
H_3Bo_3 (water-free)		0.05 g
Na_2MoO_4 x 2 H_2O		0.05 g
H_2O bidest.	ad	100 ml

Add 1 ml chloroform for preservation and store on 4°C.

4.1.3 Buffers

2x CTAB buffer

Tris/HCl 1 M, pH 7.5 - 8.0		10 ml	100 mM
CTAB		2 g	2%
NaCl		8.18 g	1.4 M
EDTA 0.5 M, pH 7.5 - 8.0		4 ml	20 mM
Sodium bisulfite		1 g	1%
H_2O bidest.	ad	100 ml	

50% PEG for yeast transformation

PEG 3800 (or 4000)		50 g	
H_2O	ad	100 ml	

sterile filtrate

4x Laemmli buffer

Tris/HCl 1 M, pH 6.8		20 ml	20 mM
Glycerol 87%		45 ml	40% v/v
SDS		8 g	8%
Bromophenol blue		0.04 g	0.04%
H_2O bidest.	ad	80 ml	

Add β-mercaptoethanol to a final concentration of 20% v/v.

10x LiAc buffer for yeast transformation

LiAc x $2H_2O$		10.2 g	1 M
adjust pH to 7.5 with acetic acid			
H_2O	ad	100 ml	

autoclave

Lysis buffer for protein purification

HEPES 1 M		50 ml	50 mM
NaCl		29.1 g	500 mM
Glycerol		400 ml	40% v/v
adjust pH to 7.0			
H_2O	ad	950 ml	
add fresh for lysis			
β-mercaptoethanol		331 µl	5 mM
Imidazol 4 M		5 ml	20 mM
Complete protease inhibitor (Roche)		10x	
DNaseI 5 mg/ml		1 ml	5 µg/µl
PMSF 1 M		1 ml	1 mM
H_2O	ad	1000 ml	

PEX buffer

HEPES 1 M, pH 7.4		50 ml	50 mM
NaCl		8 g	137 mM
EDTA 0.5 M pH 7.5 - 8.0		10 ml	5 mM
Glycerol 87%		116 ml	10% v/v
H_2O bidest.	ad	1000 ml	

Add protease inhibitors (Pepstatin A and Leupeptin to 5 µg/ml and PMSF to 5 mM) and if needed phosphatase inhibitors.

ECL solution

Tris/HCl 1M, pH 8.5		1 ml	100 mM
Cumaric acid 15 mg/ml		22 µl	
Luminol 44 mg/ml		50 µl	
H_2O_2 30%		3 µl	

Ponceau S

Trichloroacetic acid		3 g	3% w/v
Ponceau S			0.2% w/v
H_2O bidest.	ad	100 ml	

RNA precipitation buffer

NaCl		0.7 g	1.2 M
Na_3citrate x $2H_2O$		2 g	0.8 M
H_2O bidest.	ad	10 ml	

SDS gel electrophoresis buffer

Tris		60.55 g	50 mM
Glycine		288.3 g	384 mM
SDS		10 g	10% w/v
H_2O bidest.	ad	10 l	

SLN-I for yeast transformation

10x TE buffer	1 ml
10x LiAc buffer	1 ml
H_2O	8 ml

SLN-II for yeast transformation

10x TE buffer	1 ml
10x LiAc buffer	1 ml
50% PEG	8 ml

Storage buffer

HEPES 1 M		5 ml	50 mM
EDTA 0.5 M, pH 7.5 - 8		8 ml	4 mM
DTT		0.03 g	2 mM
NaCl		1.2 g	200 mM
Glycerol		40 ml	40% v/v
adjust pH to 7.0			
H_2O	ad	100 ml	

TB buffer (add ingredients in the listed order!)

PIPES		1.51 g	10 mM
$CaCl_2$		1.1 g	15 mM
KCl		9.32 g	250 mM
adjust pH to 6.7 with KOH			
$MnCl_2$		5.44 g	55 mM
H_2O bidest.	ad	500 ml	

Do not autoclave because this will oxidize the manganese. Sterile filtrate instead.

20x TBS buffer

Tris/HCl		48.4 g	200 mM
NaCl		348 g	3 M
adjust pH to 7.4 with HCl			
H_2O	ad	2 l	

10x TE buffer for yeast transformation

Tris		1.21 g	100 mM
Na_2-EDTA x $2H_2O$		0.37 g	10 mM
adjust pH to 7.5 with HCl			
H_2O	ad	100 ml	

autoclave

10x TEAM buffer

Triethanolamine		29.8 g	1 M
$MgCl_2$		0.95 g	50 mM
H_2O bidest.	ad	200 ml	

Transfer buffer for Western Blotting

Tris		24.2 g	20 mM
Glycin		112.6 g	150 mM
Methanol		2 l	20% v/v
SDS		8 g	0.08% w/v
H_2O bidest.	ad	10 l	

Yeast lysis buffer

LiCl		1.06 g	2.5 M
1 M Tris/HCl pH 8.0		500 µl	50 mM
Triton X-100		400 µl	
Na_2-EDTA x $2H_2O$		0.023 g	6.25 mM
H_2O bidest.	ad	10 ml	

4.2 Oligonucleotides

ccg-9 3' rev + vector	GCGGATAACAATTTCACACAGGAAACAGCGAATAAAGAAGCGCCACCCA
ccg9 3` fwd + TrpC	CACTTGTTTAGAGGTAATCCTTCTTTCTAGGCCGGTCATCTGATGGAC
ccg-9 3´ fwd + *hph*	CGACCGGGATCCACTTAACGTTACTGAAATCTCAGACAAAAGGTTGTGCCA
ccg-9 5' fwd + vector	GTAACGCCAGGGTTTTCCCAGTCACGACGCCAAATCATAACGCACGGAC
ccg-9 5' rev + eGFP	ACTCTCGGCATGGACGAGCTGTACAAGTAAAAAGTCACCTGGCTGTCAAG
ccg-9 5´rev + *hph*	CAAAAATGCTCCTTCAATATCATCTTCTGTGCTTGATGCTGCGATGAT
ccg-9 fwd qPCR	GGCCCAGCTTGAGACATACT
ccg-9 ORF fwd + p*QA*	CATCGCACCCAACCAGAGGTACCAAACACAATGGTTGATAGGGGGGAACC
ccg-9 ORF fwd + vector	GTAACGCCAGGGTTTTCCCAGTCACGACGATGGTTGATAGGGGGGAACC
ccg-9 ORF rev + Flag	GTAGTCTTTGTCATCATCGTCTTTGTAGTCAGCAGTAACCTCTGCCTTCTTC
ccg-9 probe	CATGCGTTTGGAGCCCAACG
ccg-9 rev qPCR	GGAGAGCAAGGTGTTGATGA
eGFP fwd + tubulin	TCACCAGATAATTCACATCCCGAAGCAAAGATGGTGAGCAAGGGCGAG
eGFP rev + vector	GTAACGCCAGGGTTTTCCCAGTCACGACGTTACTTGTACAGCTCGTCCATGC
Flag fwd	GCATGCGACTACAAAGACG
hph fwd	ACAGAAGATGATATTGAAGGAGCA
hph fwd + p*QA*	GACACCAGCGACTGCTTGTCAAGGACTCTAACAGAAGATGATATTGAAGGAGCA
hph rev + tubulin	ATCCAAGCCAACGAAGAGACTAGGAGCATAGATTTCAGTAACGTTAAGTGGATCC
p*Cyclin B* fwd Spe I	CCCCACTAGTTGTGCCATGTCAAAAACAG
p*Cyclin B* rev Not I	CCCCCGCGGCCGCCTTTAGGGAAATTACCAAAGAGA
p*Histone H1* fwd BamH I	CCCCGGATCCTATGATTTGGTTGAGGGATTT
p*Histone H1* rev Not I	CCCCCGCGGCCGCGACAAAAAGAAGGAATCAGCA
p*QA* fwd	TAGAGTCCTTGACAAGCAGTCGCT
p*QA* rev + vector	GCGGATAACAATTTCACACAGGAAACAGCTGTGTTTGGTACCTCTGGTTGGG
p*Tubulin* fwd BamH I	CCCCCCGGATCCTATGCTCCTAGTCTCTTCGTTGG
p*Tubulin* rev Not I	CCCCCCGCGGCCGCCTTTGCTTCGGGATGTGAAT
TrpC rev	CTAGAAAGAAGGATTACCTCTAAACAA
Tubulin fwd	TATGCTCCTAGTCTCTTCGTTGG
Tubulin rev	CTTTGCTTCGGGATGTGAAT

4.3 Plasmids

Plasmid	Backbone	Reference
pFH62		Heise F., unpublished work
p*frq*::*luc*	pFH62	Sancar et al., 2011
p*desat*::*luc*	pFH62	Sancar et al., 2011
p*tubulin*::*luc*	pFH62	this study
p*CycB*::*luc*	pFH62	this study
p*HistonH1*::*luc*	pFH62	this study
Δ*ccg-9*	pRS426	this study
p*QA-4*::*ccg-9-Flag*	pRS426	this study
p*ccg-9*::*ccg-9-Flag*	pRS426	this study
pRS426		Sikorski and Hieter, 1989

4.4 Strains

Strain	Genotype	Comment	Reference
frq^{+} *bd*	*ras*^{bd}, mat A		
frq^{10} *bd*	*ras*^{bd}, mat A	*frq* knockout by gene replacement	
p*frq*::*luc*	*ras*^{bd}, *His*$^{-}$, mat A		Sancar et al., 2011
p*desat*::*luc*	*ras*^{bd}, *His*$^{-}$, mat A		Sancar et al., 2011
p*tubulin*::*luc*	*ras*^{bd}, *His*$^{-}$, mat A		this study
p*CycB*::*luc*	*ras*^{bd}, *His*$^{-}$, mat A		this study
p*HistonH1*::*luc*	*ras*^{bd}, *His*$^{-}$, mat A		this study
ccg-9^{RIP}	*ras*^{bd}, *His*$^{-}$, mat A		Shinohara et al., 2002
Δ*ccg-9*	*ras*^{bd}, mating type undetermined, homokaryon	*ccg-9* knockout by gene replacement, progeny of *frq*$^{+}$ *bd* x *frq*$^{+}$ mus-52 *bd*, glufosinate sensitive	this study
p*QA-4*::*ccg-9-Flag*	*ras*^{bd}, *His*$^{-}$, p*frq*::*luc*, mat A, homokaryon	knockin by gene replacement, expresses C-terminal flag-tagged CCG-9	this study
p*ccg-9*::*ccg-9-Flag*	*ras*^{bd}, mating type undetermined, heterokaryon	knockin by gene replacement, expresses C-terminal flag-tagged CCG-9	this study
ΔNCU05041	OR74, *mus-51*, mat a, heterokaryon		Colot et al., 2006

4.5 Physiological methods

4.5.1 *Neurospora* growth conditions

For analysis of nucleic acids and proteins *Neurospora* was usually grown in submerged liquid cultures. We used Vogel`s minimal medium (Vogel, 1956) supplemented with 0.6% arginine and 2.2% glucose monohydrate as a carbon source if not stated differently. The cultures were grown with orbital shaking at 125 rpm, 25°C and constant light (LL, approx. 80 µE). Under these conditions *Neurospora* just grows in its vegetative form and conidiation is blocked. Hence, this setup allows steady state conditions over a broad range of growth parameters and is thereby most suitable to perform standard experiments on molecular biology or physiology of the organism. Mycelium was harvested with a filtering flask connected to a vacuum pump and directly frozen in liquid nitrogen.

For inoculation of liquid and solid media usually macroconidia were used, which were raised from solid cultures grown in 500 ml Erlenmeyer flask or a slant. If not stated differently for solid cultures we used standard solid medium containing Vogel`s salts supplemented with 2% glucose as a carbon source. For histidine auxotrophic mutants we supplemented histidine to a final concentration of 0.5 µg/ml. The cultures were grown at room temperature and constant light for 6 to 10 days. Conidia were harvested with 50 ml (flasks) 1 M sorbitol and filtered with sterile cheesecloth. For slants 2 ml 1 M sorbitol was used and the conidial suspension was directly poured into a reaction cup. Conidial suspensions were centrifuged at 4°C, 1500 g for 10 min for the first time, then washed twice with 50 ml or 1 ml of 1 M sorbitol and centrifuged at 4°C, 1500 g for 5 min.

4.5.2 Densitometry of growth cultures and conidial suspensions

For methods using *E. coli* or yeast exponentially growing liquid cultures were used. For this purpose optical density of the suspension was determined spectrophotometer at 420 nm with a 1 cm lightpath. An OD between 0.5 and 0.9 was considered to reflect the exponential growth phase.

For some experiments with *Neurospora* the density of conidial suspensions had to be determined in order to achieve a comparable inoculum for cultures. Densitometry was performed as described above. OD_{420} = 1 corresponds to a conidial density of 2.86 x 10^6/ml.

4.5.3 *E. coli* growth conditions

E. coli was grown on 37°C in liquid LB medium or on plates filled with LB agar. Liquid cultures were grown on an orbital shaker with 180 rpm overnight for 14 – 18 hours. If needed the medium was supplemented with ampicillin (to 100 µg/ml) or kanamycin (to 25 µg/ml) as selective markers. For further processing liquid cultures were harvested by centrifuging with 2000 g for 10 min.

4.5.4 *S. cerevisiae* growth conditions

Standard yeast cultures were grown in YPD medium on an orbital shaker with 120 rpm at 30°C and constant light. Under selection conditions yeast was grown on SDC agar or SDC liquid medium. In this study yeast was used for transformation only which is described later.

4.5.5 Crossing of *N. crassa*

Crosses were done to generate mutants with a desired genetic background and to yield homocaryotic strains. In order to cross, two strains of different mating type were needed, which are named “a” and “A”. Conidia of the strains to be crossed were inoculated on opposing sides in petri dishes filled with synthetic crossing medium (SCM). The plates were sealed with parafilm and placed on the bench to be subjected to room temperature and the daily light/dark cycles (L/D). As the vegetative mycelium grows they will eventually merge in the middle of the plate and form perithecia there. After a while the lid was exchanged by a clean one if needed because of intensive coverage with macroconidia. When ascospores became visible at the lid they were harvested with sterile water and heat activated by incubation at 60°C for 30 min. Afterwards they were spread on plating medium in a petri dish containing hygromycin as

a selection marker if needed. Colony formation was monitored daily and after two days clones were picked under a dissection microscope using a scalpel and a sterile inoculation loop. To yield a homokaryon it is necessary to select clones which have arisen from a single ascospore.

4.5.6 Determination of biomass grown in liquid culture

Biomass was determined by weighing the dry-weight of mycelial disks in liquid culture. Mycelial pads were obtained by inoculating 25 ml of standard Vogel`s medium with 0.5 x 10^6 conidia in a 50 ml reaction tube. The conidia were distributed homogenously by inverting the tube and the suspension was then filled into a 94 mm petri dish. The petri dish was then sealed with parafilm and the culture was incubated at 24°C and constant light for 48 h until a mycelial mat had formed.

Mycelial disks were stamped out with the top side (Ø approx. 8 mm) of a sterilized 1 ml pipette tip. At least five disks were immediately collected, dried at 80°C overnight and weighed to determine the mass of the starting material. Three mycelial disks were transferred into a 500 ml flask filled with 250 ml of medium consisting of Vogel`s salts supplemented with a single carbon source as indicated. The cultures were grown for 48 h, then harvested and dried at 80°C overnight to determine the dry weight on the next day.

4.5.7 Counting of macroconidia production in race tubes

Sterilized race tubes (with approx. 32 cm length) were filled with 10 ml race tube medium supplemented with indicated increments of glucose as a carbon source. Every race tube was inoculated with 1.5 x 10^6 of freshly harvested conidia. The conidia were allowed to hatch at 25°C, LL overnight (~ 16 h). From this starting point the cultures were grown for four more days (120 h) until they were harvested.

The harvesting procedure was started with filling the race tubes wit 10 ml of 1 M sorbitol followed by intense shaking. The race tubes were then placed on a teetering shaker at 4°C for 30 min. Afterwards of each race tube 2 ml of conidial suspension were transferred to a reaction cup and centrifuged for 10 min at 1500 g. Conidia were washed

with 1 ml of 1 M sorbitol and centrifugation was repeated for 5 min. The supernatant was removed completely and conidia were resuspended in 1 ml of 1 M sorbitol. The amount of conidia was determined photometrically at 420 nm.

4.5.8 Induction of macroconidiation

The method is based on a study performed by Berlin and Yanofsky in 1985 (Berlin and Yanofsky, 1985). Briefly, conidia from frq^{+} *bd* or *ccg-9*^{RIP} were harvested from cultures grown at 30°C DD in the first night and for 3 more days at 25°C, LL afterwards. Conidial density was determined photometrically. In a 1 l flask 300 ml of liquid culture (Vogel`s minimal medium with 0.75% sucrose as carbon source) were inoculated with 5 x 10^5 conidia of per ml. After 16 h of growth a first sample was taken. Petri dishes (Ø 94 mm) were filled with 10 ml of the above mentioned medium and with enough glass beads to cover approx. 75% of the bottom area. To start induction of conidiation 100 ml of wild type and approx. 170 ml (to compensate for the growth defect) of ccg-9^{RIP} culture were then harvested on a filter paper which was placed in the petri dishes. Petri dishes were placed in the incubator without a lid, just surrounded by moistened paper towel and covered with a huge petri dish (Ø 145 mm). Cultures were incubated in LL at 25°C and harvested 8 h and 24 h after commencement of induction.

4.5.9 Transformation of *Neurospora crassa*

To generate genetically modified strains of *Neurospora crassa*, macroconidia were transformed with linearized or circular DNA by electroporation. Conidia were harvested as described above and carefully purified to get rid of contaminating material and salts. Finally after the last centrifugation step the sorbitol was removed to yield a very viscous conidial suspension. For transformation 1 µg of DNA (the volume should not exceed 5 µl) and 70 µl of the suspension were pipetted into an electroporation cuvette. The mixture was incubated for 15 min on ice and then electroporated with 1.5 KV, 25 µF at 600 Ω. The conidia were immediately taken up in ice cold 1 M sorbitol. Then 200 µl of conidial suspension were pipetted into 10 ml of liquid top agar (Take care! The temperature should not exceed 50°C.), mixed by inverting several times and then

poured on bottom agar. The cultures were incubated at 30°C monitoring colony formation on a daily basis.

4.5.10 Generating *Neurospora* knockin- and knockout-strains by gene replacement

To create knockin- or knockout-strains frq$^+$ *bd* or frq$^+$ *bd mus-52* strains were used for primary transformation. The frq$^+$ *bd mus-52* lacks an enzyme which is involved in repair of DNA double-stranded breaks by non-homologous end-joining and shows a reduced number of ectopic construct insertions (Ninomiya Y. et al. 2004). Successfully transformed frq$^+$ *bd mus-52* strains were checked for homologous integration of the knockout construct. Afterwards they were backcrossed to wild type frq$^+$ *bd* to cross out the *mus-52* deletion and to yield a homokaryon. Since the *mus-52* deletion mediates Ignite- (glufosinate-) resistance, the strains were tested for growth on solid medium containing 250 µg/ml of Ignite. Ignite-sensitive strains were chosen for further work. When frq$^+$ *bd* was used for transformation, a homokaryon was generated by purification. For this purpose macroconidia were grown and spread on bottom agar under selective conditions. In all strains complete deletion of the wild type gene was tested by qPCR. Furthermore the copy number of the hygromycin resistance was analyzed to exclude ectopic insertions.

4.6 Biochemical and cellular assays

4.6.1 Luciferase assay for real-time gene expression monitoring

For this assay transcriptional fusion was used. Promoters were cloned into pFH62 plasmid to drive expression of the firefly luciferase. The plasmid was then transformed into a histidine auxotrophic mutant. Histidine autotrophs were picked and further selected for luciferase signal. To monitor luciferase signal in 96-well plates luciferase medium A and B were used supplemented with 150 µM luciferin. It is important to note, that the medium contains 0.02 g/ml sorbose as a growth inhibitor. In the presence of sorbose *Neurospora* grows slowly with a morphology similar to bacterial plaques

instead of fast filamentous growth with subsequent asexual development. This phenomenon is called “sorbose toxicity” and it prevents instant formation of conidia as these are metabolically inactive and will not give any luciferase signal at all. For race tube assays race tube medium with 0.1% glucose was used. Each well was inoculated with 20,000 freshly harvested conidia suspended in 2.5 µl of sorbitol. Conidia were allowed to hatch for 24 h at 25°C in constant darkness. Afterwards cultures were treated according to the synchronization scheme as indicated in the results part before recording was started.

4.6.2 Trehalose phosphorylase assay

This assay was performed with a discontinuous system. In a first reaction trehalose (50 mM final concentration) was used as a substrate either with or without inorganic phosphate (KH_2PO_4 50 mM final concentration) in a HEPES buffered solution (HEPES 25 mM, $MgCl_2$ 10 mM final concentration). 10 µg of purified protein were used for the assay. Control reactions were prepared either without substrate, without enzyme or with protein purified from a Δ*ccg-9* knockout strain (mock purification). The mixture was incubated at 30°C for 1.5 h with occasional shaking (1000 rpm, for 5 - 10 sec per min). Afterwards 5 µl of trehalose mixture were added to the second reaction:

1st reaction		
trehalose	[0.5 M]	5.0µl
KH_2PO_4/ H_2O	[0.2 M / -]	12.5µl
HEPES / $MgCl_2$	[50 mM / 20 mM]	25.0µl
enzyme / mock	[10 µg]	3.0µl
H_2O		4.5µl
		50.0µl
incubate at 30°C for 1.5 h		

2nd reaction		
1st reaction		5.0 µl
ATP	[50 mM]	0.4 µl
NADP	[20 mM]	1.0 µl
10x TEAM		2.0 µl
Hexokinase	[75 U/ml]	0.2 µl
G6P-DH	[35 U/ml]	0.4 µl
H_2O		11.5 µl
		20.0 µl
incubate at 30°C for 2 h		

Condensed water was centrifuged briefly in between. Finally the samples were immediately put on ice and OD_{340} was determined.

4.7 Methods of molecular biology

4.7.1 Generating chemocompetent *E. coli* cells

Chemocompetent cells were generated with a method found by Inoue and coworkers in 1990 (Inoue et al., 1990). From a preculture grown overnight 500 ml of SOB medium were inoculated to a density of OD_{600} = 0.1 in a 3 l baffled flask. The culture was grown for approximately 18 h at 18°C to reach a final OD_{600} of 0.6 and then cooled down on ice for 10 min. The cell suspension was centrifuged for 10 min at 2,500 g and 4°C, then the supernatant was discarded and the cells resuspended in 160 ml of ice cold TB buffer. Again the cells were incubated on ice for 10 min and centrifuged for 10 min at 2,500 g and 4°C. After discarding the supernatant cells were carefully resuspended in 40 ml of ice cold TB buffer and DMSO was added to a final concentration of 7%. After incubation on ice for further 10 min the cells were aliquoted to 50 µl and immediately frozen on liquid nitrogen. For long term storage the cells were kept on -80°C.

4.7.2 Transformation of chemocompetent *E. coli* cells

E. coli cells were thawn on ice for 15 min. To 50 µl of cell suspension 5 µl of plasmid solution was added. The cell suspension was mixed carefully and incubated on ice for 15 min. Then the cells were heat shocked for 90 sec, immediately placed on ice and incubated for further 5 min. 200 µl of SOC medium were added and the suspension was incubated in a shaker at 37°C for 60 min. The cells were then spread on LB agar plates containing the according selection marker.

4.7.3 Isolation of plasmid DNA from *E. coli* ("Miniprep" and "Midiprep")

Plasmids were isolated according to a kit protocol delivered with the NucleoBond® PC 20/100 kit (MACHEREY-NAGEL, Düren). After purification of the plasmid with a column the DNA was distributed evenly to 2 ml reaction tubes, precipitated by adding 0.7 volumes of isopropanol and pelleted by centrifugation for 30 min at 25,000 g and 4°C. Afterwards the pellet was washed with 1 ml of 70% EtOH, dried and dissolved in HPLC-grade water.

4.7.4 Preparation of genomic DNA extracts from *Neurospora crassa*

Genomic DNA was extracted from approx. 200 µl of ground mycelium by adding 500 µl of prewarmed (60°C) 2x CTAB buffer and incubating on 60°C for 30 min. Further 500 µl of a phenol/chloroform/isoamylalcohol (25:24:1) mixture were added and the samples were incubated on a turning wheel for 10 min at room temperature. After centrifugation at 2000 g for 10 min the aqueous supernatant was transferred to a fresh tube and the phenol-chloroforem extraction was repeated once. The final extract was incubated for 1 h with RNase A (1 µl from a 10 mg/ml stock on 1000 µl) at room temperature. DNA was precipitated by adding 0.7 volumes of isopropanol and mixing. The precipitate was finally pelleted by centrifuging for 30 min with 25,000 g at 4°C, washed with 70% EtOH, dried briefly and resolved in ultrapure water on 4°C overnight.

4.7.5 Polymerase chain reaction (PCR)

For routine polymerase chain reaction like for clone checks *Taq* polymerase (Bioron GmbH, Ludwigshafen) was used. Phusion® and Q5® high fidelity polymerases (New England Biolabs, Ipswich, USA) were used for cloning experiments. Reactions were performed based on the manufacturer`s protocol recommendations. Just the annealing temperature and the extension time were individually adjusted depending on the amplicon and the primers used. The basic protocols are depicted in the table below. Annealing temperatures were calculated using the NEB T_m calculator:
https://www.neb.com/tools-and-resources/interactive-tools/tm-calculator#.T_Pr8tlKFI4

polymerase	*Taq*	Phusion®	Q5®
initial denaturation	94°C, 2´	98°C, 30´	98°C, 30´
cycles	30x	35x	35x
denaturation	94°C, 10´´	98°C, 10´´	98°C, 10´´
annealing	55 - 68°C, 20´´	50 - 72°C, 30´´	50 - 72°C, 30´´
extension	1´/kb	30´´/kb	30´´/kb
final extension	72°C, 5´	72°C, 10`	72°C, 2´

Depending on complexity of the template extension times and template amount were varied. For plasmid DNA 1 – 10 ng per 50 µl reaction volume were used whereas for genomic DNA we used 50 – 100 ng. For genomic DNA as well as for long amplicons (>5 kb) extension time was increased.

A typical PCR mix was pipetted as depicted in the following scheme:

component	final conc.	volume
Template	[variable]	x µl
5 x buffer		10 µl
dNTPs	[200 µM each]	1 µl
fwd primer	[500 nM]	2.5 µl
rev primer	[500 nM]	2.5 µl
polymerase	[1 U]	0.5 µl
H_2O		50 - x µl
		50 µl

4.7.6 Purification of PCR products

PCR products were purified by using the Wizard® SV Gel and PCR purification system (Promega GmbH, Mannheim). The purification was performed according to the manufacturer´s protocol.

4.7.7 Determination of nucleic acid concentration

Concentration of dissolved nucleic acids was determined using a NanoDrop spectrophotometer. To assess the preparation quality, amount of impurities was analyzed by the OD 260/280 ratio was measured. For DNA a ratio of >1.8, for RNA a ratio >2.0 is considered as pure.

4.7.8 Molecular cloning

Restriction digestion of plasmid and insert DNA

For restriction digestion 1 µg of DNA was used for a 50 µl reaction. If possible at least two reactions were set up to compensate for a loss of material during the purification procedure. The reaction was performed for 1 h at 37°C with an excess of enzyme (approx. 1.5 U per 50 µl) to guarantee quantitative digestion of the products. Linearized plasmid DNA was dephosphorylated by adding 1.5 U of Calf Intestinal Phosphatase (CIP) directly to the restriction digestion mix and incubating for at least 30 more minutes. Restriction enzymes were heat inactivated if possible and DNA was purified over a column.

Ligation of plasmid and insert DNA

For ligation reactions 100 ng of linearized plasmid DNA were used. Insert DNA was added in molar excess of 1:3. The reaction mixture was incubated for 10 to 15 minutes at room temperature and immediately used for transformation of *E. coli* cells.

4.7.9 Preparing knockin- and knockout-constructs by yeast transformation

Yeast transformation

Yeast transformation has been performed according to published protocols (Colot et al., 2006). 50 ml YPD were inoculated with yeast grown in an overnight preculture to OD_{600} = 0.2. The culture was grown to OD_{600} = 0.7 - 0.8 and then centrifuged for 5 min at 3,600 g and room temperature. The cells were resuspended in 500 µl SLN-1 buffer and incubated in a turning wheel for 10 min at room temperature. After centrifugation

(3 min, 3,600 g, RT) the supernatant was discarded and the cells were resuspended in 250 µl SLN-2 buffer. For the transformation pRS426 plasmid was linearized with EcoRI and XhoI and purified. To 50 µl of yeast cells 120 ng plasmid, 20 to 50 ng of fragment DNA, 100 µg of salmon sperm DNA as well as 300 µl SLN-2 buffer were added and carefully mixed by pipetting. The mixture was incubated on a turning wheel for 30 min at room temperature followed by a heat shock at 42°C for 15 min and brief incubation on ice for 3 min 1 ml of H_2O was added and the suspension was centrifuged at 3,600 g for 3 min. The supernatant was discarded. The cell pellet was resuspended in 1 ml of YPD and the cells were incubated on 30°C for 1 h. After another centrifugation step (3,600 g, 3 min) the cells were resuspended in 150 µl of H_2O and spread out on a selective plate (SDC -Ura).

Yeast DNA preparation

To check for the successful recombination of PCR fragments to the desired construct 1.5 ml overnight cultures of yeast clones were grown. The suspensions were centrifuged for 30 sec at full speed and the pellet was resuspended in 100 µl of yeast lysis buffer. The same volume of a phenol/chloroform/isoamylalcohol mixture (25:24:1) and some glass beads (approx. 0.2 g) were added and the samples were vortexed for at least 2 min. After addition of 100 µl H_2O and subsequent vortexing (15 sec) the samples were centrifuged at full speed and room temperature for 5 min. The aqueous phase was then transferred to a fresh tube and 2.5 volumes of ice cold EtOH (100%) were added. For the precipitation the samples were incubated at 4°C on a rotation wheel for 15 min and then centrifuged at full speed and room temperature for 30 min. The pellet was washed with 1 ml of 70% EtOH, air dried and resolved in an appropriate volume of water.

4.7.10 Gene expression analysis

Preparing total RNA extracts

For total RNA extraction approximately 200 µl of ground mycelium was filled into a 2 ml reaction cup. 1 ml of FstTri RNA/DNA/Protein Extraction Reagent (Axon Labortechnik, Kaiserslautern) was added and the sample was shaken for 10 min at 800 rpm and room

temperature. 200 µl of chloroform were added, the sample was briefly vortexed and subsequently shaken for 5 min at 800 rpm and room temperature. Phases were separated by centrifugation at 12,000 g and 4°C for 20 min and the aqueous phase was transferred to a fresh reaction tube. RNA was precipitated by adding 250 µl isopropanol and 250 µl precipitation solution. The sample was incubated at room temperature for 10 min with shaking at 800 rpm and then centrifuged for 10 min at 12,000 g and 4°C. The supernatant was discarded and the pellet was washed twice with 75% EtOH, air dried for 3 min and resuspended in HPLC grade water supplemented with RNase inhibitor (80 U per 70 µl). Integrity of RNA was examined on an agarose gel, then samples were frozen in liquid nitrogen and stored at -80°C.

Single stranded cDNA synthesis

For reverse transcription of RNA the Maxima First Strand cDNA Synthesis Kit (Thermo Fisher Scientific Biosciences GmbH, St. Leon-Rot) was used. cDNA synthesis was performed as described in the manufacturer´s protocol using 1 µg of RNA, incubating for 10 min at 25°C followed by 50°C for 30 min. The reaction was terminated by heat inactivation on 85°C for 5min. cDNA was diluted 1:10 for use in qPCR and stored at -20°C.

Semiquantitative Real-Time PCR (qPCR)

qPCR was used for semiquantitative comparison of transcript abundance in different samples as well as for copy number estimation between different strains on a genomic level. For the qPCR reaction TaqMan probes were used that carried a 5´-FAM and a 3´-TAMRA label. Template amounts were 5 µl of 1:10 diluted cDNA (see above) or 50 ng of genomic DNA. Enzyme and nucleotides came with the TaqMan® Gene Expression Master Mix (Life Technologies GmbH, Darmstadt). The experiments were performed using a 96-well-plate format with triplicates for each sample and a reaction volume of 20 µl. As endogenous standard *28s* or *actin* RNA was taken for transcript determination or the *wc-1* locus for measuring the genomic copy number.

4.8 Protein analysis

4.8.1 Preparation of total protein extracts from *Neurospora crassa*

Total protein extracts were prepared by adding 500 µl PEX buffer supplemented with protease inhibitors to 500 µl of ground mycelium. The suspension was incubated on ice for 30 min with occasional vortexing and finally centrifuged with 10,000 g at 4°C for 10 min. The supernatant was transferred to a fresh tube and centrifugation was repeated with 20,000 g for 10 min at 4°C. The resulting supernatant was used for further protein analysis.

4.8.2 Preparation of protein extracts from asexual structures

Asexual structures were generated and isolated according to a method published by Bailey-Shrode and Ebbole (Bailey-Shrode and Ebbole, 2004). Briefly, mycelium grown in liquid Vogel´s medium was harvested on filter paper. Adding a second filter paper on top the mycelium was now placed in a petri dish containing solid Vogel´s medium supplemented with 1.5% sucrose and 0.45% agar. As conidial structures grew through the top filter paper they were carefully harvested using a scalpel and frozen in liquid nitrogen for further processing. Total protein extracts were prepared as described above.

4.8.3 Determination of protein concentration

Protein concentration was determined by the Bradford method (Bradford, 1976). For this purpose a 5x Bradford reagent (Carl Roth GmbH & Co. KG, Karlsruhe) was diluted and filtered. For the assay samples were diluted 1:10 and 10 µl of the dilution were added to 990 µl of Bradford reagent. The samples were incubated for 5 min at room temperature and then the OD_{595} was measured with a spectrophotometer using a 1 cm lightpath. The protein concentration was calculated in mg/ml by multiplying the OD with an empirical value of 42.

4.8.4 SDS polyacrylamide gel electrophoresis (SDS-PAGE)

Discontinuous SDS-PAGE was performed according to Laemmli (Laemmli, 1970). For this purpose large gels were used that allow separation of proteins over a distance of about 10 – 12 cm and a stacking gel with a length of about 2 cm. The recipe for a commonly used SDS gel with 12/0.5% acrylamide is depicted below.

1M Tris pH 8.8	6.5 ml
H_2O	3.4 ml
30 % acrylamide, 0.5% bisacrylamide	6.8 ml
10 % SDS	167 µl
10 % APS	200 µl
TEMED	20 µl

For a gel with 14 lanes 300 µg of protein were loaded, for 18 and more lanes 200 µg were sufficient. The total protein lysates were adjusted to the same volume with PEX buffer before 4x Laemmli buffer was added. The total protein lysates were adjusted to the same volume with PEX buffer before 4x Laemmli buffer was added. Then the samples were boiled on 95°C for 5 min and loaded on the gel. The proteins were allowed to migrate into the stacking gel with an initial voltage of 80 V until the running front reached the resolving gel. Separation of the proteins was performed with 200 V or with the current limited to 4 mA overnight.

4.8.5 Transfer of proteins to a nitrocellulose membrane – Western Blotting

After SDS gel electrophoresis proteins were blotted on a nitrocellulose membrane by using a semi-dry approach. The membrane as well as the SDS gel were preincubated in blot buffer for 5 min. For the blot a sandwich assembly was used with the gel and the membrane surrounded by three Whatman® paper on top and on the bottom. Each layer was saturated properly with blot buffer and bubbles were removed carefully with a glass slant. The lid of the chamber was firmly put on top of the sandwich and arrested (but not pressed down!) with screws. The transfer was done with 300 mA for 2.5 h. Success of

the transfer was examined by staining the membrane with Ponceau S solution. The Ponceau S was washed off with blot buffer and the membrane was washed twice with TBS to prepare for further analysis.

4.8.6 Immunodetection of proteins

Immobilized proteins were detected by tandem immunolabelling with specific antibodies. To avoid unspecific binding of the antibodies to the membrane the latter was blocked by incubation in 5% milk powder in TBS for 45 min. Afterwards, the first antibody was added and the membrane was incubated for further two hours or overnight. Free antibody was washed off four times with TBS for 5 min. The membrane was incubated in the secondary antibody, to which the horse radish peroxidase is coupled, for 1.5 h at room temperature. Then it was washed four times with TBS for 5 min. Proteins were detected by chemiluminescence using ECL solution. For this purpose the TBS was drained from the membrane by a paper towel and the membrane was incubated in the ECL solution for 20 sec. The signal was exposed to Super RX films (Fujifilm, Düsseldorf).

4.8.7 Purification of proteins from total extracts

Histidine-tagged proteins were purified from total extracts using a HisTrap^{TM} FF column prepacked with a Ni Sepharose^{TM} 6 Fast Flow matrix (GE Healthcare Bio-Sciences, Uppsala, Sweden). For protein purification a modified lysis buffer was used compared to standard PEX buffer (see above). Ground mycelium was resuspended in 100 ml buffer and incubated on ice for 30 min with occasional vortexing. The suspension was centrifuged for 15 min at 3,000 g at 4°C and the supernatant was transferred to clean tubes. The pellets were resuspended in further 100 ml buffer and extraction was repeated for further 30 min followed by centrifugation for 15 min at 3,500 g and 4°C. All supernatants were pooled and centrifuged for 30 min at 64,000 g and 4°C. Supernatants were transferred to clean tubes and stored on ice until used.

The column (1 ml) was washed with 5 ml water and subsequently equilibrated with 10 ml lysis buffer (no β-mercaptoethanol!). Extracts were loaded with a flow-rate of 0.75 ml/min and the flowthrough was collected. Subsequent steps were performed with a flow-rate of 1 ml/min. For a first washing step the column was washed with 10 ml high-salt buffer (lysis buffer + 1000 mM NaCl + 5 mM β-mercaptoethanol). The first 2.5 ml were discarded (W_0) and the rest was collected (W_1). Subsequently the column was washed with 3 ml lysis buffer (+ 5 mM β-mercaptoethanol) (W_2). Proteins were eluted using 3.5 ml elution buffer (lysis buffer + 250 mM imidazole + 5 mM β-mercaptoethanol) per fraction. The first 2.5 ml were discarded directly (E_0). Then the column was incubated for 30 min before elution of the subsequent fraction was started (E_1, E_2…). Elution fractions E_1 and E_2 were directly rebuffered using a PD-10 desalting column (GE Healthcare Bio-Sciences, Uppsala, Sweden) and stored at -80°C.

4.9 Bioinformatical methods

4.9.1 Analysis of bioluminescence traces

For detrending and rhythm analysis of bioluminescence traces MultiCycle™ software (revision 1.39, Actimetrics Inc., Illinois, USA) was used. The traces were plotted as the running average based on a 24 h periodicity without smoothing.

4.9.2 Multiple sequence alignments

Sequence alignments were performed using the online tool ClustalW2 with the default settings (www.ebi.ac.uk/Tools/msa/clustalw2).

4.9.3 Analysis of RNAseq data (Sancar, 2014)

The analysis of RNAseq data was based on reads which could be mapped to annotated exons of a *N. crassa* NC10 genome. For aligning the sequence reads Bowtie was used (Langmead et al., 2009). The samples were normalized based on the size factor formula (Anders and Huber, 2010). Genes induced during asexual development at 8h or

24h were identified by differential gene expression analysis. A non-negative binomial distribution (NB) was assumed for the number of reads (G_i).

$$Gi \approx \mathrm{NB}(\mu i, \sigma i) \quad \text{with } \mu i = \text{mean and } \sigma i = \text{variance}$$

Even though two biological replicates were available the variance of the datasets was estimated using Local Regression and Likelihood analysis (locfit) with R. The two-sided p-value was calculated using an adapted form of the “exact” test (Robinson and Smyth, 2008).

$$p = \frac{\sum_{f(a,b) \leq f(G_{i,treat}, G_{i,control})} f(a\,, b)}{\sum f(a\,, b)}$$

$a + b = G_{i,treat} + G_{i,control}$ with $a, b \in 0\ldots(G_{i,treat} + G_{i,control})$.
$G_{i,treat}$ and $G_{i,control}$ are the read counts of any mapped gene after air exposure (8h and 24h) or under control conditions (0h).
$f(a, b) = f(a) \times f(b)$

Genes with a p-value of $p < 0.05$ were considered significantly induced after 8h or 24h compared to control conditions (0h).

4.9.4 Statistics

Statistical analysis was performed using GraphPad Prism for Windows (GraphPad Software, San Diego, California, USA, revision 4.03, 2005). Variance between paired groups was analyzed with a 2-way ANOVA including the Bonferroni post-test. $p < 0.05$ was considered as a significant difference.

5 References

1. Anders, S., and Huber, W. (2010). Differential expression analysis for sequence count data. *Genome Biol* **11**(10): R106

2. Bailey, L. A., and Ebbole, D. J. (1998). The fluffy gene of *Neurospora crassa* encodes a Gal4p-type C6 zinc cluster protein required for conidial development. *Genetics* **148**(4): 1813-20

3. Bailey-Shrode, L., and Ebbole, D. J. (2004). The fluffy gene of *Neurospora crassa* is necessary and sufficient to induce conidiophore development. *Genetics* **166**(4): 1741-9

4. Ballario, P., Talora, C. Galli, D., Linden, H., and Macino, G. (1998). Roles in dimerization and blue light photoresponse of the PAS and LOV domains of *Neurospora crassa* white collar proteins. *Mol Microbiol* **29**(3): 719-29

5. Ballario, P., Vittorioso, P., Magrelli, A., Talora, C., Cabibbo, A., and Macino, G. (1996). White collar-1, a central regulator of blue light responses in *Neurospora*, is a zinc finger protein. *EMBO J* **15**(7): 1650-7

6. Baylis, J. R., and DeBusk, A. G. (1967). Estimation of the frequency of multinucleate conidia in microconidiating strains. *Neurospora Newslett* **11**: 9.

7. Beadle, G. W., and Tatum, E. L. (1945). *Neurospora.* 2. Methods of producing and detecting mutations concerned with nutritional requirements. *Am J Bot* **31**: 678-686

8. Belden, W. J., Larrondo, L. F., Froehlich, A. C., Shi, M., Chen, C. H., Loros, J. J., and Dunlap. J. C. (2007). The band mutation in Neurospora crassa is a dominant allele of ras-1 implicating RAS signaling in circadian output. *Genes Dev* **21**(12): 1494-505

9. Bell, W. et al. (1992). Characterization of the 56-kDa subunit of yeast trehalose-6-phosphate synthase and cloning of its gene reveal its identity with the product of CIF1, a regulator of carbon catabolite inactivation. *Eur J Biochem* **209**(3): 951-9

10. Bell-Pedersen, D., Shinohara, M. L., Loros, J. J., and Dunlap, J. C. (1996). Circadian clock-controlled genes isolated from Neurospora crassa are late night- to early morning-specific. *Proc Natl Acad Sci* **93**(23): 13096-101

11. Belocopitow, E., and Marechal, L. R. (1970). Trehalose phosphorylase from Euglena gracilis. *Biochem Biophys Acta* **198**(1): 151-4

12. Bennett, L. D., Beremand, P., Thomas, T. L., and Bell Pedersen, D. (2013). Circadian activation of the mitogen-activated protein kinase MAK-1 facilitates rhythms in clock-controlled genes in Neurospora crassa. *Eucaryot Cell* **12**(1): 59-69

13. Berlin, V., and Yanofsky, C. (1985). Isolation and characterization of genes differentially expressed during conidiation of Neurospora crassa. *Mo Cell Biol* **5**(4): 849-55

14. Berlin, V., and Yanofsky, C. (1985). Protein changes during the asexual cycle of Neurospora crassa. *Mol Cell Biol* **5**(4): 839-48

15. Blazquez, M. A., Lagunas, R., Gancedo, C., and Gancedo, J. M. (1993). Trehalose-6-phosphate, a new regulator of yeast glycolysis that inhibits hexokinases. *FEBS Lett* **329**(1-2): 51-4

16. Blazquez, M. A., Santos, E., Flores, C. L., Martinez-Zarpater, J. M., Salinas, J., and Gancedo, C. (1998). Isolation and molecular characterization of the Arabidopsis TPS1 gene, encoding trehalose-6-phosphate synthase. *Plant J* **13**(5): 685-9

17. Borkovich, K. A. et al. (2002). Lessons from the genome sequence of Neurospora crassa: tracing the path from genomic blueprint to multicellular organism. *Microbiol Mol Biol Rev* **68**(1): 1-108

18. Brand, W. H. (1953). Zonation in a prolineless strain of *Neurospora*. *Mycologia* **45**(2): 194-208

19. Cabib, E., and Leloir, L. F. (1959). The biosynthesis of trehalose phosphate. *J Biol Chem* **231**(1): 259-75

20. Candy, D. J., and Kilby, B. A. (1959). Site and mode of trehalose biosynthesis in the locust. *Nature* **183**(4675): 1594-5

21. Carpenter, J. F., and Crowe, J. F. (1989). An infrared spectroscopic study of the interactions of carbohydrates with dried proteins. *Biochemistry* **28**(9): 3916-22

22. Castro-Longoria, E., Brody, S., and Bartnicki-Garcia, S. (2007). Kinetics of circadian band development in *Neurospora crassa*. *Fungal Genet Biol* **44**(7): 672-81

23. Castro-Longoria, E., Brody, S., and Bartnicki-Garcia, S. (2005). Kinetics of circadian band development in Neurospora crassa. *Fungal Genet Biol* **44**(7): 672-81

24. Colombo, S., Ronchetti, D., Thevelein, J. M., Winderickx, J., and Martegani, E. (2004). Activation state of the Ras2 protein and glucose-induced signaling in Saccharomyces cerevisiae. *J Biol Chem* **279**(45): 46715-22

25. Colot, H. V., et al. (2006). A high-throughput gene knockout procedure for *Neurospora* reveals functions for multiple transcription factors. *Proc Natl Acad Sci USA* **103**(27): 10352-7

26. Correa, A., and Bell-Pedersen, D. (2002). Distinct signaling pathways from the circadian clock participate in regulation of rhythmic conidiospore development in Neurospora crassa. *Eucaryot Cell* **1***(*2): 273-80

27. Czupryna, J., and Tsourkas, A. (2011). Firefly luciferase and RLuc8 exhibit differential sensitivity to oxidative stress in apoptotic cells. *PloS One* **6**(5): e20073

28. d´Enfert, C., Bonini, B. M., Zapella, P. D., Fontaine, T., da Silva, M., and Terenzi, H. F. (1999). Neutral trehalases catalyze intracellular trehalose breakdown in the filamentous fungi Aspergillus nidulans and Neurospora crassa. *Mol Microbiol* **32**(3): 471-83

29. Davis, R. H. (2000). *Neurospora*, contributions of an model organism. New York, *Oxford University Press*

30. De Virgilio, C., Hottiger, T., Dominquez, J., Boller, T., and Wiemken, A. (1994). The role of trehalose synthesis for the acquisition of thermotolerance in yeast. I. Genetic evidence that trehalose is a thermoprotectant. *Eur J Biochem* **219**(1-2): 179-86

31. Dean Allison, S., Chang, B., Randolph, T. W., and Carpenter, J. F. (1999). Hydrogen bonding between sugar and protein is responsible for inhibition of dehydration-induced protein unfolding. *Arch Biochem Biophys* **365**(2): 289-98

32. dÉnfert, C., Bonini, B. M., Zapella, P. D., Fontaine, T., da Silva, A. M., and Terenzi, H. F. (1999). Neutral trehalases catalyse intracellular trehalose breakdown in the filamentous fungi Aspergillus nidulans and Neurospora crassa. *Mol Microbiol* **32**(3): 471-83

33. Dong, W., Qu, Y. B., and Gao, P. J. (1995). Regulation of cellulase synthesis in mycelial fungi: participation of ATP and cyclic-AMP. *Biotechnol Lett* **17**: 593-598

34. Eastmond, P. J., et al. (2002). Trehalose-6-phosphate synthase 1, which catalyses the first step in trehalose synthesis, is essential for Arabidopsis embryo maturation. Plant J **29**(2): 225-35

35. Eis, C., and Nidetzky, B. (1999). Characterization of trehalose phosphorylase from Schizophyllum commune. *Biochem J* **341**(Pt2): 385-93

36. Elbein, A. D. (1974). The metabolism of α,α-trehalose. *Adv Carbohyd Chem Biochem* **30**: 227-56

37. Enright, J. T. (1967). Temperature compensation in short-duration time-measurement by an intertidal amphipod. *Science* **156**(3781): 1510-2

38. Flavell, R. B., and Woodward, D. O. (1971). Metabolic role, regulation of synthesis, cellular localization, and genetic control of the glyoxylate cycle enzymes in *Neurospora crassa*. *J Bacteriol* **105**(1): 200-10

39. Froehlich, A. C., Liu, Y., Loros, J. J., and Dunlap, J. C. (2002). White Collar-1, a circadian blue light photoreceptor, binding to the frequency promoter. *Science* **297**(5582): 815-9

40. Froehlich, A. C., Loros, J. J., and Dunlap, J. C. (2003). Rhythmic binding of a WHITE COLLAR-containing complex to the frequency promoter is inhibited by FREQUENCY. *Proc Natl Acad Sci USA* **100**(10): 5914-9

41. Garceau, N. Y., Liu, Y., Loros, J. J., and Dunlap, J. C. (1997). Alternative initiation of translation and time-specific phosphorylation yield multiple forms of the essential clock protein FREQUENCY. *Cell* **89**(3): 469-76

42. Giæver, H. M., Styrvold, O. B., Kaasen, I., and Ström, A. M. (1988). Biochemical and genetic characterization of osmoregulatory trehalose synthesis in Escherichia coli. *J Bacteriol* **170**(6): 2841-9

43. Gooch, V. D., et al. (2008). Fully codon-optimized luciferase uncovers novel temperature characteristics of the Neurospora clock. *Eucaryot Cell* **7**(1): 28-37

44. Gooch, V. D., et al. (2014). A kinetic study of the effects of light on circadian rhythmicity of the frq promoter of Neurospora crassa. *J Biol Rhythms* **29**(1): 38-48

45. Görl, M., Merrow, M., Huttner, B., Johnson, J., Roenneberg, T., and Brunner, M. (2001). A PEST-like element in FREQUENCY determines the length of the circadian period in *Neurospora crassa*. *EMBO J* **20**(24): 7074-84

46. Hager, K. M., and Yanofsky, C. (1990). Genes expressed during conidiation in Neurospora crassa: molecular characterization of con-13. *Gene* **96**(2): 153-9

47. Hanks, D. L., and Sussaman, A. S. (1969). Control of trehalase synthesis in *Neurospora crassa*. *Amer J Bot* **56**(10): 1160-66

48. Harmer, S. L. et al. (2000). Orchestrated transcription of key pathways in *Arabidopsis* by the circadian clock. *Science* **290**(5499): 2110-3

49. He, Q., Cheng, P., Yang, Y., Wang, L., Gardner, K. H., and Liu, Y. (2002). White collar-1, a DNA binding transcription factor and a light sensor. *Science* **297**(5582): 840-3

50. Heise, F. (2007). Subzelluläre Verteilung des zentralen Uhrenproteins FREQUENCY in der circadianen Uhr von Neurospora crassa. PhD thesis, University of Heidelberg, Germany

51. Hong, C. I., et al. (2014). Circadian rhythms synchronize mitosis in Neurospora crassa. *Proc Natl Acad Sci USA* **111**(4): 1397-402

52. Hottiger, T., Boller, T., and Wiemken, A. (1987). Rapid changes of heat and desiccation tolerance correlated with changes of trehalose content in Saccharomyces cerevisiae cells subjected to temperature shifts. *FEBS Lett* **210**(1): 113-5

53. Hurley, J. M., et al. (2014). Analysis of clock-regulated genes in Neurospora reveals widespread posttranscriptional control of metabolic potential. *Proc Natl Acad Sci USA* **111**(48): 16995-7002

54. Kaasen, I., Falkenberg, P., Styrvold, O. B., and Ström, A. R. (1992). Molecular cloning and physical mapping of the otsBA genes, which encode the osmoregulatory trehalose pathway of Escherichia coli: evidence that transcription is activated by katF (AppR). *J Bacteriol* **174**(3): 889-98

55. Kandror, O., DeLeon, A., and Goldberg, A. L. (2002). Trehalose synthesis is induced upon exposure of *Escherichia coli* to cold and is essential for viability at low temperatures. *Proc Natl Acad Sci USA* **99**(15): 9727-32

56. Kim, J. D., Kaiser, K., Larive, C. K., and Borkovich, K. A. (2011). Use of 1H nuclear magnetic resonance to measure intracellular metabolite levels during growth and asexual sporulation in Neurospora crassa. *Eucaryot Cell* **10**(6): 820-31

57. Koike, N., Yoo, S. H., Huang, H. C., Kumar, V., Lee, C., Tim, T. K., and Takahashi, J. S. (2012). Transcriptional architecture and chromatin landscape of the core circadian clock in mammals. *Science* **338**(6105): 349-54

58. Langmead, B., Trapnell, C., Pop, M., and Salzberg, S. L. (2009). Ultrafast and memory-efficient alignment of short DNA sequences to the human genome. *Genome Biol* **10**(3): R25

59. Larrondo, L. F., Loros, J. J., and Dunlap, J. C. (2012). High-resolution spatiotemporal analysis of gene expression in real time: in vivo analysis of circadian rhythms in Neurospora crassa using a FREQUENCY-luciferase translational reporter. *Fungal Genet Biol* **49**(9): 681-3

60. Linden, H., and Macino, G. (1997). White collar 2, a partner in blue-light signal transduction, controlling expression of light-regulated genes in *Neurospora crassa*. *EMBO J* **16**(1): 98-109

61. Liu, Y., Garceau, N. Y., Loros, J. J., and Dunlap, J. C. (1997). Thermally regulated translational control of FRQ mediates aspects of temperature responses in the Neurospora circadian clock. *Science* **89**(3): 477-86

62. Liu, Y., Loros, J., and Dunlap, J. C. (2000). Phosphorylation of the *Neurospora* clock protein FREQUENCY determines its degradation rate and strongly influences the period length of the circadian clock. *Proc Natl Acad Sci USA* **97**(1): 234-9

63. Madi, L., McBride, S. A., Bailey, L. A., and Ebbole, D. J. (1997). Rco-3, a gene involved in glucose transport and conidiation in Neurospora crassa. *Genetics* **146**(2): 499-508

64. Maerz, S., et al. (2008). The nuclear Dbf2-related kinase COT1 and the mitogen-activated protein kinases MAK1 and MAK2 genetically interact to regulate filamentous growth, hyphal fusion and sexual development in Neurospora crassa. *Genetics* **179**(3): 1313-25

65. Malzahn, E., and Ciprianidis, S., Kaldi, K., Schafmeier, T., and Brunner, M. (2010). Photoadaptation in *Neurospora* by competitive interaction of activating and inhibitory LOV domains. *Cell* **142**(5): 762-72

66. Mandels, G. R., Vitols, R., and Parrish, F. W. (1965). Trehalose as an endogenous reserve in spores of the fungus Myrothecium verrucaria. *J Bacteriol* **90**(6): 1589-98

67. Maruta, K., Mitsuzumi, H., Kubota, M., Chaen, H., Fukuda, S., Sugimoto, T., and Kurimoto, M. (1996). Cloning and sequencing of a cluster of genes encoding novel enzymes of trehalose biosynthesis from thermophilic archaebacterium Sulfolobus acidocaldarius. *Biochem Biophys Acta* **1291**(3): 177-81

68. Matsuo, T., Yamaguchi, S., Mitsui, S., Emi, A., Shimoda, F., and Okamura, H. (2003). Control Mechanism of the Circadian Clock for Timing of Cell Division *in Vivo*. *Science* **302**(5643): 255-59

69. McDonald, M. J., and Rosbash, M. (2001). Microarray analysis and organization of circadian gene expression in *Drosophila*. *Cell* **107**(5): 567-78

70. Nishimoto, T., Nakano, M., Nakada, T., Chaen, H., Fukuda, S., Kurimoto, M., and Tsujisaka, Y. (1996). Purification and properties of a novel enzyme, trehalose synthase, from Pimelobacter sp. R48. *Biosci Biotechnol Biochem* **60**(4): 640-4

71. Olmedo, M. et al. (2010). Regulation by blue light of the fluffy gene encoding a major regulator of conidiation in Neurospora crassa. *Genetics* **184**(3): 651-8

72. Park, G., et al. (2011). Global analysis of serine-threonine protein kinase genes in Neurospora crassa. *Eucaryot Cell* **10**(11): 1553-64

73. Park, G., Pan, S., and Borkovich, K. A. (2008). Mitogen-activated protein kinase cascade required for regulation of development and secondary metabolism in Neurospora crassa. *Eukaryot Cell* **10**(11): 1553-64

74. Phillips, C. M., Iavarone, A. T., and Marletta, M. A. (2011). Quantitative proteomic approach by cellulose degradation in *Neurospora crassa. J Proteome Res* **10**(9): 4177-85

75. Plesofsky, N., and Brambl, R. (1999). Glucose metabolism in Neurospora is altered by heat shock and by disruption of HSP30. *Biochem Biophys Acta* **1449**(1): 73-82

76. Prequeiro, A. M., Liu, Q., Baker, C. L., Dunlap, J. C., and Loros, J. J. (2006). The Neurospora checkpoint kinase 2: A regulatory link between the circadian and cell cycles. *Science* **313**(5787): 644-9

77. Purvis, J. E., Yomano, L. P., and Ingram, L. O. (2005). Enhanced Trehalose Production Improves Growth of Escherichia coli under Osmotic Stress. *Appl Environ Microbiol* **71**(7): 3761-9

78. Qu, Q., Lee, S. J., and Boss, W. (2004). TreT, a novel trehalose glycosyltransferring synthase of the hyperthermophilic archaeon Thermococcus litoralis. *J Biol Chem* **279**(46): 47890-7

79. Querfurth, C., Diernfellner, A. C., Gin, E., Malzahn, E., Höfer, T., and Brunner, M. (2011). Circadian conformational change of the *Neurospora* clock protein FREQUENCY triggered by clustered hyperphosphorylation of a basic domain. *Mol Cell* **43**(5): 713-22

80. Querfurth, C., Diernfellner, A., Heise, F., Lauinger, L., Neiss, A., Tataroglu, O., Brunner, M., and Schafmeier, T. (2007). Posttranslational regulation of *Neurospora* circadian clock by CK1a-dependent phosphorylation. *Cold Spring Harb Symp Quant Biol* 72: 177-83

81. Ring, R. A. (1977). Cold hardiness of the bark beetle scolytus ratzeburgi coleoptera scolytidae. *Norw J Ent* **24**(2): 125-36

82. Roberts, A. N., Berlin, V., Hager, K. M., and Yanofsky, C. (1988). Molecular analysis of a Neurospora crassa gene expressed during conidiation. *Mol Cell Biol* **8**(6): 2411-8

83. Robinson, M. D., and Smyth, G. K. (2008). Small-sample estimation of negative binomial dispersion, with applications to SAGE data. *Biostatistics* **9**(2): 321-32

84. Rossier, C., Oulevey, N., and Turian, G. (1973). Electron microscopy of selectively stimulated microconidiogenesis in wild type *Neurospora crassa*. *Arch Mikrobiol* **91**(4): 345-353

85. Rudolph, B. R., Chandrasekhar, E., Gaber, B. P., and Nagumo, M. (1990). Molecular modelling of saccharide-lipid interactions. *Chem Phys Lipids* **53**(2-3): 243-61

86. Ruepp, A., et al. (2004). The FunCat, a functional annotation scheme for systematic classification of proteins from whole genomes. *Nucleic Acids Res* **32**(18): 5539-45

87. Saito, K., Yamazaki, H., Ohnishi, Y., Fujimoto, S., Takahashi, E., and Horinouchi, S. (1998). Production of trehalose synthase from a basidiomycete, Grifola frondosa, in Escherichia coli. *Appl Microbiol Biotechnol* **50**(2): 193-8

88. Sancar, G. et al. (2011). A global circadian repressor controls antiphasic expression of metabolic genes in Neurospora. *Mol Cell* **44**(5): 687-97

89. Sancar, G., et al. (2012). A global circadian repressor controls antiphasic expression of metabolic genes in Neurospora. *Mol Cell* **44**(5): 687-97

90. Sancar, S. (2014). GATA type transcription factors SUB1 and WCC cooperate in nucleosome dynamics and transcription activation. PhD thesis, University of Heidelberg, Germany

91. Sargent, M. L., and Woodward, D. O. (1969). Gene-enzyme relationships in *Neurospora*. *J Bacteriol* **97**(2): 867

92. Schafmeier, T., Diernfellner, A., Schäfer, A., Dintsis, O., Neiss, A., and Brunner, M. (2008). Posttranslational regulation of *Neurospora* circadian clock by CK1a-dependent phosphorylation. *Genes Dev* **22**(24): 3397-402

93. Schafmeier, T., Haase, A., Kaldi, K., Scholz, J., Fuchs, M., and Brunner, M. (2005). Transcriptional feedback of Neurospora circadian clock gene by phosphorylation-dependent inactivation of its transcription factor. *Cell* **122**(2): 235-46

94. Schmit, J. C., and Brody, S. (1975). Neurospora crassa conidial germination: role of endogenous amino acid pools. *J Bacteriol* **124**(1): 232-42

95. Schmoll, M., Schuster, A. Silva Rdo, N., and Kubicek, C. P. (2009). The G-alpha protein GNA3 of Hypocrea jecorina (Anamorph Trichoderma reesei) regulates cellulase gene expression in the presence of light. *Eucaryot Cell* **8**(3): 410-420

96. Schuster, A., Tisch, D., Seidl-Seiboth, V., Kubiceck, C. P., and Schmoll, M. (2012). Roles of protein kinase A and adenylate cyclase in light-modulated cellulase regulation in Trichoderma reesei. *Appl Environ Microbiol* **78**(7): 2168-78

97. Shear, C. L., and Dodge, O. B. (1927). Life histories and heterothallism of the red bread-mold fungi of the *Monilia sitophila* group. *J Agric Res* **34**: 1019-1042

98. Shi, L., Sutter, B. M., Ye, X., and Tu, B. P. (2010). Trehalose is a key determinant of the quiescent metabolic state that fuels cell cycle progression upon return to growth. *Mol Biol Cell* **21**(12): 1982-90

99. Shinohara, M. L., Correa, A., Bell-Pederson, D. Dunlap, J. C., and Loros, J. J. (2002). Neurospora clock-controlled gene 9 (ccg-9) encodes trehalose synthase: circadian regulation of stress responses and development. *Eucaryot Cell* **1**(1): 33-43

100. Sikorski, R. S., and Hieter, P. (1989). A system of shuttle vectors and yeast host strains designed for efficient manipulation of DNA in Saccharomyces cerevisiae. *Genetics* **122**(1): 19-27

101. Smith, K. M., et al. (2010). Transcription factors in light and circadian clock signaling networks revealed by genomewide mapping of direct targets for neurospora white collar complex. *Eucaryot Cell* **9**(10): 1549-56

102. Sømme, L. (1967). The effect of temperature and anoxia on haemolymph composition and supercooling in three overwintering insects. *J Insect Physiol* **13**:805-14

103. Sømme, L. (1982). Supercooling and winter survival in terrestrial arthropods. *Comp Biochem Physiol* **73**(4): 519-43

104. Springer, M. L., and Yanofsky, C. (1989). A morphological and genetic analysis of conidiophore development in Neurospora crassa. *Genes Dev* **3**(4): 559-71

105. Storch, K. F. et al. (2002). Extensive and divergent circadian gene expression in liver and heart. *Nature* **417**(6884): 78-83

106. Sun, J., and Glass, N. L. (2001). Identification of the CRE-1 Cellulolytic Regulon in Neurospora crassa. *PLoS ONE* **6**(9): e25654

107. Sussman, A. S., and Lingappa, B. T. (1959). Role of Trehalose in Ascospores of Neurospora Tetrasperma. *Science* **130**(3385): 1343

108. Sussmann, A. S., Garret, M. K., Sargent, M., and Yu, S. A. (1971). Isolation, mapping, and characterization of trehalaseless mutants of Neurospora crassa. *J Bacteriol* **108**(1): 59-68

109. Tanno, K. (1964). High sugar levels in the solitary bee *Ceratina*. *Low Temp Sci Ser* B **22**: 51-7

110. Teichert, I., Steffens, E. K., Schnaß, N., Fränzel, B., Krisp, C., Wolters, D. A., and Kück, U. (2014). PRO40 Is a Scaffold Protein of the Cell Wall Integrity Pathway, Linking the MAP Kinase Module to the Upstream Activator Protein Kinase C. *PLoS Genet* **10**(9): e1004582

111. Thevelein, J. M. (1984). Regulation of trehalose mobilization in fungi. *Microbiol rev* **48**(1): 42-59

112. Thevelein, J. M., and Hohmann, S. (1995). Trehalose synthase: guard to the gate of glycolysis in yeast? *Trends Biochem Sci* **20**(1): 3-10

113. Tian, C, et al. (2009). Systems analysis of plant cell wall degradation by the model filamentous fungus Neurospora crassa. *Proc Natl Acad Sci USA* **106**(52): 22157-62

114. Tu, B. P., Kudlicki, A., Rowicka, W., and McKnight, S. L. (2005). Logic of the Yeast Metabolic Cycle: Temporal Compartmentalization of Cellular Processes. *Science* **310**(5751): 1152-8

115. Tu, B. P., Mohler, R. E., Liu, J. C., Dombek, K. M., Young, E. T., Synovec, R. E., and McKnight, S. L. (2007). Cyclic changes in metabolic state during the life of a yeast cell. *Proc Natl Acad Sci USA* **104**(43): 16886-91

116. Van Aelst, L., et al. (1993). Molecular cloning of a gene involved in glucose sensing in the yeast Saccharomyces cerevisiae. *Mol. Microbiol*. **8**(5), 927–943

117. van Dijken, A. J., Schluepmann, H., and Smeekens, S. C. (2004). Arabidopsis trehalose-6-phosphate synthase 1 is essential for normal vegetative growth and transition to flowering. *Plant Physiol* **135**(2): 969-77

118. Vitalini, M. W., de Paula, R. M., Goldsmith, C. S., Jones, C. A., Borkovich, K. A., and Bell-Pedersen, D. (2007). Circadian rhythmicity mediated by temporal regulation of the activity of p38 MAPK. *Proc Natl Acad Sci USA* **104**(46): 18223-8

119. Vogel, G., Aeschbacher, R. A., Müller, J. Boller, T., and Wiemken, A. (1998). Trehalose-6-phosphate phosphatases from Arabidopsis thaliana: identification by functional complementation of the yeast tps2 mutant. *Plant J* **13**(5): 673-83

120. Wahl, V et al. (2013). Regulation of flowering by trehalose-6-phosphate signaling in Arabidopsis thaliana. *Science* **339**(6120): 704-7

121. Wang, Y., Pierce, M., Schnepper, L., Güldal, C. G., Zhang, X., Tavazoie, S., and Broach, J. R. (2004). Ras and Gpa2 mediate one branch of a redundant glucose signaling pathway in yeast. *PLoS Biol* **2**(5): E128

122. Wannet, W. J. B., Op den Camp, H. J. M., Wisselink, H. W., van der Drift, C., Van Griensven, L. J. L. D., and Vogels, G. D. (1998). Purification and characterization of trehalose phosphorylase from the commercial mushroom *Agaricus bisporus*. *Biochem Biophys Acta* **1425**(1): 177-88

123. White, C., Lee, D. B., and Free, S. J. (1985). Neurospora trehalase and its structural gene. *Genetics* **110**(2): 217-27

124. Wu, J., Zhang, N., Hayes, A., Panoutsopoulou, K., and Oliver, S. G. (2004). Global analysis of nutrient control of gene expression in Saccharomyces cerevisiae during growth and starvation. *Proc Natl Acad Sci USA* **101**(9): 3148-53

125. Xu, F. X., Dai, R. P., Goh, S. R., Zheng, L., and Luo, Y. (2009). Logic of a mammalian metabolic cycle: an oscillated NAD+/NADH redox signaling regulates coordinated histone expression and S-phase progression. *Cell Cycle* **8**(5): 773-9

126. Yang, Y., He, Q., Cheng, P., Wrage, P., Yarden, O., and Liu, Y. (2004). Distinct roles for PP1 and PP2A in the *Neurospora* circadian clock. *Genes Dev*. 18, 255-260.

127. Yazdi, M. T., Radford, A., Keen, J. N., and Woodward, J. R. (1990). Cellulase production by *Neurospora crass*: Purification and characterization of cellulolytic enzymes. *Enzyme Microb Technol* **12**: 120-23

128. Yoneyama, Y., and Lever, J. E. (1988). Apical trehalase expression associated with cell patterning after inducer treatment of LLC-PK1 monolayers. *J Cell Physiol* **131**(3): 330-41

129. Yoshida, Y., Iiqusa, H., Wang, N., and Hasunuma, K. (2011). Cross-talk between the cellular redox state and the circadian system in Neurospora. *PLoS One* **6**(12): e282277

130. Yoshida, Y., Maeda, T., Lee, B., and Hasunuma, K. (2008). Conidiation rhythm and light entrainment in superoxide dismutase mutant in Neurospora crassa. *Mol Genet Genomics* **279**(2): 193-202

131. Zimmerman, W. F., Pittendrigh, C. S., and Pavlidis, T. (1968). Temperature compensation of the circadian oscillation in drosophila pseudoobscura and its entrainment by temperature cycles. *J Insect Physiol* **14**(5): 669-84

132. Zink, M. W. (1967). Catabolite repression of malic dehydrogenase in *Neurospora crassa. Can J Microbiol* **13**(9): 1296-8

133. Znameroski, E. A., Coradetti, S. T., Roche, C. M., Tsai, J. C., Ivarone, A. T., Cate, J. H., and Glass, N. L. (2012). Induction of lignocellulose-degrading enzymes in Neurospora crassa by cellodextrins. *Proc Natl Acad Sci USA* **109**(16): 6012-7

6 Appendices

6.1 Supplementary figures

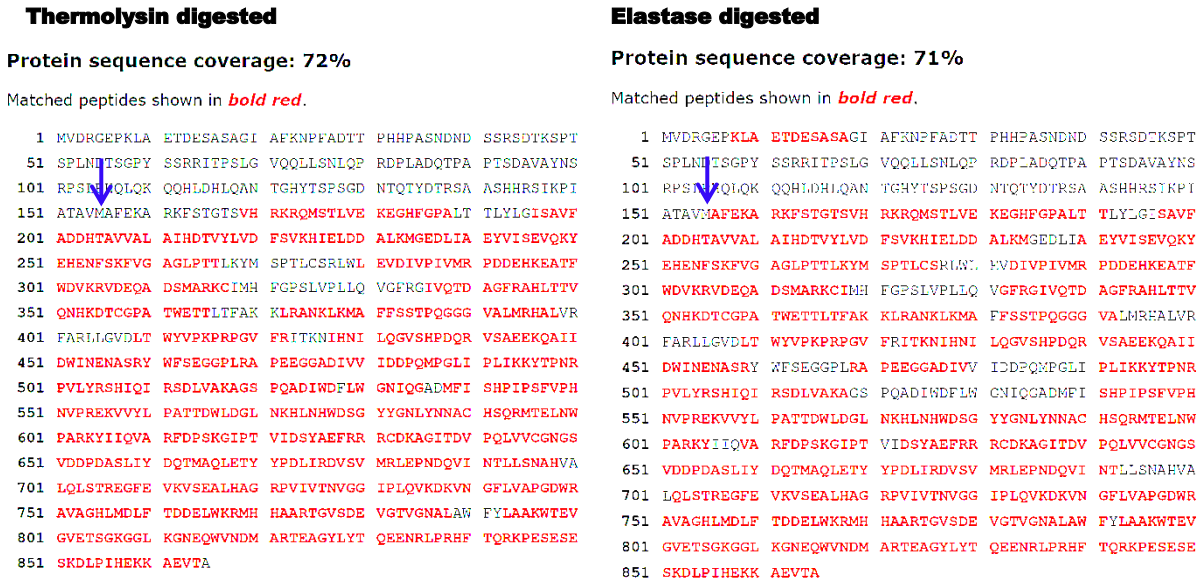

Figure S1: Analysis of the short CCG-9 isoform by mass spectrometry

CCG-9-Flag protein was purified by affinity purification and the short isoform was analyzed by mass spectrometry. The entirety of found peptides cover more than 90% of the short CCG-9 isoform but less than 10% of the N-terminal region upstream of M155 (blue arrow).

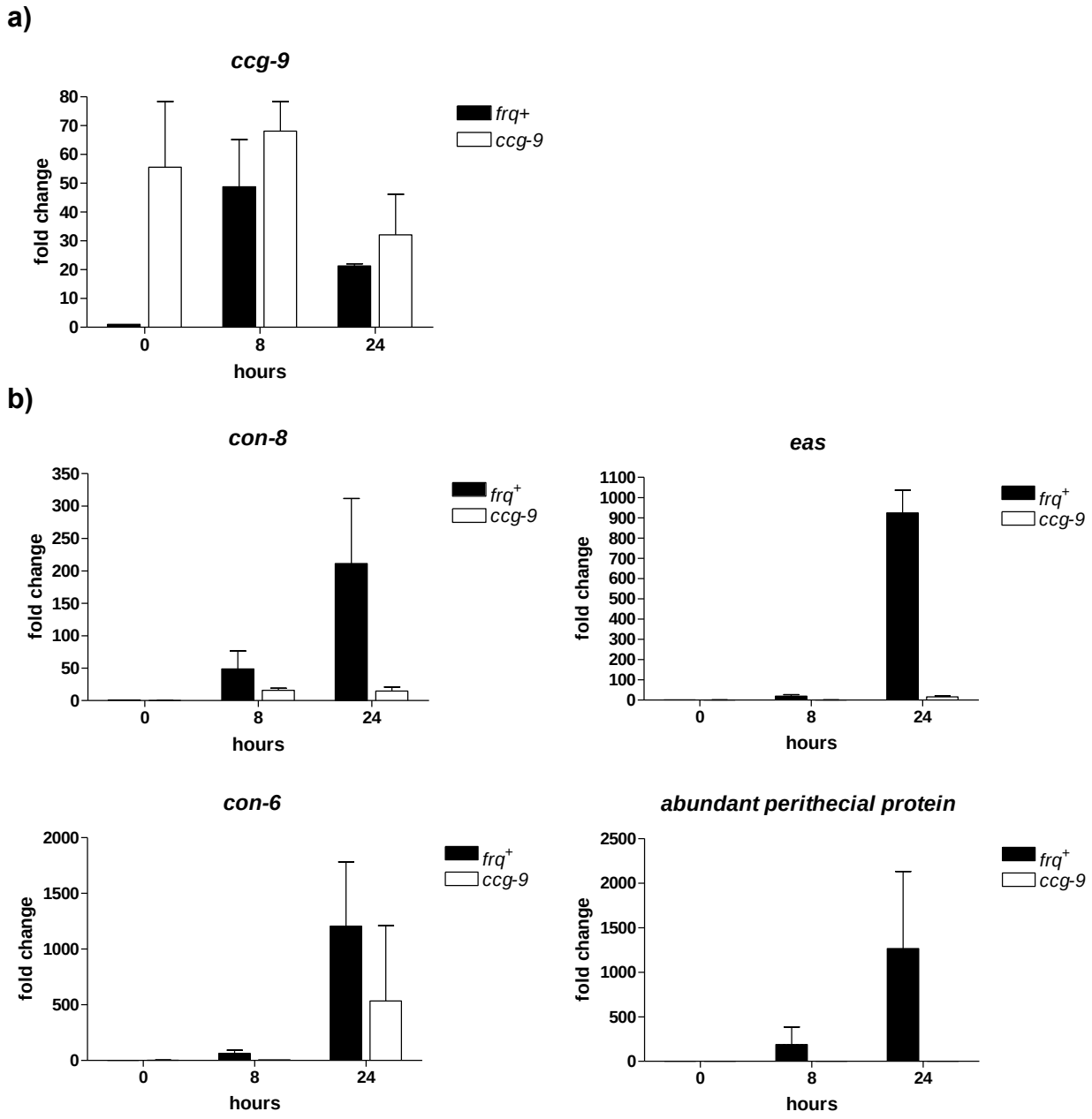

Figure S2: Expression of *ccg-9* and conidiation specific genes during asexual development

Expression of *ccg-9* is significantly induced under standard conditions (0h) in *ccg-9*^{RIP} compared to the wild type (*frq*$^{+}$) **(a)**. Upon air exposure conidiation specific genes are clearly induced in the wild type but not in *ccg-9*^{RIP} **(b)**. The diagrams show the fold change normalized to the mean expression at 0 h (iquid culture) as well as 8h and 24h after air exposure. Error bars show the standard deviation of the mean (n=2).

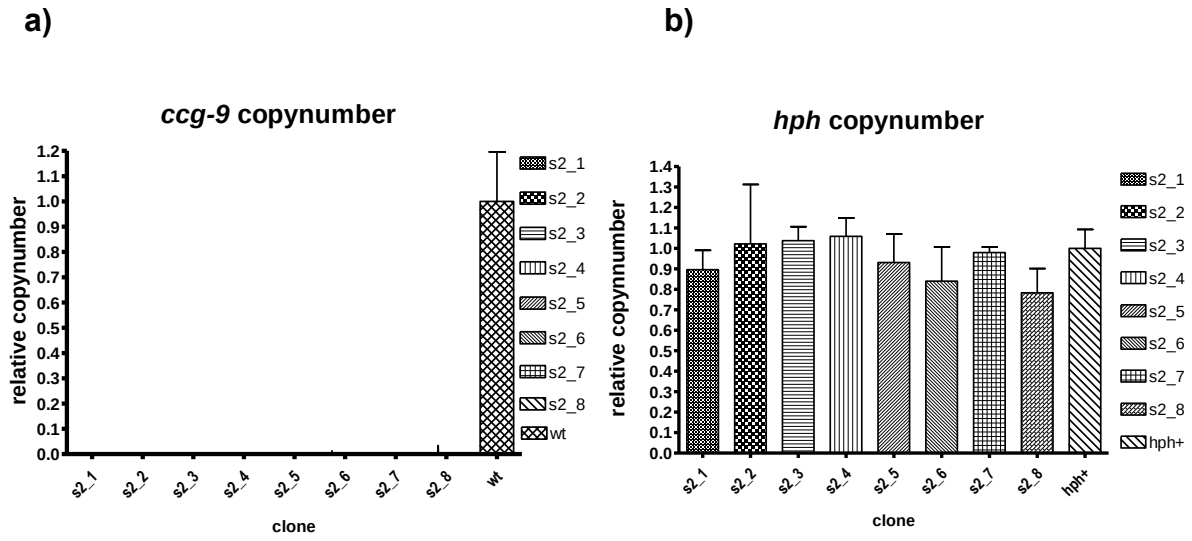

Figure S3: Validation of the Δ*ccg-9* knockout strain

Eight different clones (s2_1 to s2_8) obtained from the same cross were tested for deletion of the *ccg-9* gene. None of them showed a valid *ccg-9* copy in contrast to the wild type (wt) **(a)**. All clones showed a comparable copynumber of the hph gene indicating single copy insertion of the resistance marker **(b)**. The diagrams show the fold change normalized to a reference sample (wt or *hph+*). Error bars show the 95% confidence intervall (n=2).

target: ccg-9

	Cт Mean	ΔCт Mean	ΔΔCт	RQ
		(= Cт(ccg-9) - Cт(28s))	(= ΔCт(X) - ΔCт (wt))	(= $2^{(-\Delta\Delta Ct)}$)
wt	30,01	21,35	0	1,00
wt 8h	28,38	18,38	-2,97	7,83
s2_2	36,22	28,68	7,33	0,01
s2_2 8h	36,75	28,09	6,74	0,01
m6_4	37,47	29,75	8,40	0,00
m6_4 8h	36,11	26,09	4,75	0,04
l10_4	36,29	28,00	6,65	0,01
l10_4 8h	36,96	27,58	6,24	0,01
H2O	36,03	-	-	-

target: 28s

	Cт Mean
wt	8,67
wt 8h	10,00
s2_2	7,54
s2_2 8h	8,66
m6_4	7,72
m6_4 8h	10,02
l10_4	8,29
l10_4 8h	27,96
H2O	35,17

Table S4: Raw data of *ccg-9* transcript quantification by qPCR

Due to poor expression of *ccg-9* under standard conditions C_T values were close to background even in the wilt type (wt) samples. Therefore, cultures were subjected to air in order to induce *ccg-9* transcription (8h). Induction of *ccg-9* transcript could be detected in the wild type sample but not in the knockout strains.

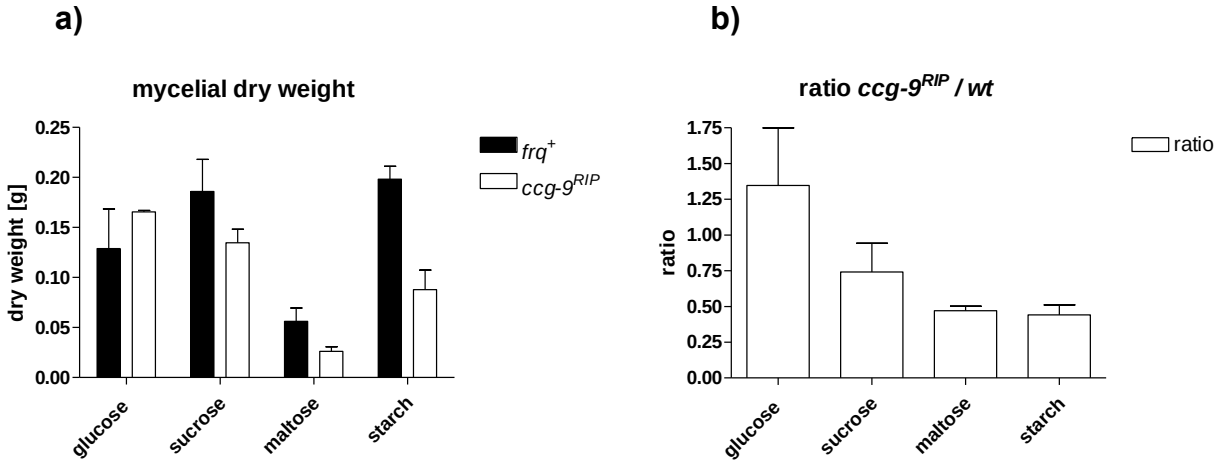

Figure S5: The *ccg-9*^{RIP} mutant shows impaired vegetative growth on complex carbohydrates compared to wild type

Mycelial disks were stamped out of cultures grown in petri dishes (Vogel´s + 2% glucose) and triplicates were transferred to liquid cultures containing Vogel´s minimal medium supplemented with the indicated carbon source (2% w/v). The mycelia were grown for 48h, harvested and dried at 80°C overnight. The diagrams show the absolute dry weight of the cultures **(a)** and the ratio between *ccg-9*^{RIP} and wild type dry weight (**b**). Error bars show the standard deviation of the mean (n=2).

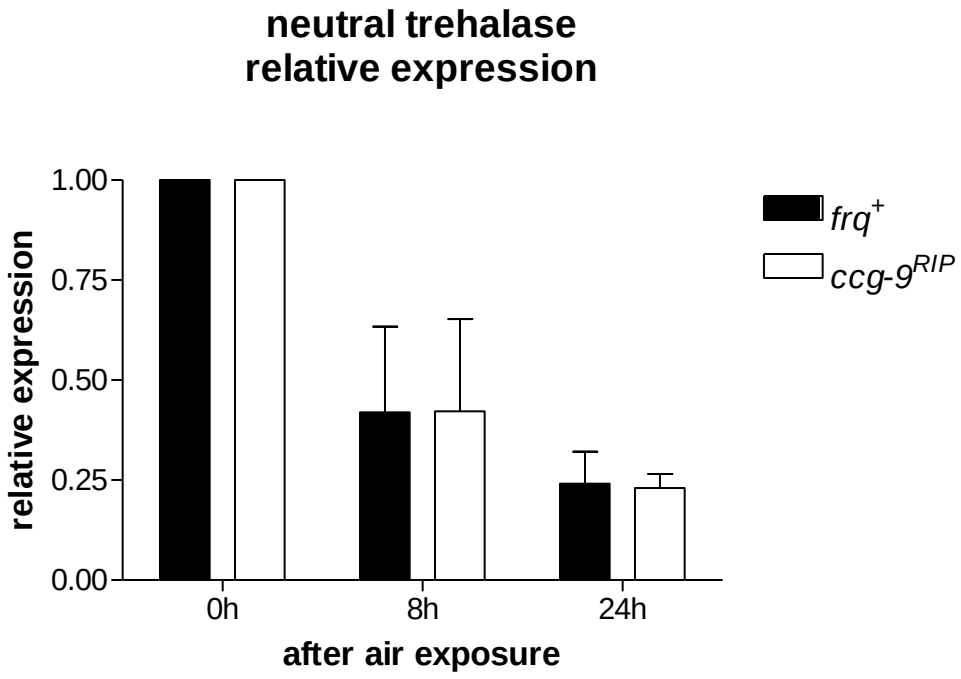

Figure S6: Neutral trehalase (NCU04221) is repressed during asexual development

The diagram shows the average of relative expression levels during asexual development normalized to standard liquid culture conditions (0h). Error bars show the standard deviation of the mean (n=2).

6.2 Abbreviations

ada-1	*all development altered-1*
APS	ammonium persulfate
bd	*band*
cAMP	cyclic adenosinemonophosphate
ccg-9	*clock controlled gene-9*
CCR	carbon catabolite repression
CK1a	CASEIN KINASE 1a
CTAB	cetyltrimethylammonium bromide
DD	constant darkness
DTT	dithiothreitol
ECL	enhanced chemiluminescence
EDTA	ethylenediaminetetraacetic acid
EtOH	ethanol
FAM	6-carboxyfluorescein
FRQ	FREQUENCY
G6P-DH	Glucose-6-phophate Dehydrogenase
h	hours
HEPES	4-(2-hydroxyethyl)-1-piperazineethanesulfonic acid
HPLC	high performance liquid chromatography
L / D	light / dark cycles
LL	constant light
MAK-1/-2	MITOGEN ACTIVATED PROTEIN KINASE-1 / -2
min	minutes
NaCl	sodium chloride
NADPH	nicotinamide adenine dinucleotide phosphate
NMR	nuclear magnetic resonance
OD	optical density
Pfu	*Pyrococcus furiosus.*
PIPES	1,4-Piperazinediethanesulfonic acid

PMSF	phenylmethylsulfonyl fluoride
QA	quinic acid
RIP	Repeat Induced Point mutation
ROS	reactive oxygen species
SDS	sodium dodecyl sulfate
sec	seconds
SNPs	single nucleotide polymorphisms
T6P	trehalose-6-phosphate
TAMRA	tetramethylrhodamine
Taq	*Thermus aquaticus*
TBS	tris-buffered saline
TEMED	N,N,N′,N′-tetramethylethan-1,2-diamin
TPP	TREHALOSE-6-PHOSPHATE PHOSPHATASE
TPS	TREHALOSE-6-PHOSPHATE SYNTHASE
TreP	TREHALOSE PHOSPHORYLASE
UV	ultra violet light
vol	volumes
WC-1	WHITE COLLAR-1
WC-2	WHITE COLLAR-2
WCC	White Collar Complex
X-ray	gamma radiation